CHAPTER IV

RESULTS AND DISCUSSIONS

4.1 Factorial Design

A quicker way of calculating the effects was by Yates Algolithm. There are five main effects: (A, B, C, D and E); ten two-factor interactions: (AB, AC, AD, AE, BC, BD, BE, CD, CE, DE); ten three-factor interactions: (ABC, ABD, ABE, ACD, ACE, ADE, BCD, BCE, BDE, CDE); five four-factor interactions: (ABCD, ABCE, ABDE, ACDE, BCDE); and one five-factor interaction (ABCDE).

4.1.1 Tensile Properties

Secant Modulus at 2 % Strain

The normal probability cumulative plot of the 2 % secant modulus is shown in Figure 4.1. All effects that lie along the line are negligible, whereas those far from the line are significant effect.

All variables, A, B, C, D and E are found to have significant effect on the 2 % secant modulus. Significant two-factor interactions is (BE), significant four-factor interactions are (ABCD, ABCE).

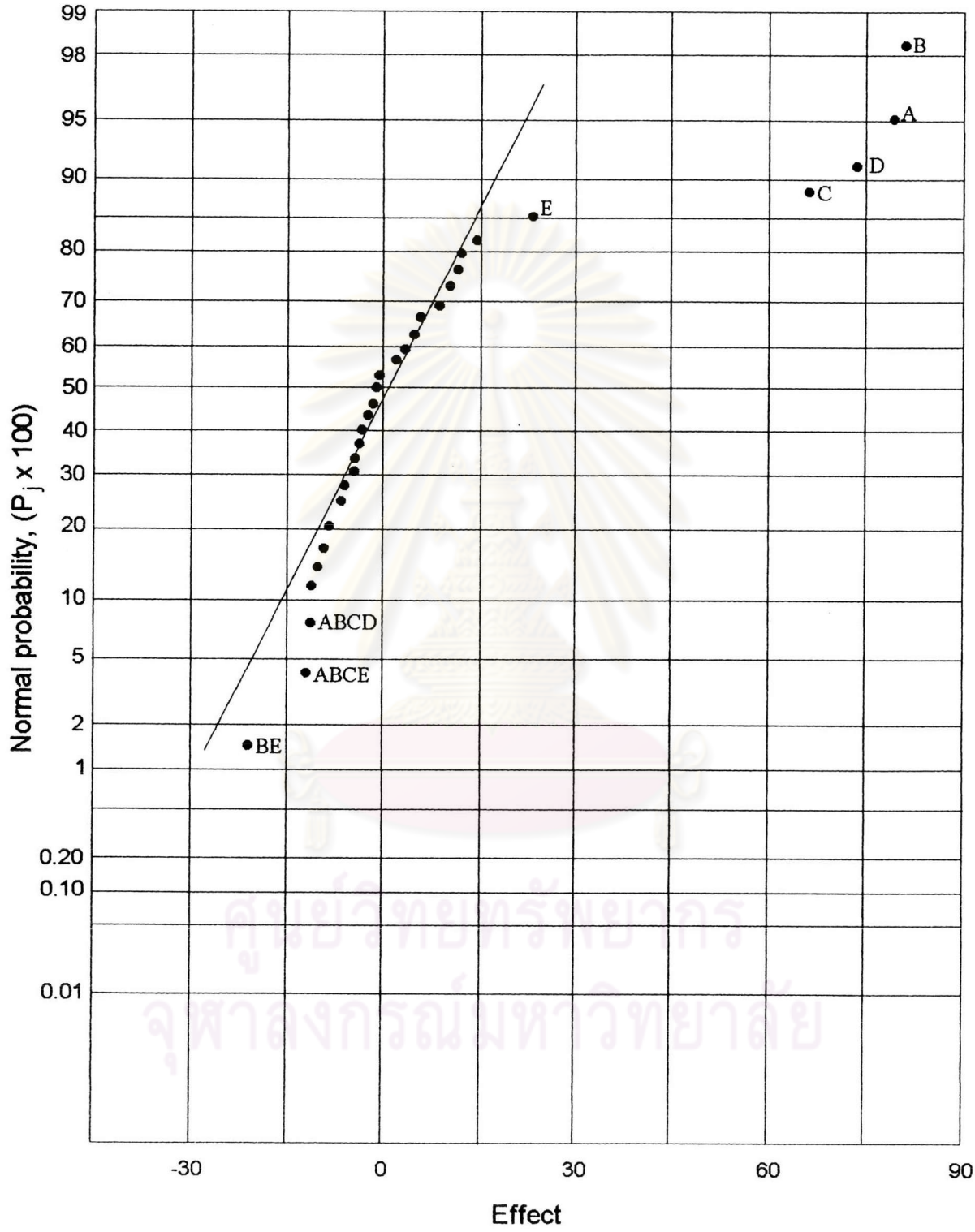

Figure 4.1: The normal probability cumulative plot of 2% secant modulus.

The 2 % secant modulus of unfilled and filled-HDPE is shown in Figure 4.2.

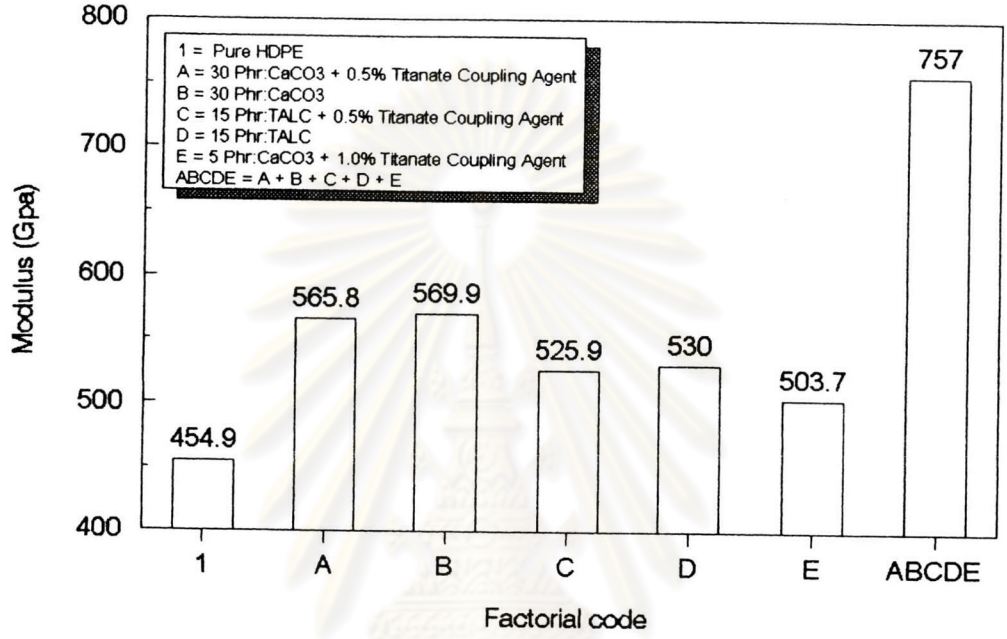

Figure 4.2: The 2 % secant modulus of unfilled and filled-HDPE.

In Figure 4.2, an addition of $CaCO_3$, talc, carbon black and a combination of (ABCDE) content by 30, 15, 5 and 95 phr increases the secant modulus by 24.8, 16.1, 10.7 and 66.4 % respectively.

0.2 % Offset Yield Stress

The normal probability cumulative plot of the 0.2 % offset yield stress is shown in Figure 4.3

The variable of A, B, C and D are significant effect of yield stress.

The effect of significant two-factor interactions (BE), significant three-factor (ABE) and significant four-factor interactions (BCDE).

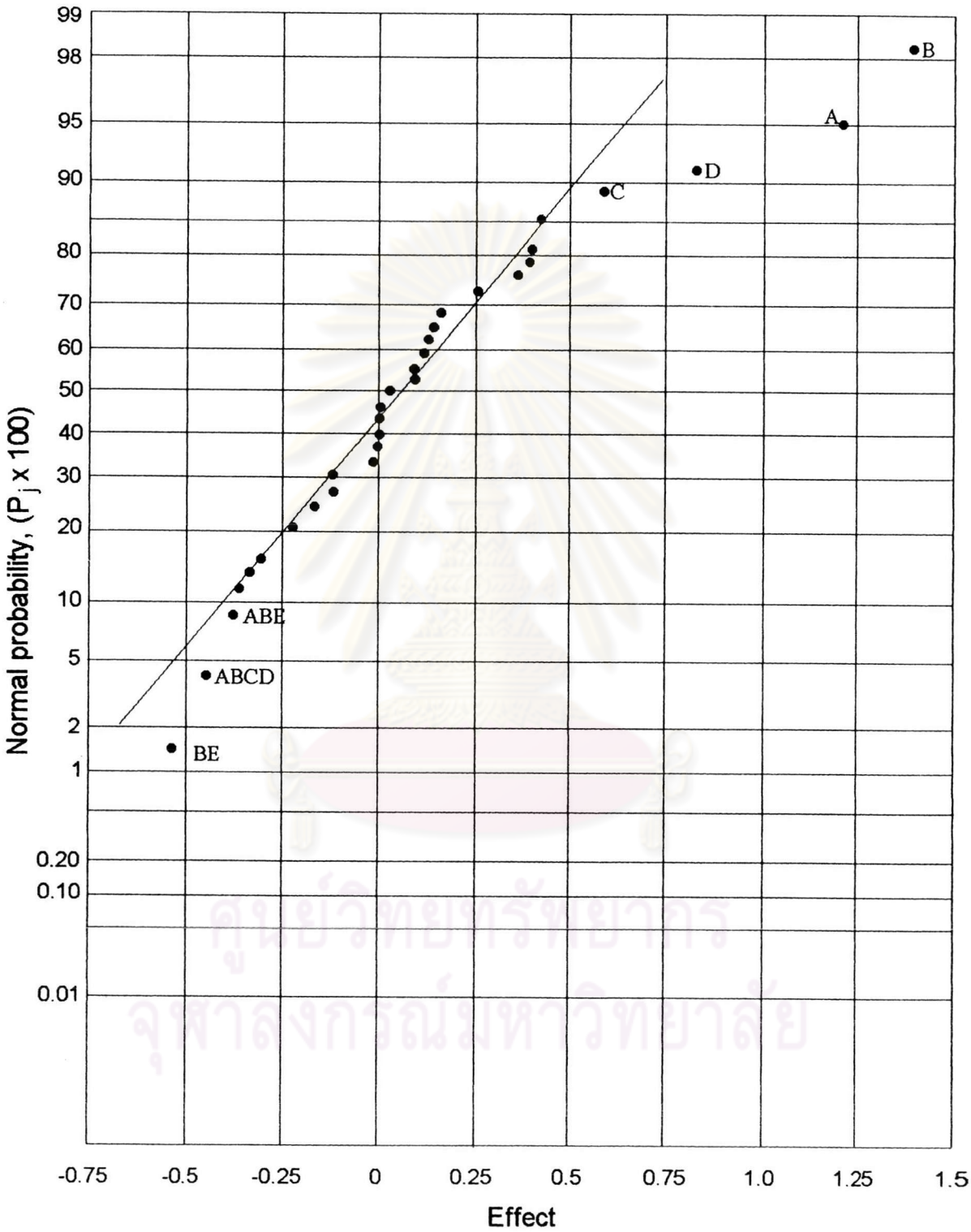

Figure 4.3: The normal probability cumulative plot of 0.2% offset yield stress.

The 0.2 % offset yield stress of filled-HDPE is shown in Figure 4.4.

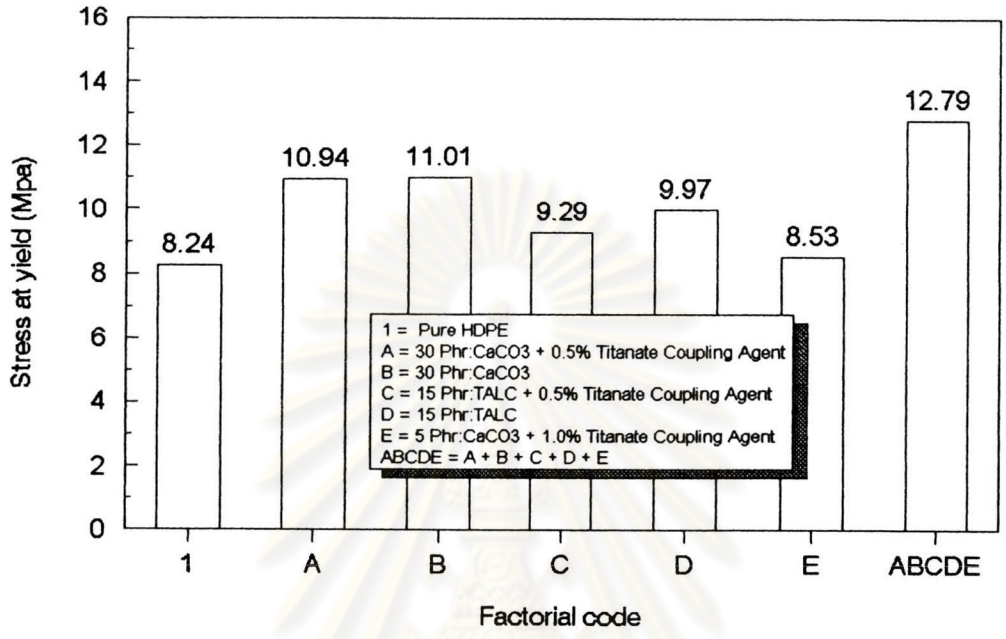

Figure 4.4: The 0.2 % offset yield stress of filled-HDPE.

In Figure 4.4, an addition of $CaCO_3$, talc, carbon black and a combination of (ABCDE) content by 30, 15, 5 and 95 phr increases yield stress by 33.2, 16.9, 3.5 and 55.2 % respectively.

0.2 % Offset yield strain

The normal probability cumulative plot of 0.2 % offset yield strain is shown in Figure 4.5.

The variable of A, B, C and D are found to have significant effect of the 0.2 % offset yield strain. The significant two-factor interaction is (AD, CE), significant three-factor is (ABE) and significant four-factor interactions (BCDE).

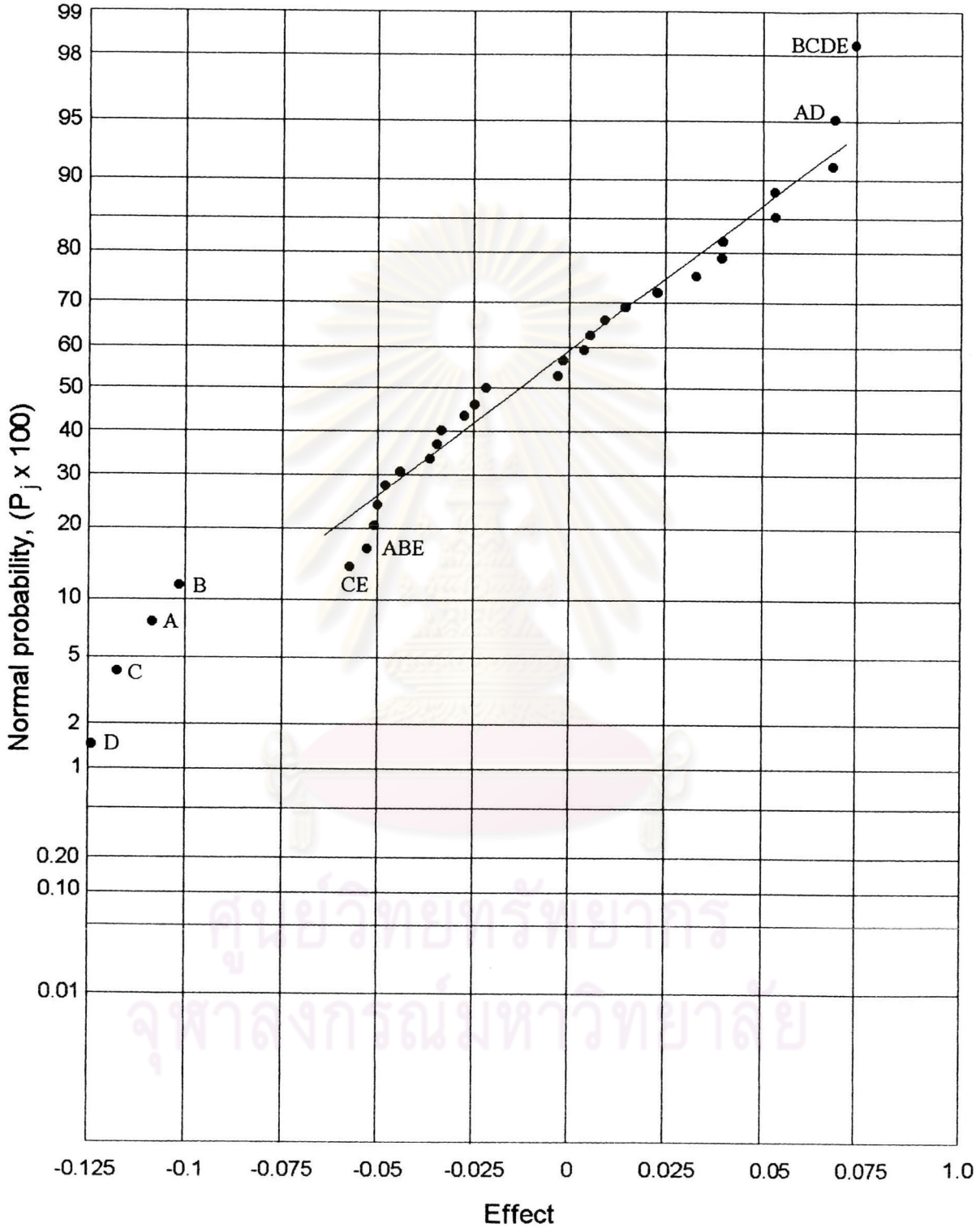

Figure 4.5: The normal probability cumulative plot of 0.2% offset yield strain.

The 0.2 % offset yield strain of filled-HDPE is shown in Figure 4.6.

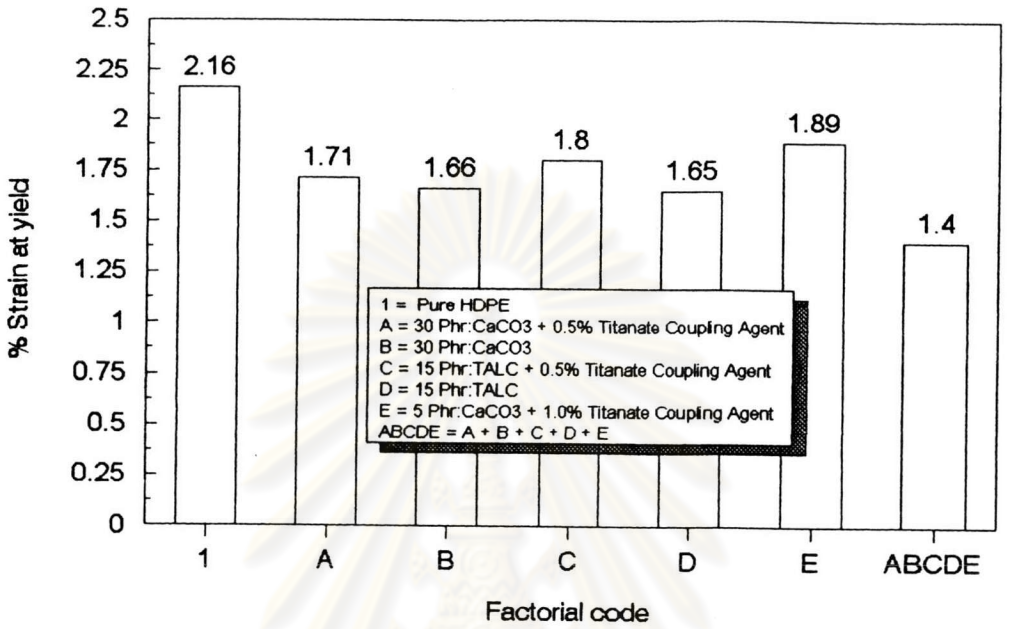

Figure 4.6: The 0.2 % offset yield strain of filled-HDPE .

In Figure 4.6, an addition of $CaCO_3$, talc, carbon black and a combination of (ABCDE) content by 30, 15, 5 and 95 phr decreases 0.2 % offset yield strain by 22, 20.1, 12.5 and 35.2 % respectively.

4.1.2 Hardness

The normal probability cumulative plot of hardness shown in Figure 4.7.

The variables of A, B and E are found to have significant effect on the hardness. Significant two-factor interaction is (BE) and significant three-factor interaction is (ABE).

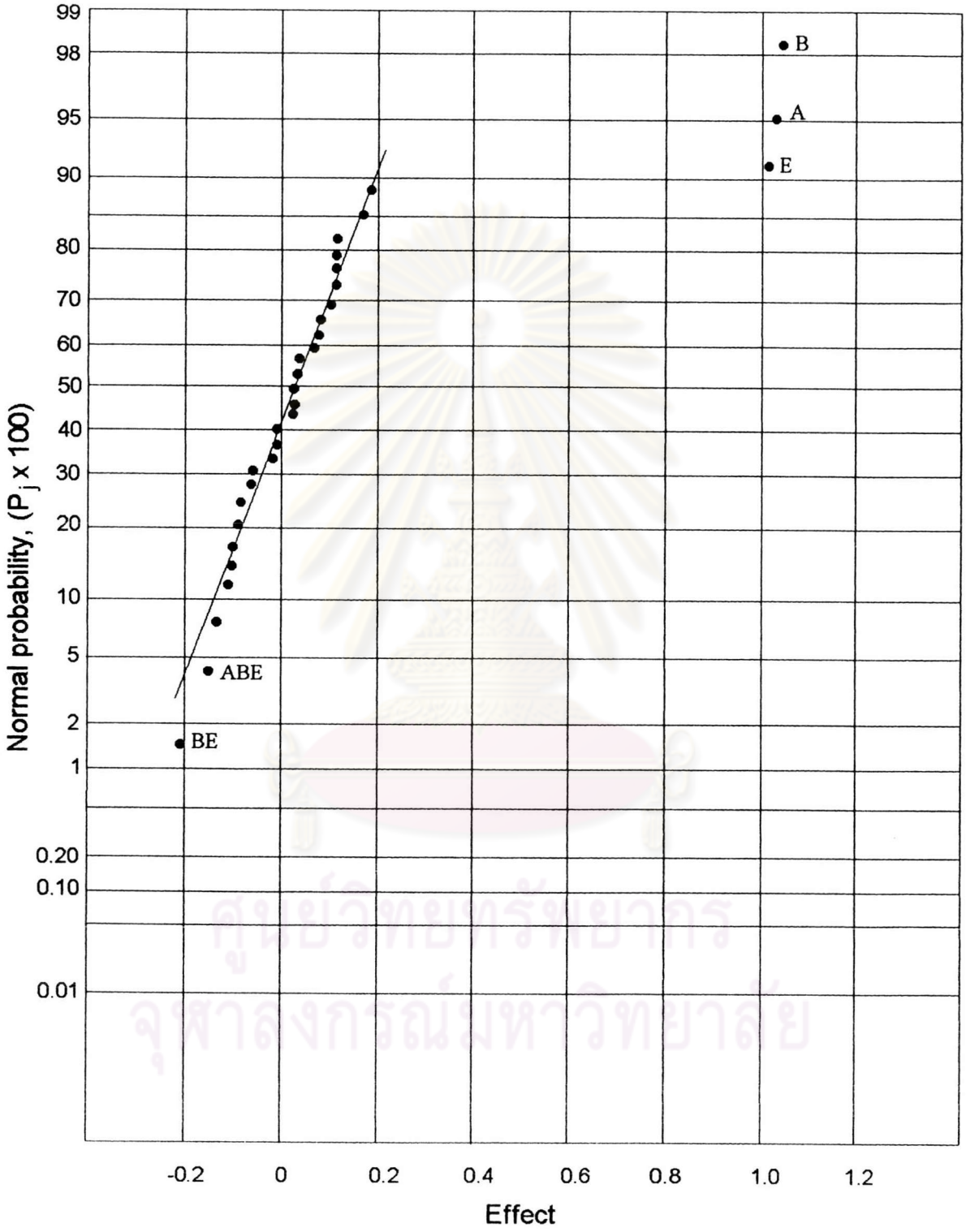

Figure 4.7: The normal probability cumulative plot of hardness.

The hardness of filled-HDPE is shown in Figure 4.8.

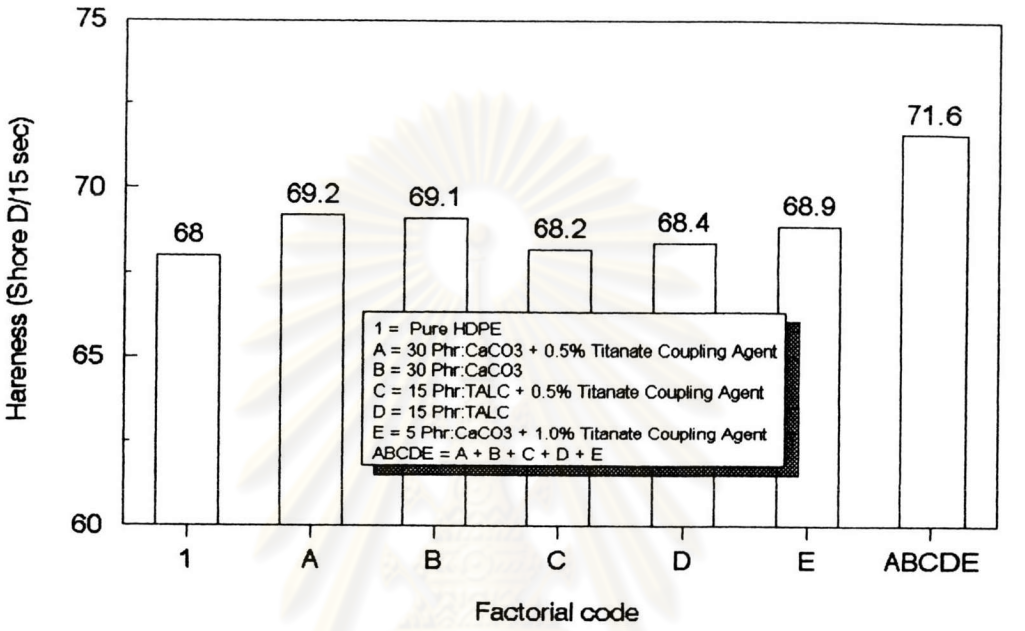

Figure 4.8: The hardness of filled-HDPE.

In Figure 4.8, an addition of $CaCO_3$, talc, carbon black and a combination of ABCDE content by 30, 15, 5 and 95 phr increase hardness by 1.7, 0.4, 1.3 and 5.3 % respectively.

4.1.3 Izod Impact Strength

The normal probability cumulative plot of Izod impact strength shown in Figure 4.9.

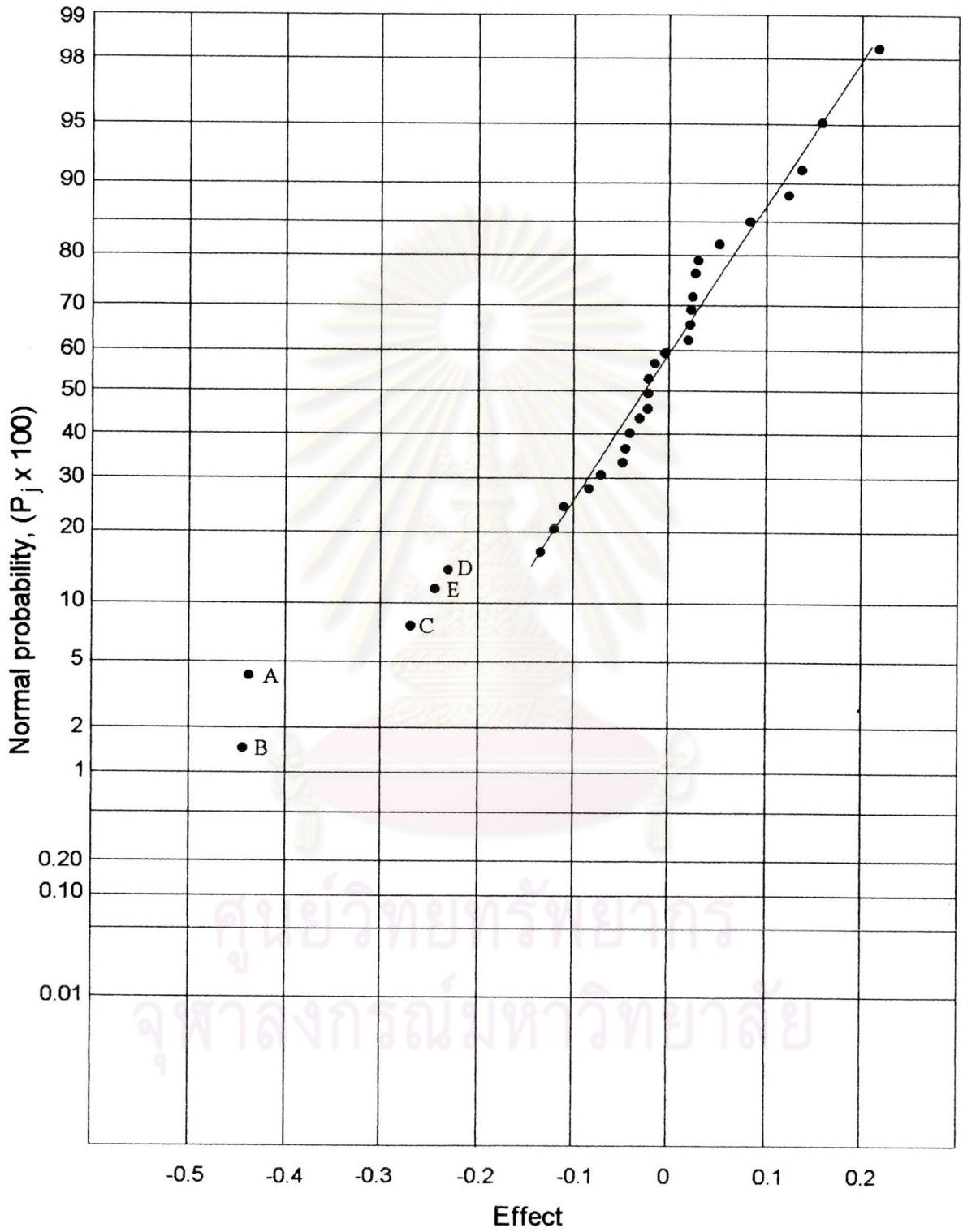

Figure 4.9: The normal probability cumulative plot of Izod impact strength.

The variables of A, B, C, D and E are found to have significant effect on the Izod impact strength.

The Izod impact strength of filled-HDPE is shown in Figure 4.10.

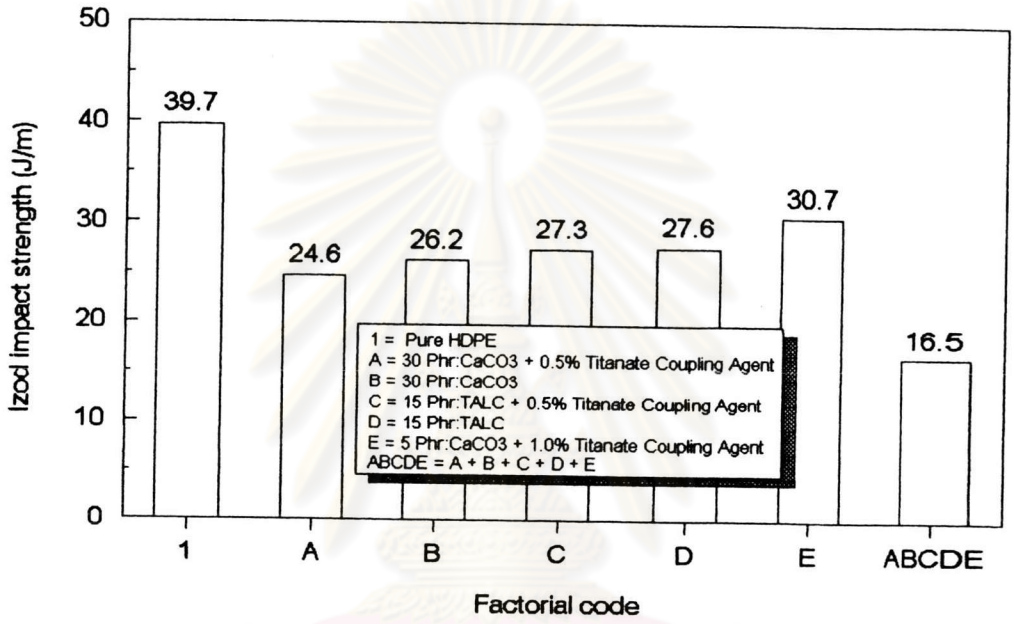

Figure 4.10: The Izod impact strength of filled-HDPE.

In Figure 4.10, an addition of $CaCO_3$, talc, carbon black and a combination of ABCDE content by 30, 15, 5 and 95 phr decrease Izod impact strength by 36.0, 30.9, 22.7 and 58.4 % respectively.

4.1.4 Falling Weight

Absorption Impact Energy

The normal probability cumulative plot of absorption impact energy shown in Figure 4.11.

All variables, A, B, C, D and E are found to have significant effect on the absorption impact energy. All effect two and higher factor interactions of A, B, C, D and E are significant interactions.

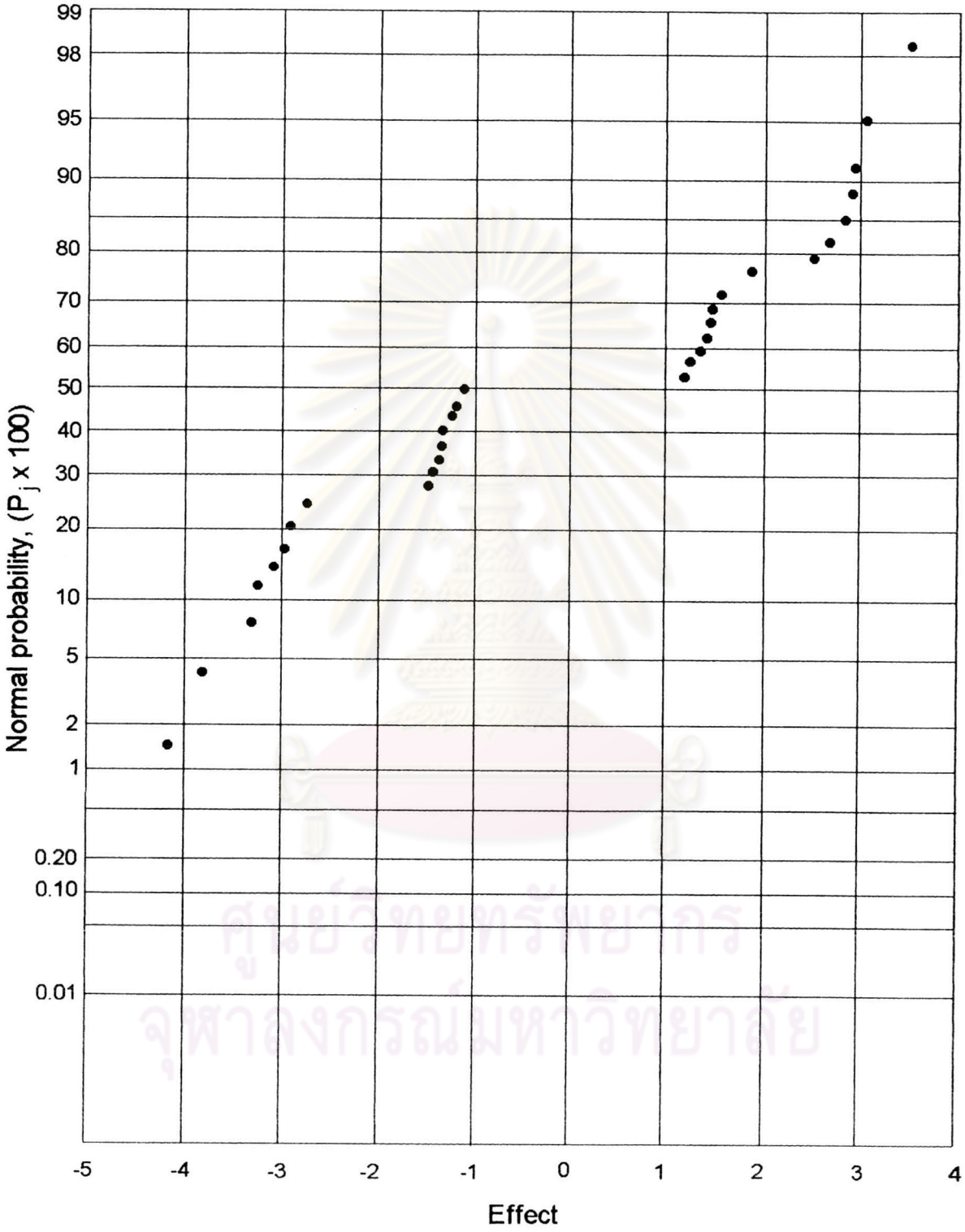

Figure 4.11: The normal probability cumulative plot of absorption impact energy.

The absorption impact energy of filled-HDPE is shown in Figure 4.12.

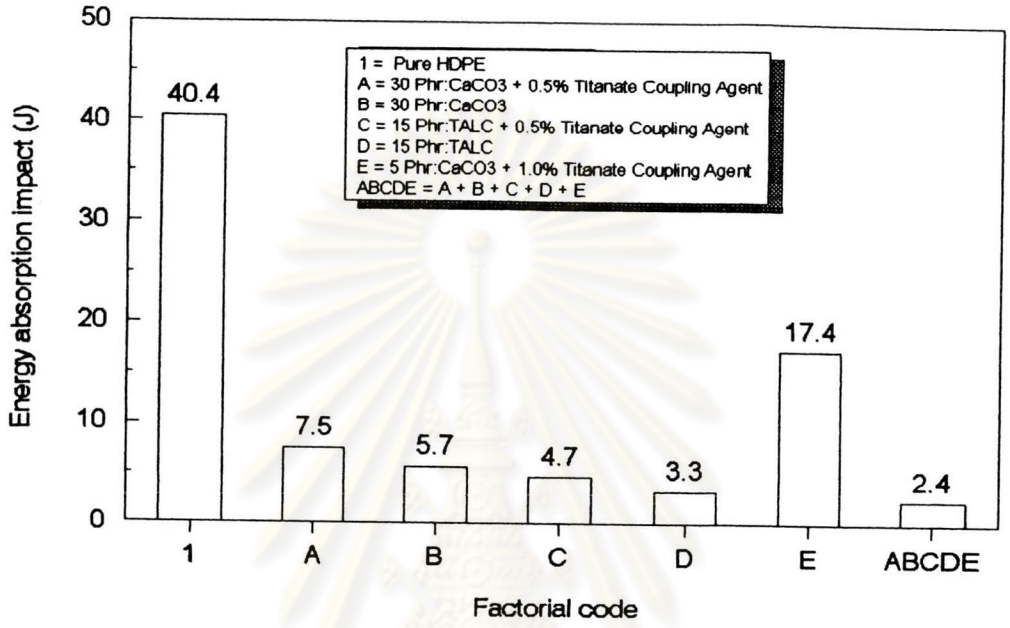

Figure 4.12: The absorption impact energy of filled-HDPE.

In Figure 4.12, an addition of $CaCO_3$, talc, carbon black and a combination of ABCDE content by 30, 15, 5 and 95 phr decrease absorption impact energy by 83.7, 90.1, 56.9 and 94.1 % respectively.

Falling weight impact cracking deformation

The normal probability cumulative plot of falling weight impact cracking deformation is shown in Figure 4.13.

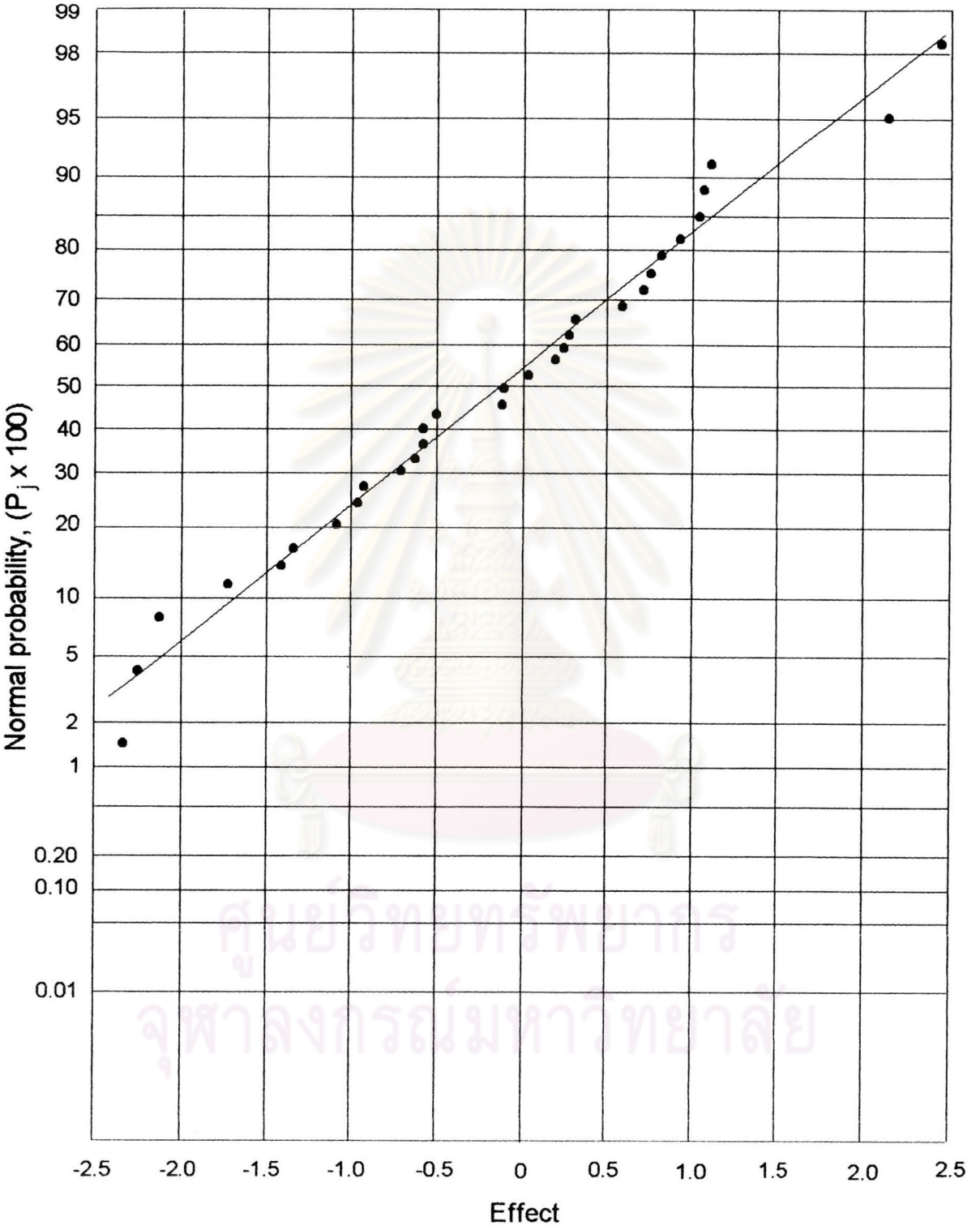

Figure 4.13: The normal probability cumulative plot of falling weight impact cracking deformation.

All variables, A, B, C, D and E are not found to have significant effect on the of falling weight impact cracking deformation. All effect two and higher factor interactions of A, B, C, D and E are not significant interactions.

The falling weight impact cracking deformation of filled-HDPE is shown in Figure 4.14.

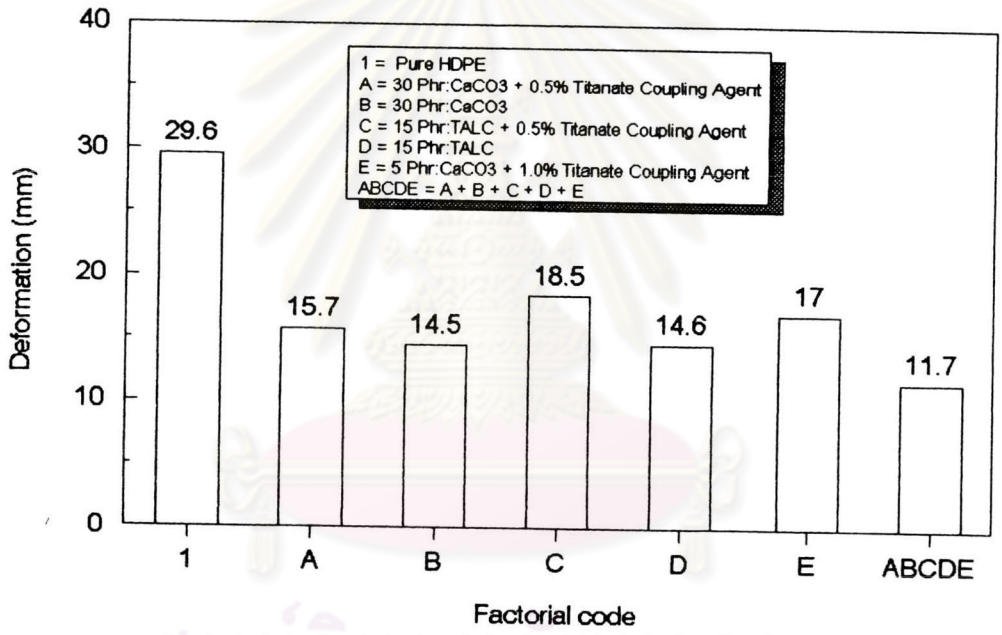

Figure 4.14: The falling weight impact cracking deformation of filled-HDPE.

In Figure 4.14, an addition of $CaCO_3$, talc, carbon black and a combination of ABCDE content by 30, 15, 5 and 95 phr decrease falling weight impact cracking deformation by 49.0, 44.1, 42.6 and 60.5 % respectively.

4.1.5 Differential Scanning Calorimeter (DSC)

Melting Point Temperature

The normal probability cumulative plot of melting point temperature is shown in Figure 4.15.

All variables, A, B, C, D and E are not found to have significant effect on the melting point temperature. Significant three-factor interactions are (ACE, ABE).

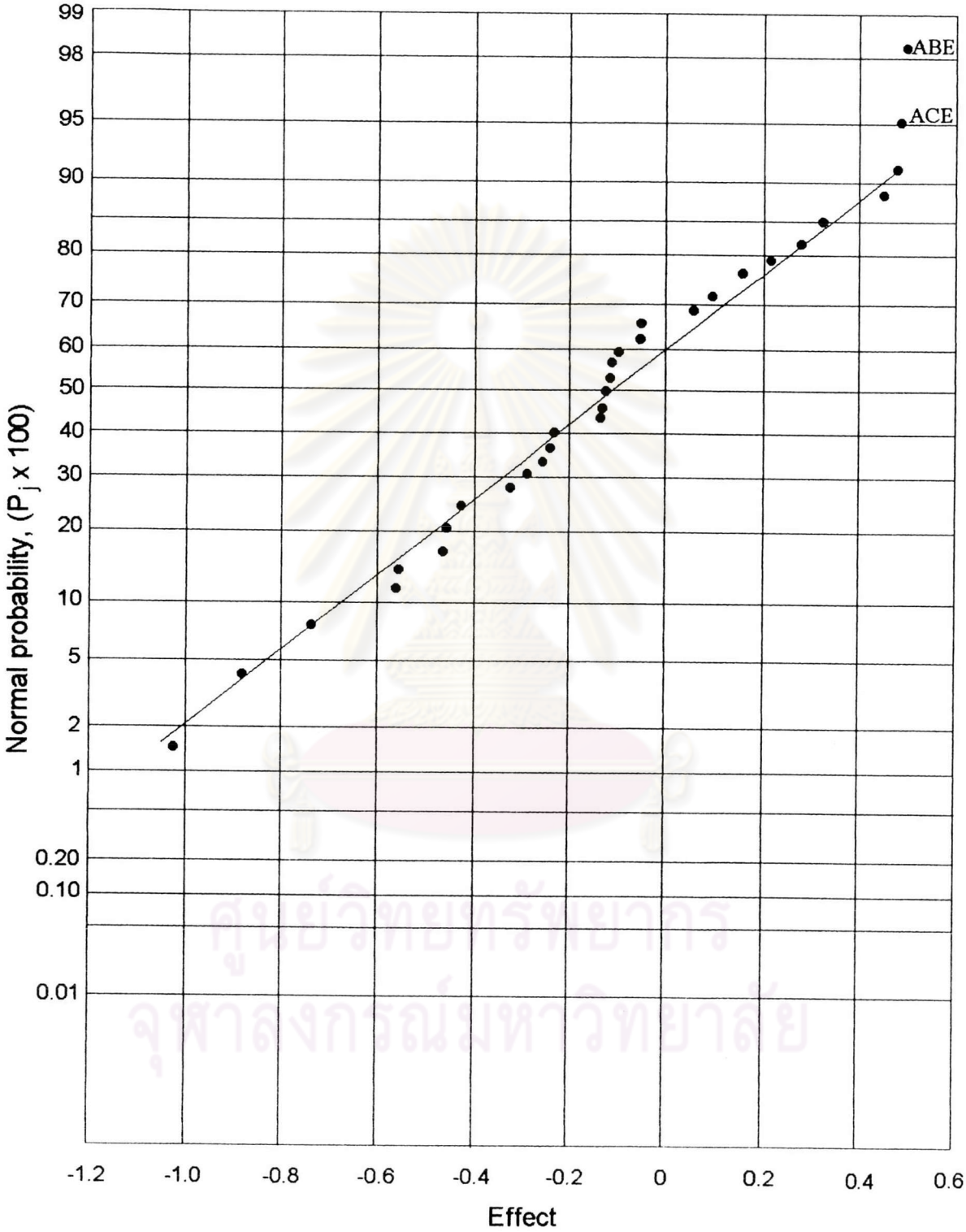

Figure 4.15: The normal probability cumulative plot of melting point temperature.

The melting point temperature of filled-HDPE is shown in Figure 4.16.

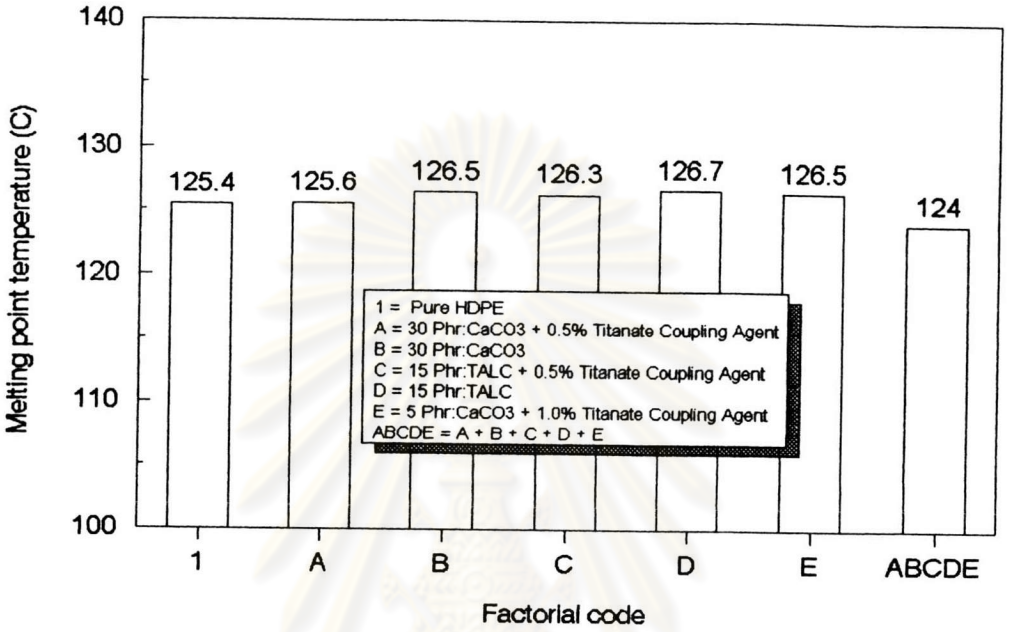

Figure 4.16: The melting point temperature of filled-HDPE.

In Figure 4.16, an addition of $CaCO_3$, talc, carbon black and a combination of ABCDE content by 30, 15, 5 and 95 phr do not change the melting point temperature of filled-HDPE.

Percent Crystallinity

The normal probability cumulative plot of percent crystallinity is shown in Figure 4.17.

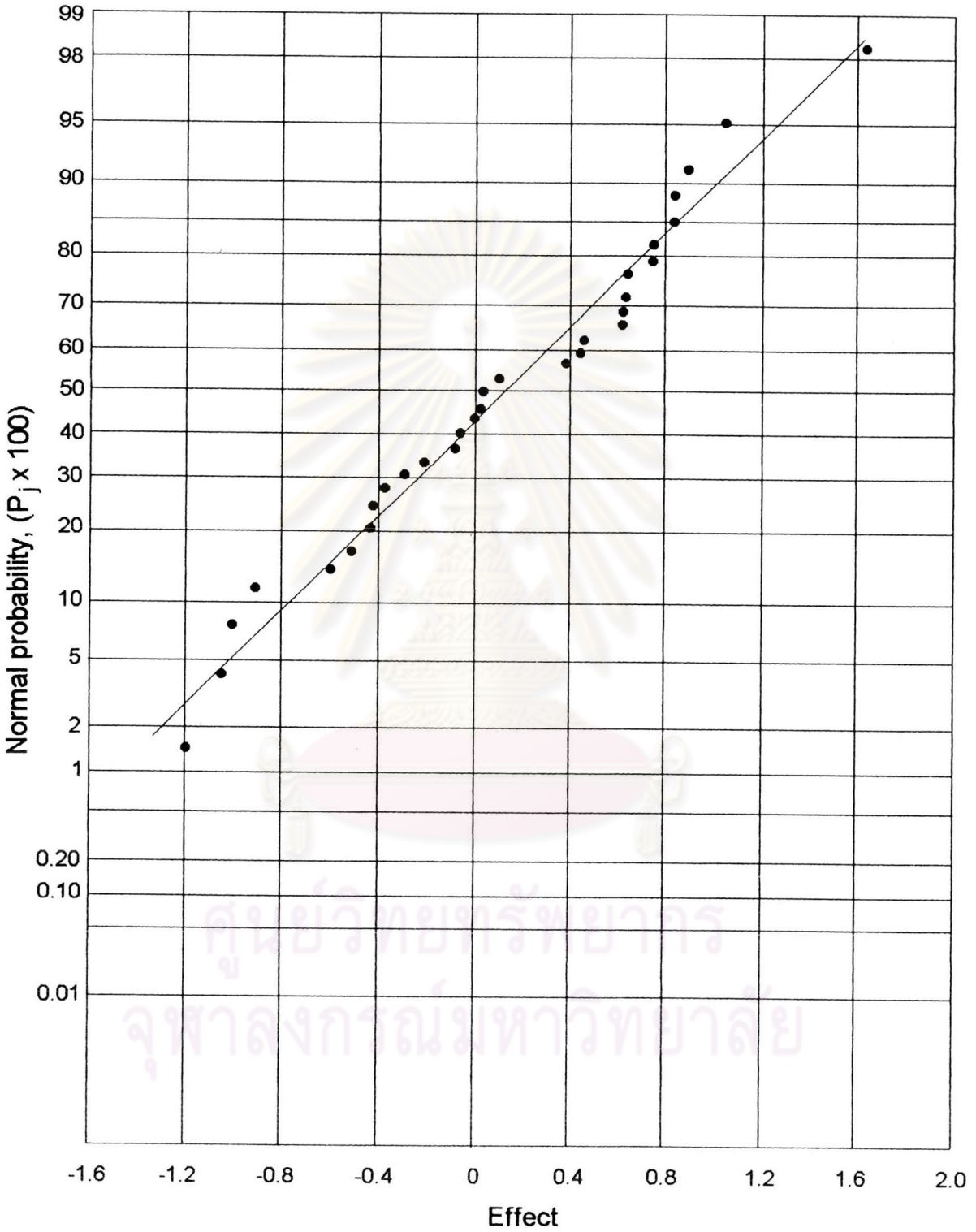

Figure 4.17: The normal probability cumulative plot of percent crystallinity.

All variables, A, B, C, D and E are not found to have significant effect on the percent crystallinity. All effect of two and higher factor interactions of A, B, C, D and E are not significant interactions.

The percent crystallinity of filled-HDPE is shown in Figure 4.18.

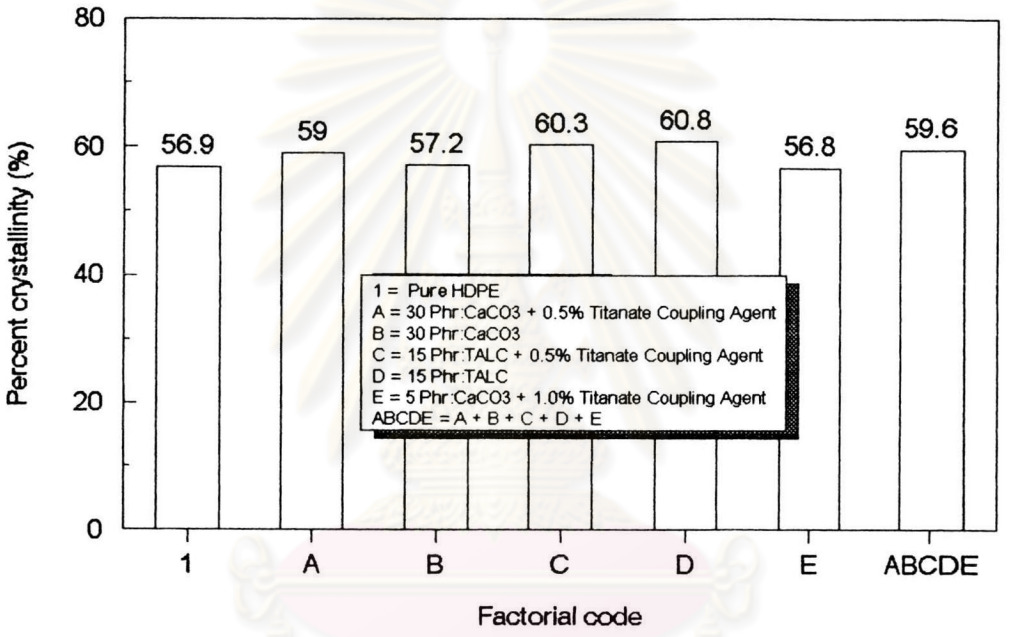

Figure 4.18: The percent crystallinity of filled-HDPE .

In Figure 4.18, an addition of $CaCO_3$, talc, carbon black and a combination ABCDE content by 30, 15, 5 and 95 phr do not change the percent crystallinity of filled-HDPE.

4.1.6 Heat Deflection Temperature.

The normal probability cumulative plot of heat deflection temperature is shown in Figure 4.19.

The variables of A, B, C and D are found to have significant effect on the of heat deflection temperature. All effect of two and higher factor interactions of A, B, C, D and E are not significant interactions.

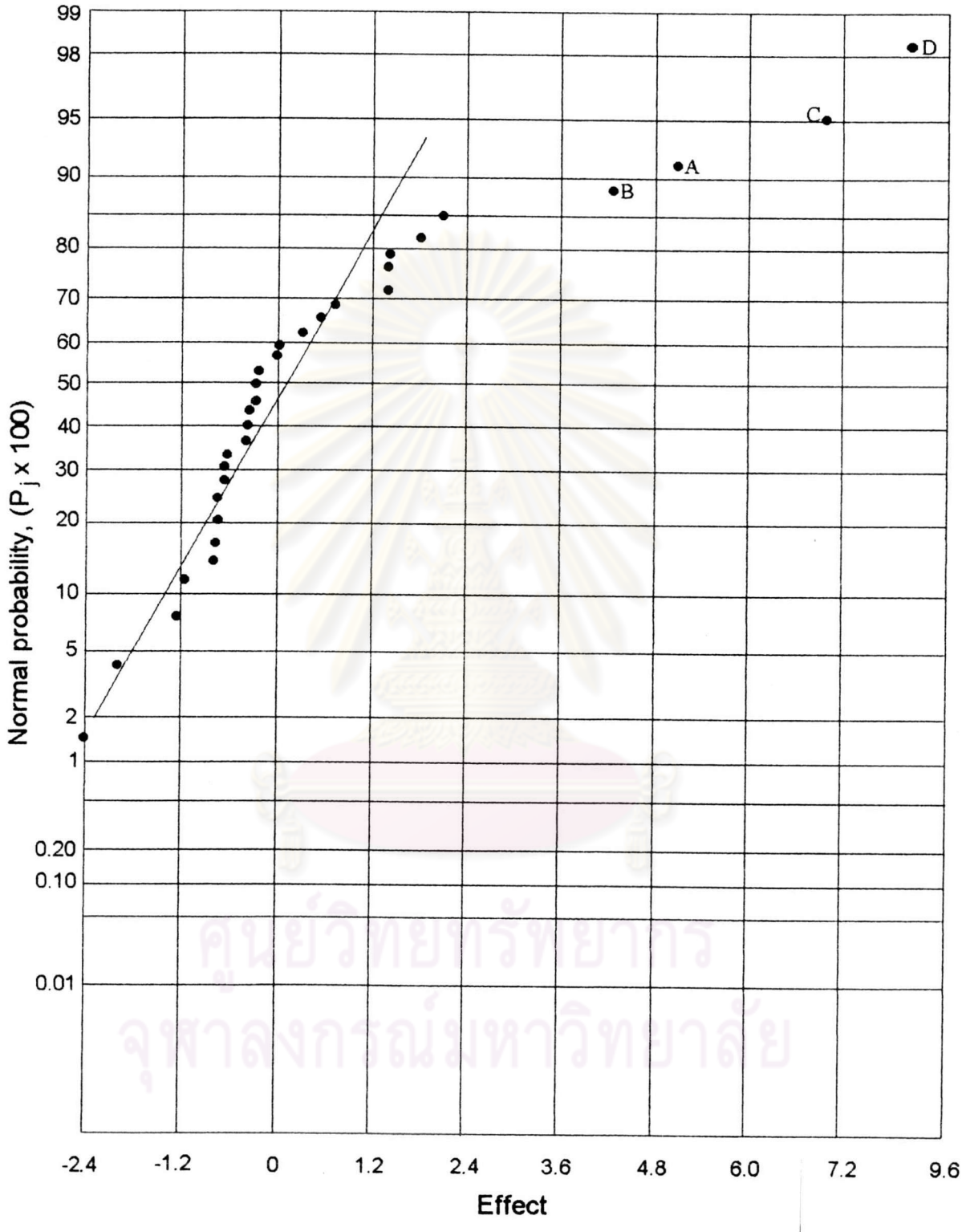

Figure 4.19: The normal probability cumulative plot of heat deflection temperature.

The heat deflection temperature of filled-HDPE is shown in Figure 4.20.

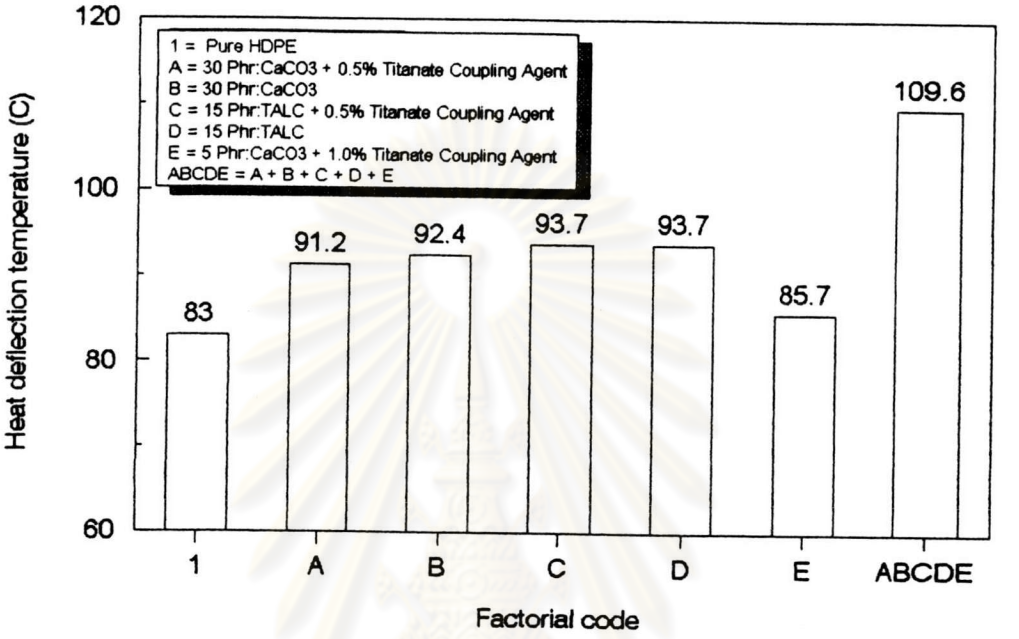

Figure 4.20: The heat deflection temperature of filled-HDPE.

In Figure 4.20, an addition of $CaCO_3$, talc, carbon black and a combination of ABCDE content by 30, 15, 5 and 95 phr increase heat deflection temperature by 10.6, 12.9, 3.2 and 32.0 % respectively.

4.1.7 Glass Transition Temperature

The glass transition temperature of filled-HDPE is shown in Figure 4.21.

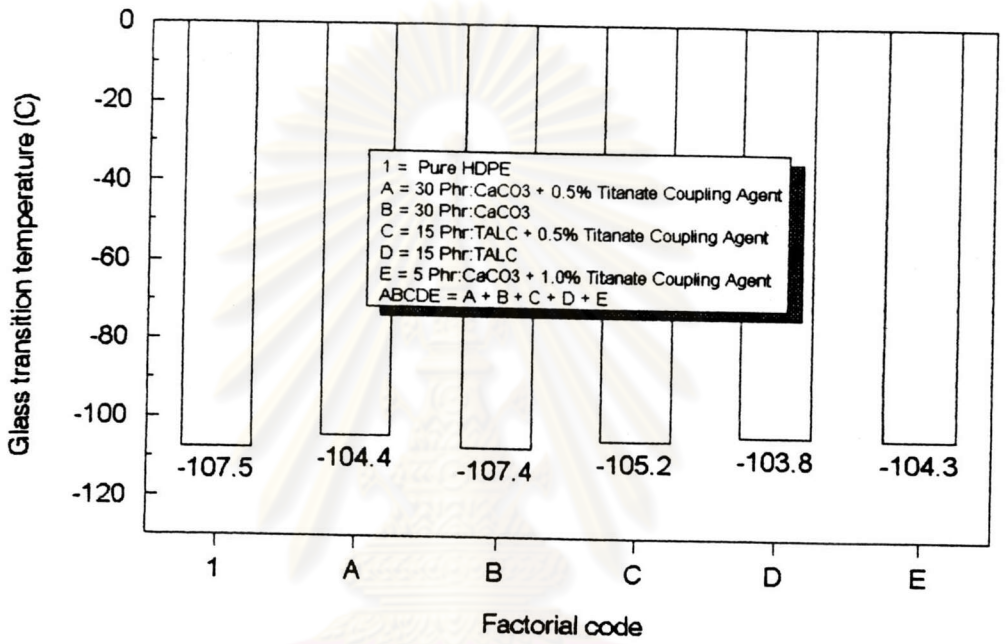

Figure 4.21: The glass transition temperature of filled-HDPE.

In Figure 4.21, an addition of $CaCO_3$, talc, carbon black and a combination of ABCDE content by 30, 15, 5 and 95 phr do not change the glass transition temperature of filled-HDPE.

4.1.8 Density

The density of filled-HDPE is shown in Figure 4.22.

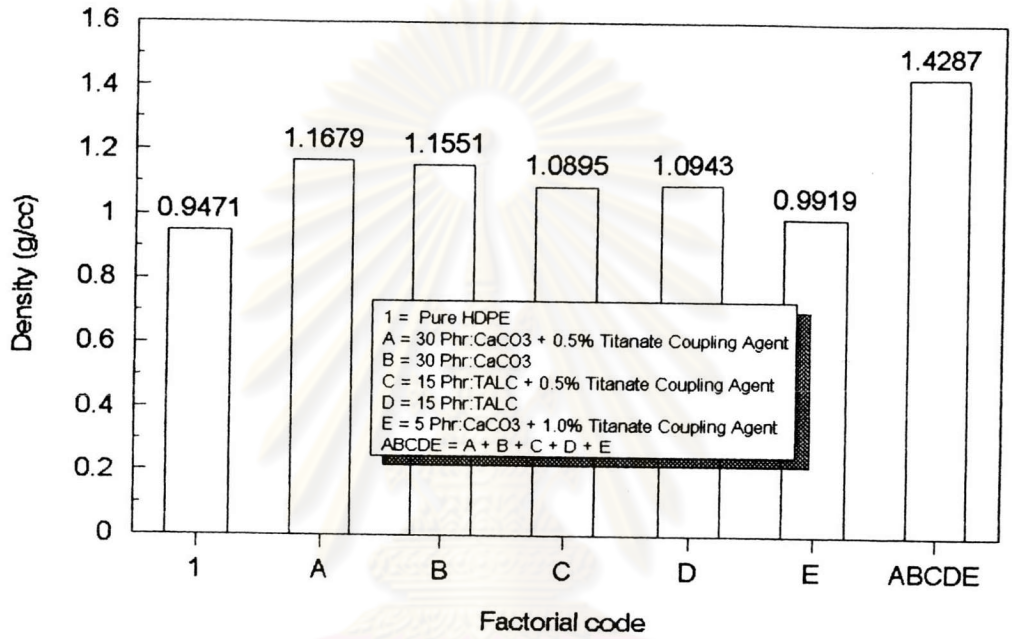

Figure 4.22: The density of filled-HDPE.

In Figure 4.22, an addition of $CaCO_3$, talc, carbon black and a combination of ABCDE content by 30, 15, 5 and 95 phr increase density by 22.6, 15.3, 4.7 and 50.8 % respectively.

4.2 Mixing

A plot of torque and melting temperature against the time of mixing was obtained for the HDPE composites of all compositions. A sample of the plots of the torque required for mixing over the mixing periods of 10 is shown in Figure 4.23. The record was done by using the Mixer Evaluation Software installed in the computer interfaced with the mixer. Peak torque appears directly after charging the sample which was initially cold and unmelted. The mixing torque is high but it gradually decreases as the HDPE melts. The mixing torque eventually becomes stable after mixing for approximately 3 min.

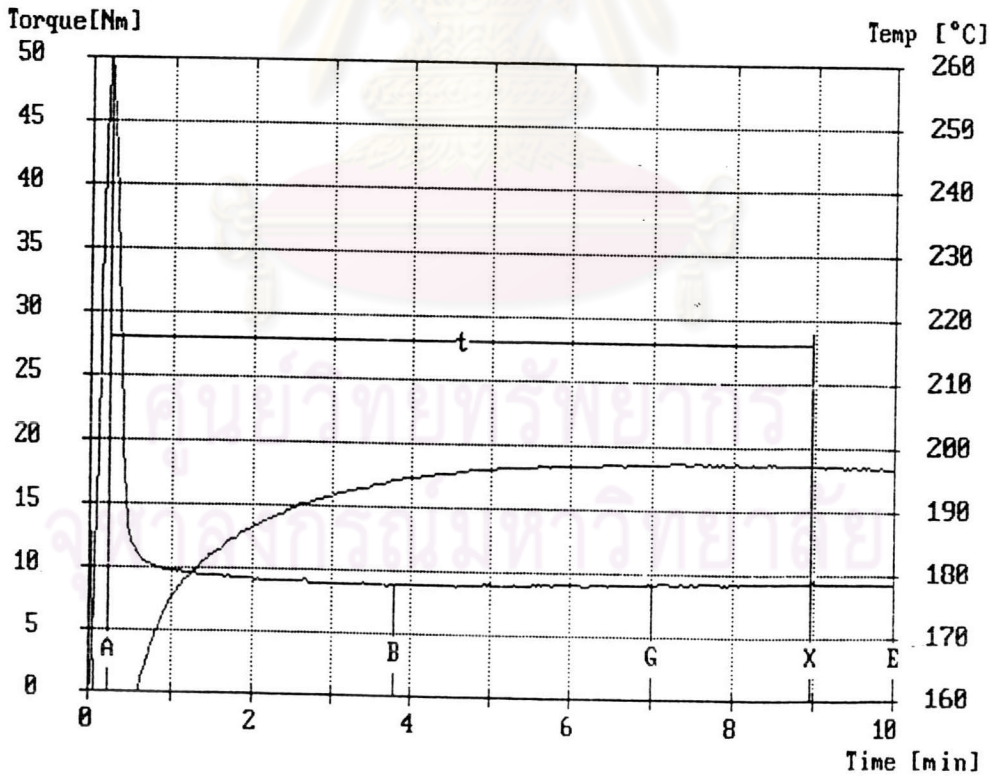

Figure 4.23: Torque-time curve during compounding of HDPE composites.

As the fillers content increases, the mixing torque associated with all samples seen to rise as shown in Figure 4.24. This enhancement is believed to due to the presence of the fillers particles among the HDPE matrix. Hence, the mobility of the molecular chains of HDPE is reduced and thus the flow is limited. With the addition of more fillers particles, a greater amount of energy or torque energy is required for mixing than that associated with the pure HDPE.

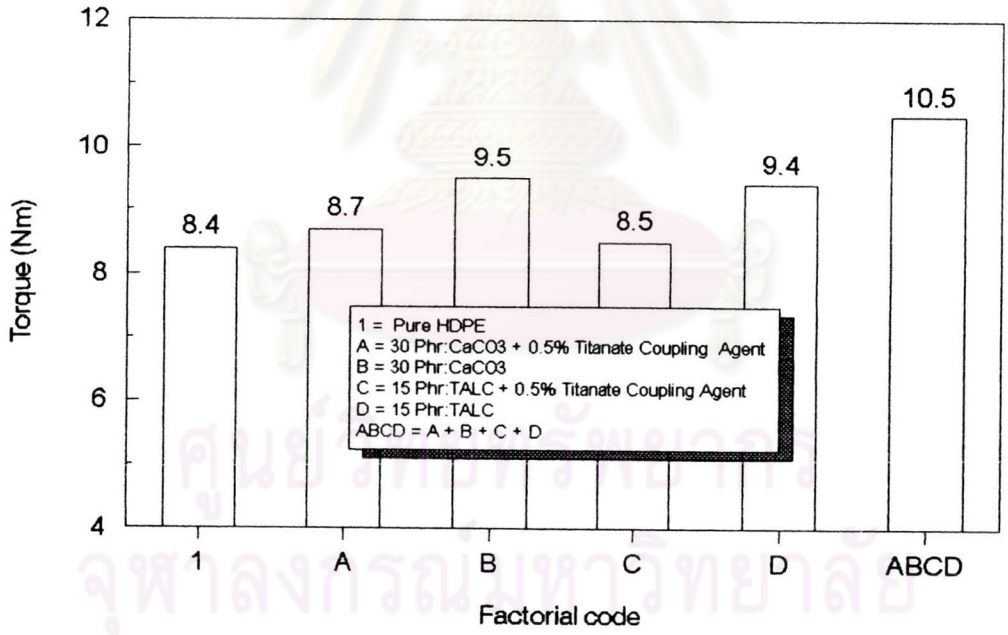

Figure 4.24: The effect of fillers content, coupling agent on torque at 10 min mixing time.

The fillers particles have a tendency tend to form aggregates which are called agglomerates. The agglomeration has a great effect on the mixing properties. As shown in Figure 4.24, the higher torque for untreated $CaCO_3$ (B) and TALC (D) implies that there may have been higher degree of agglomeration of particles than the system with surface treated fillers (A and C), as show in Figures 4.25 to 4.28. The surface treatment of the fillers, i.e. $CaCO_3$ and talc by titanate coupling agent decreases the torque required to the level close to that required for mixing pure HDPE. Hence, it seems that the titanate coupling agent serves as an external lubricant during the mixing process of the HDPE composites. Consequently the flow properties are improved while the energy consumption and machinery wear may be reduced. On an industrial scale, the increase in the flow properties may lead to enhancement in the production rate.

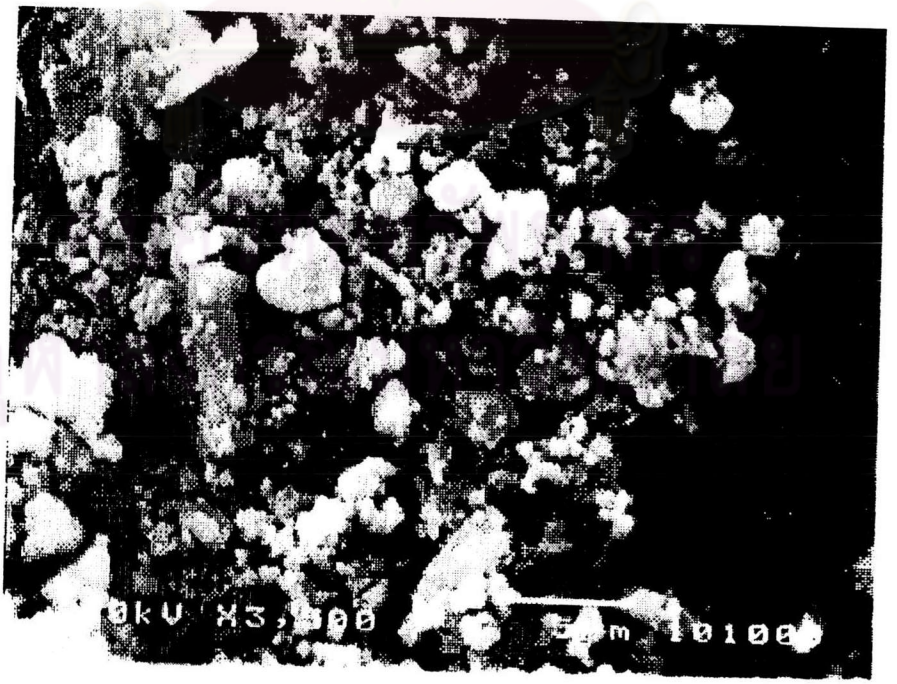

Figure 4.25: Scanning electron micrograph of $CaCO_3$ + 0.5% titanate coupling agent.

Figure 4.26: Scanning electron micrograph of $CaCO_3$ without any coupling agent.

Figure 4.27: Scanning electron micrograph of TALC + 0.5 % titanate coupling agent.

Figure 4.28: Scanning electron micrograph of TALC/without any coupling agent.

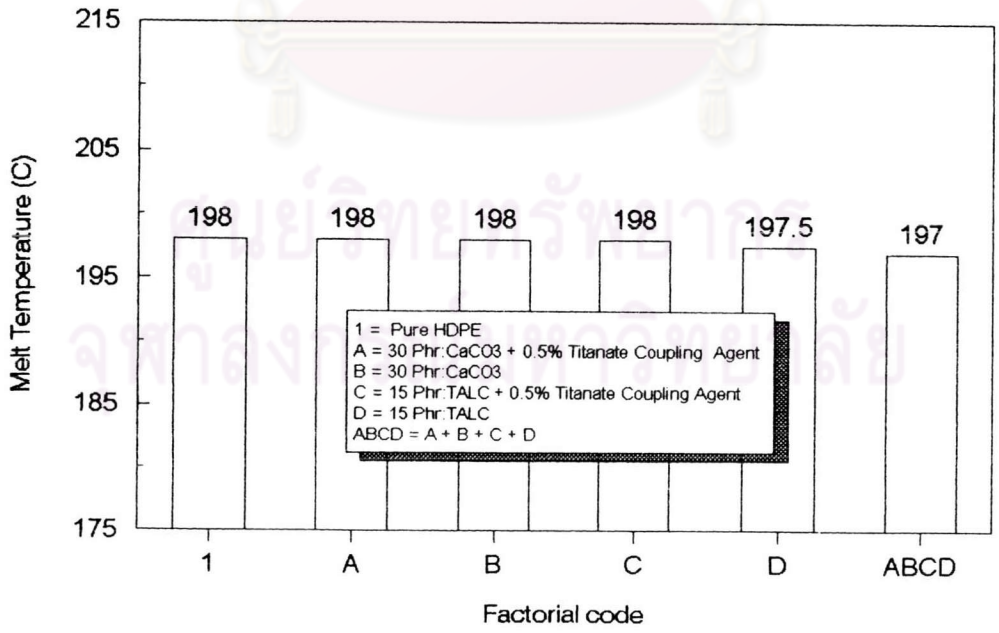

Figure 4.29: The effect of the fillers content and the titanate coupling agent on the melt temperature after mixing for 10 min.

Figure 4.29 shows the melting temperature of unfilled and filled HDPE. The melting temperature remains relatively constant despite the change in the filler content and the presence of a coupling agent in the system. However, the melt temperature of all filled and unfilled HDPE are higher than the set temperature of 190°C. This is because during compounding, there may be a slight enhancement in the temperature due to the high shear stress and the latent heat of fusion of polyethylene .

4.3 Mechanical Properties of $CaCO_3$-filled HDPE

4.3.1 Tensile Test

The tensile stress-strain behavior of pure HDPE and filled HDPE with and without the titanate coupling agents are shown in Figures .4.30 to 4.35. The tensile stress-strain behavior of pure HDPE is a typical one of ductile plastic. The curve shows clearly the extrinsic yield point and the necking which arises due to non-uniform plastic deformation. Pure HDPE has a modulus of elasticity of about 454.8 MPa. The extrinsic yield stress is at the level of 8.25 MPa. The pure HDPE was tested to fracture. The elongation at break is about 1600 %.

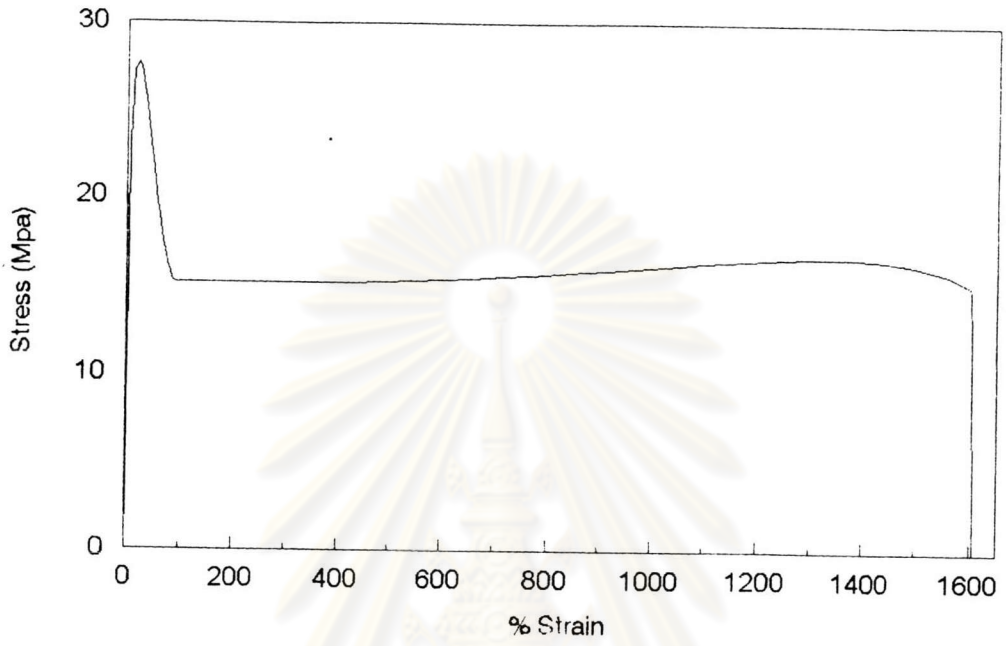

Figure 4.30: Stress-strain curve of pure HDPE.

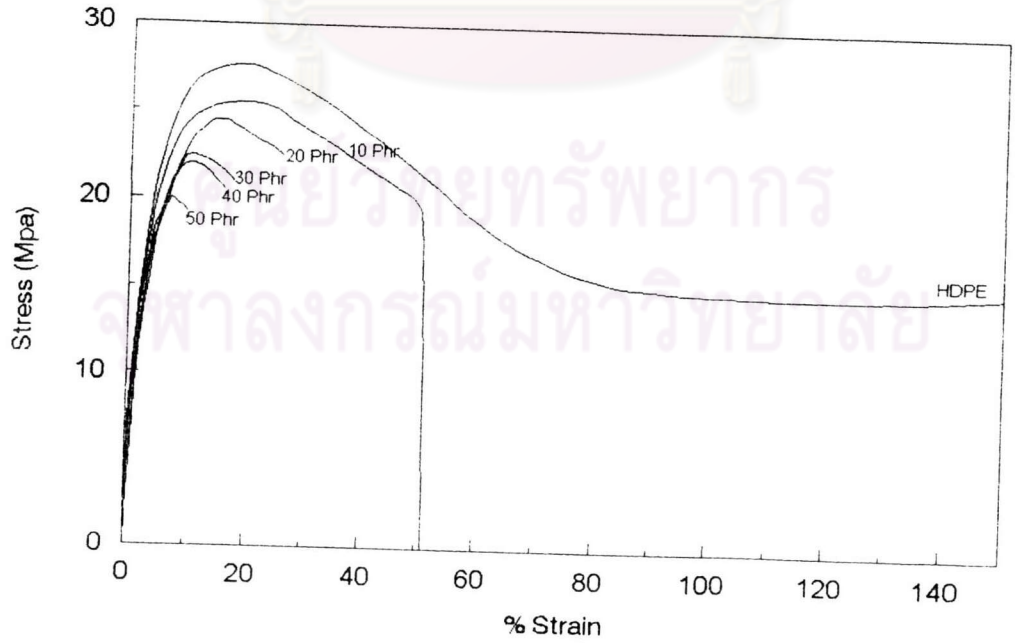

Figure 4.31: Stress-strain curve of HDPE/$CaCO_3$.

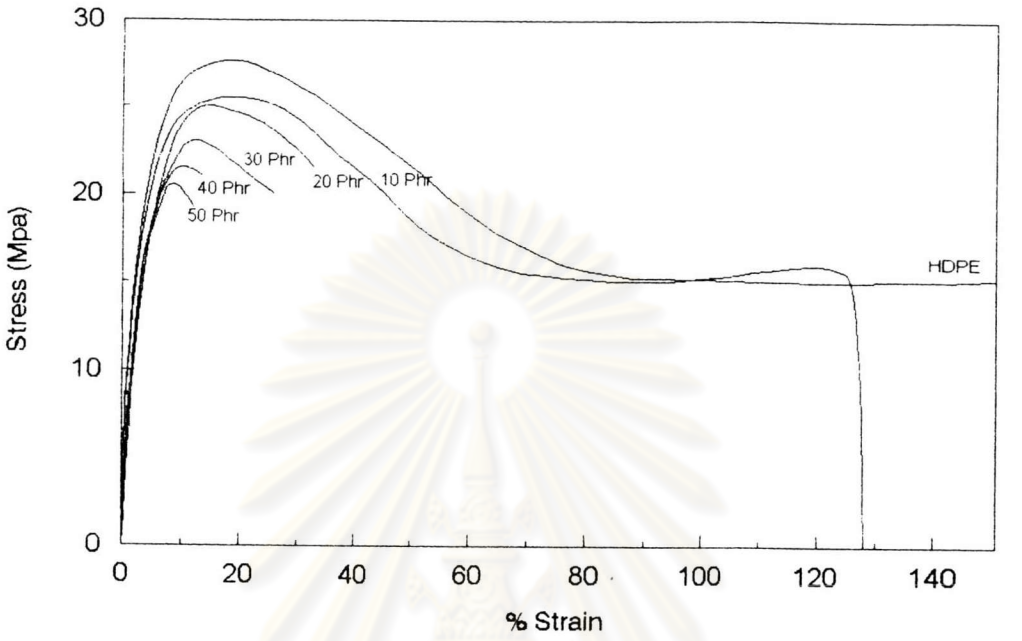

Figure 4.32: Stress-strain curve of HDPE/$CaCO_3$/0.5% titanate coupling agent.

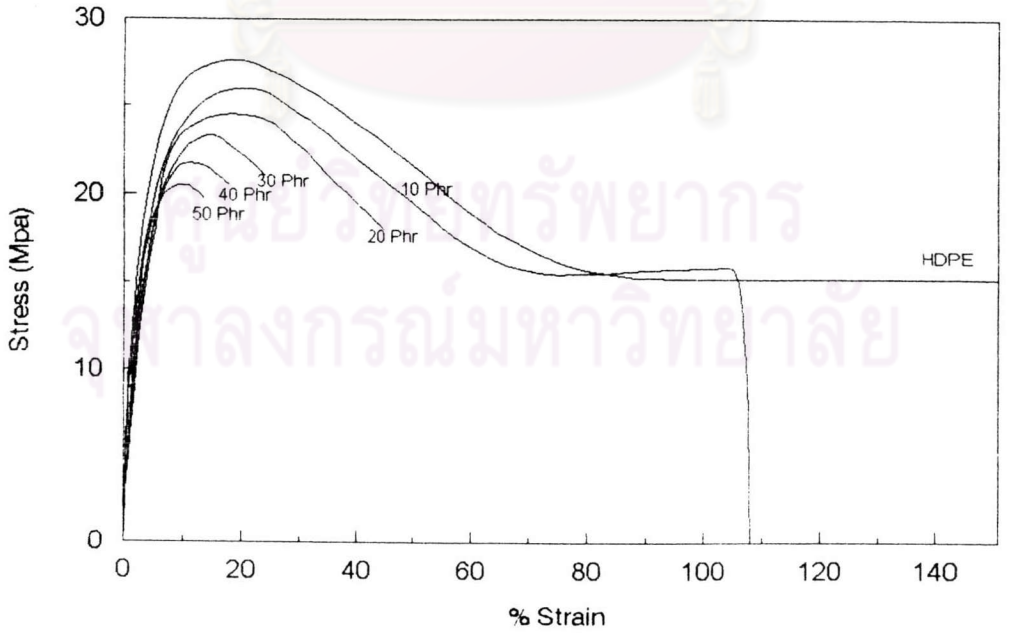

Figure 4.33: Stress-strain curve of HDPE/$CaCO_3$/0.75% titanate coupling agent.

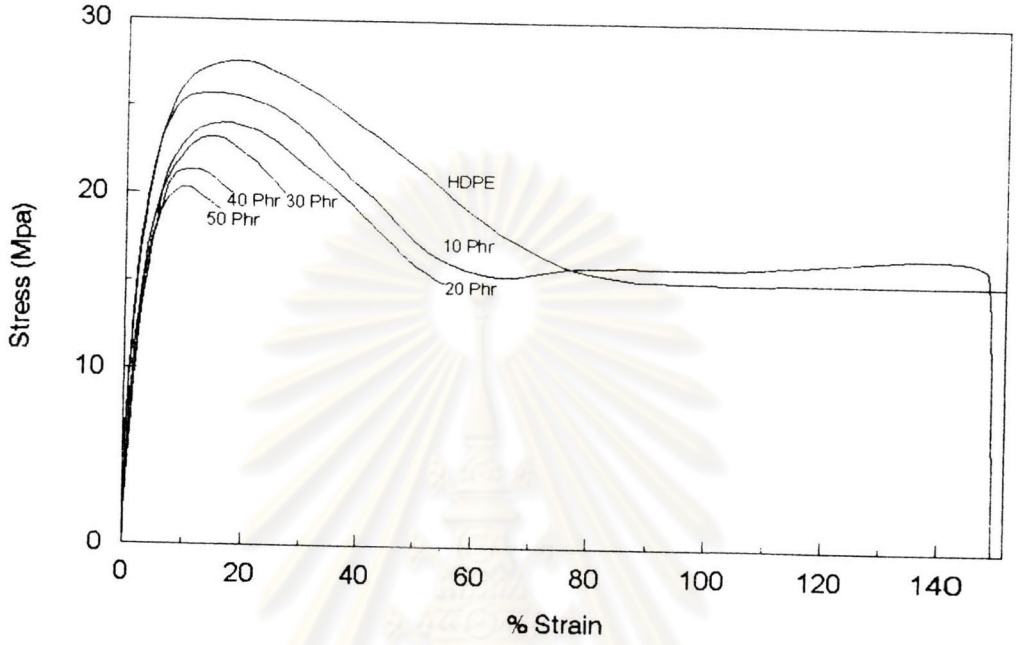

Figure 4.34: Stress-strain curve of HDPE/$CaCO_3$/1.0% titanate coupling agent.

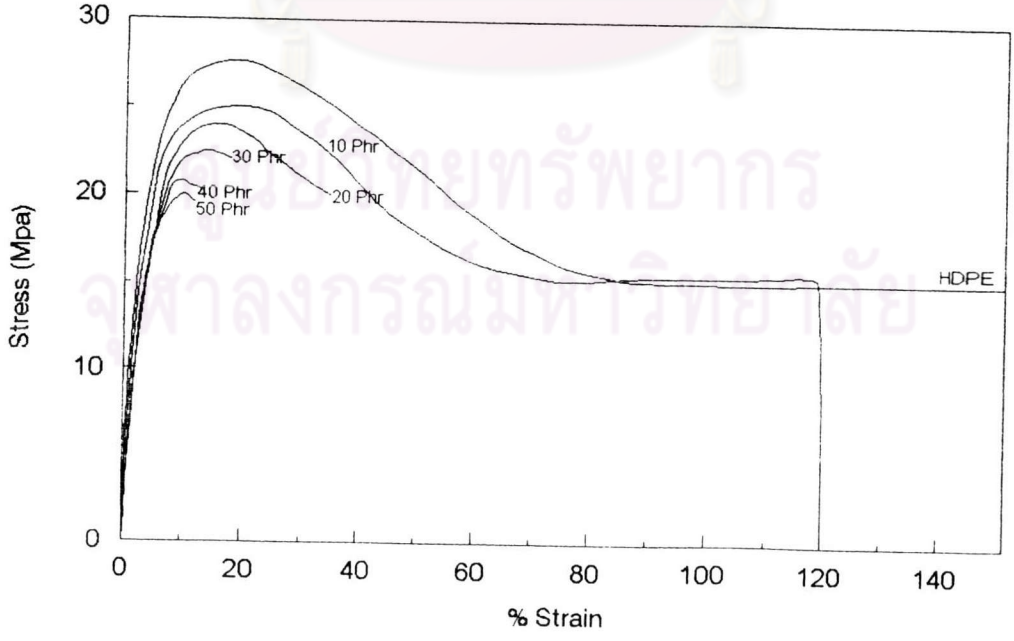

Figure 4.35: Stress-strain curve of HDPE/$CaCO_3$/1.5% titanate coupling agent.

Figures 4.31 to 4.35 show the effect of $CaCO_3$ and titanate coupling agent on the tensile properties. The stress-strain behavior is strongly affected by the $CaCO_3$ content. The fracture strain gradually decreases as the $CaCO_3$ content increases. The stress-strain curve with the lowest amount of $CaCO_3$ at 10 phr, has a ductile manner close to that of the unfilled HDPE. Those with greater content of $CaCO_3$, i.e. more than 10 phr, tend to be brittle. The addition of the titanate coupling are clearly increase the fracture strain for the HDPE with 10 phr $CaCO_3$.

The deformation exhibits by the pure HDPE is believed to be the consequence of the chain mobility induced by the external tensile stress. AT the Hookean's region or the initial portion of the stress-strain curve, the elastic deformation in the HDPE chains arises due to bond stretching. This is shown schematically in Figure 4.36. As the applied stress is increased, the long HDPE chains because uncoiled. This corresponds to the pre-yielding region of the stress-strain curve. Further stretching beyond the yield point, the HDPE chains are permanently deformed due to chain slippage. The yield point is the onset of plastic deformation.

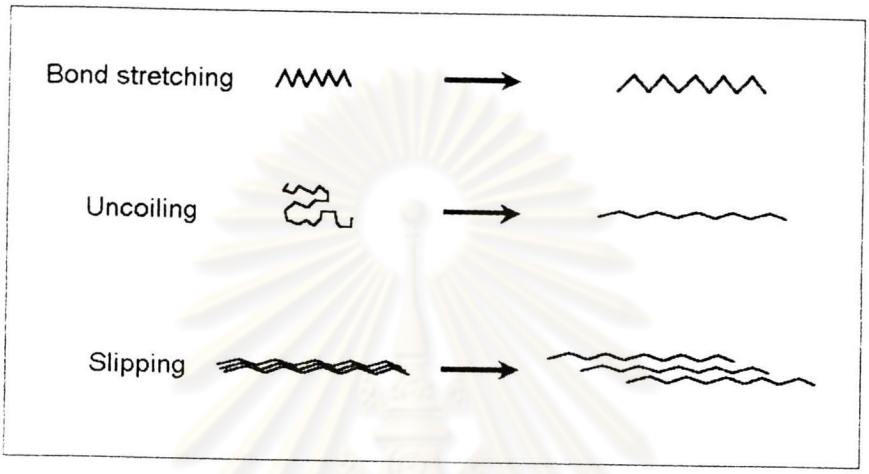

Figure 4.36: The polymer chain deformation of ductile semi-crystalline polymer in the tensile properties.

If the plastic deformation is non-uniform, necking will take place in the tensile specimen. The failure of pure HDPE is clearly a ductile one.

For HDPE and several polymers, after reaching the yield point, the stress drops to a lower yield stress. The tensile specimen begins to decrease locally in width, i.e. necking within the specimen gauge length.

The conventional tensile stress-strain relationship of a polymer is a function of the temperature and the strain rates as shown in Figure 4.37.

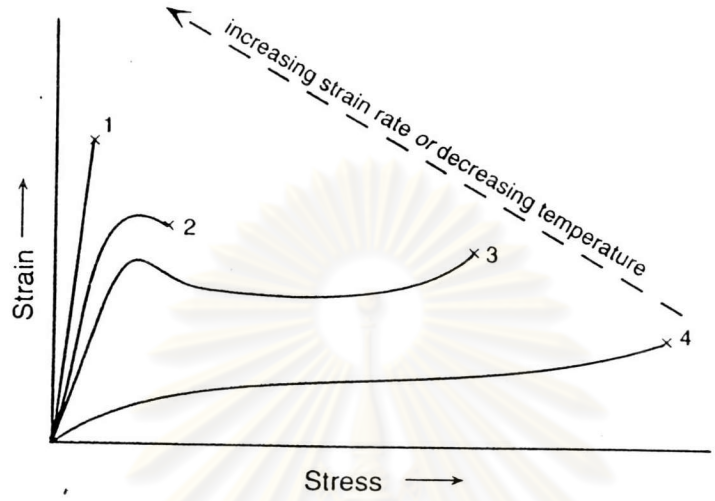

Figure 4.37: Typical stress-strain curves of polymers.

Increasing the strain rates has a similar effect to decreasing the temperature of testing. Inevitably, both factors have a significant effect on the failure behavior of the polymers from ductile to brittle fracture of the polymers. Both the stress and the strain are affected.

The results studies by S. Matsuoka [64] on the tensile behavior of polyethylene truly support the above theory. Their studies were summarized in the plot as shown in Figure 4.38.

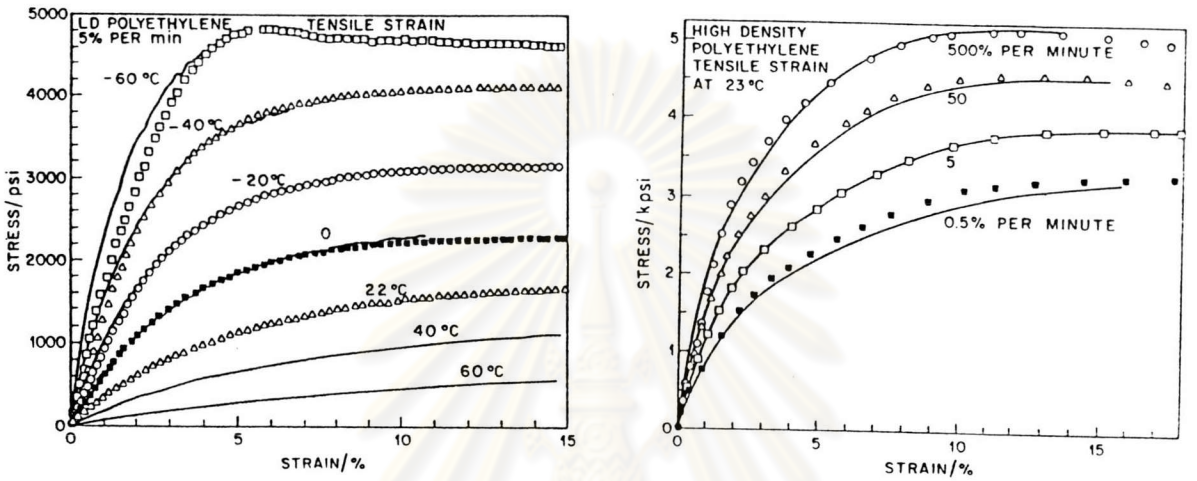

(a) (b)

Figure 4.38: Effect of (a) temperature and (b) strain rates for the tensile properties of polyethylene.

The strain rate selected for the present test is 5 mm/min. This corresponds to the minimum rate specified in the ASTM D-638.

For HDPE and several polymers, after reaching yield point, the stress drops to a lower yield stress or draw stress. The tensile specimen begins to decrease locally in width, i.e. necking within the specimen gauge length. Further, the cross-section area of necking does not change and neck propagates along the length of the gauge length until the sample finally breaks.

The process of neck propagation of HDPE occurs between above glass transition temperature of -105.5°C and the melting point temperature of 127°C. This is also called cold drawing. The mechanism of necking usually occurs at the chain folded lamellae within the spherulite in the HDPE. When HDPE specimens are stretched by uniaxial stress, the lamellae slip rigidly past one another and align in the direction of the applied stress. Microscopic change of the chains and their alignment during the formation of necking is shown schematically in Figure 4.39.

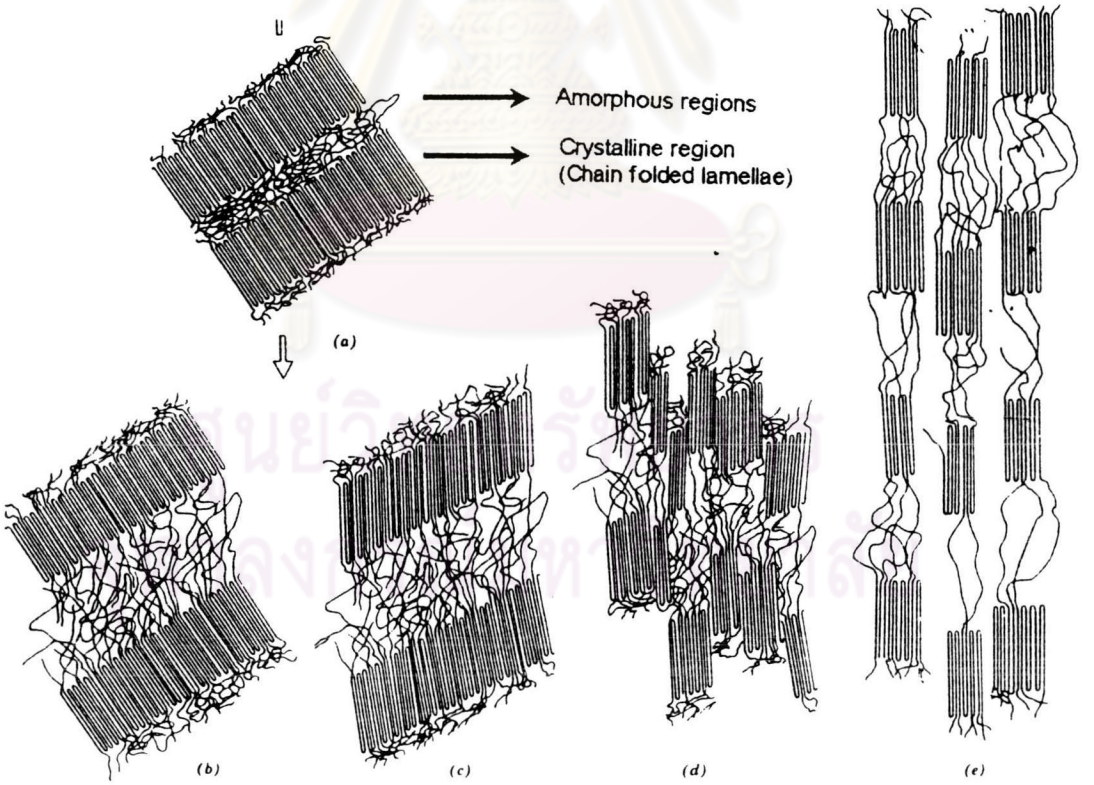

Figure 4.39: Steps in the deformation during necking of crystalline region of HDPE.

The tensile properties are calculated in term of the stress at yield, % strain at yield, modulus of elasticity, the maximum stress, the stress at break, the strain at break and the energy required to break the specimens.

The yield point of polymers usually define as an increasing of strain without any increasing of stress. The HDPE composite with high filler content does not have a clear yield point. Hence, a 0.2 % offset yield stress is reported in the present study. In the cause of the modulus of elasticity, the 2 % secant modulus will be estimated.

The area under the stress-strain curve is proportional to the energy required to break the HDPE.

The effect of the $CaCO_3$ content and the titanate coupling agent concentrations on the modulus of the $CaCO_3$-filled HDPE is shown in Figure 4.40.

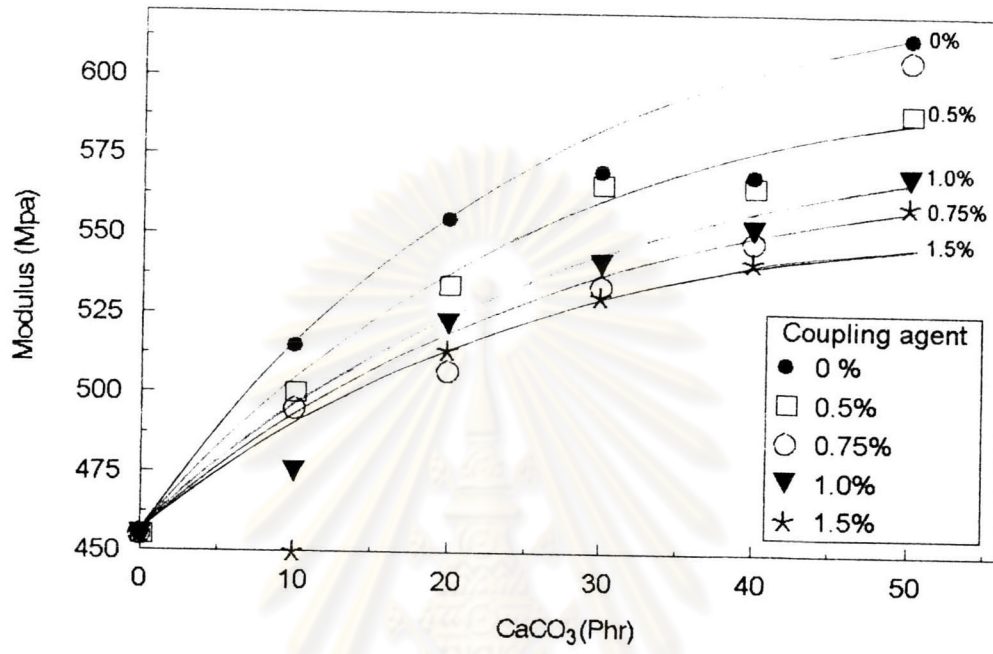

Figure 4.40: The modulus of the unfilled and $CaCO_3$-filled HDPE, with and without the titanate coupling agent.

In Figure 4.40, for the $CaCO_3$-filled HDPE systems with and without the titanate coupling agent, the modulus of elasticity apparently increases with the $CaCO_3$ content. This may be due to the stiffness imparted by the $CaCO_3$. The incorporation of the titanate coupling agent into the system decreases the modulus of elasticity as compared with the untreated system. The decrease in the modulus of elasticity with increasing concentration of the titanate coupling agent may be attributed to the plasticizing action cause by the titanate coupling agent.

For the untreated $CaCO_3$ system in Figure 4.40, an increase in the $CaCO_3$ content from 10, 20, 30, 40 and 50 phr results in an increase in the

corresponding modulus by 12.8, 22.0, 27.5, 31.4 and 34.8 % respectively in comparison with that of the virgin HDPE.

For the 0.5 % titanate coupling agent treated $CaCO_3$ system in Figure 4.40, an increase in the $CaCO_3$ content from 10, 20, 30, 40 and 50 phr results in an increase in the corresponding modulus by 9.7, 17.8, 23.8, 27.2 and 29.8 % respectively in comparison with that of the virgin HDPE.

For the $CaCO_3$-filled HDPE system with 0.75 % titanate coupling agent, an increase in the $CaCO_3$ content from 10, 20, 30, 40 and 50 phr results in an increase in the corresponding modulus increase by 8.4, 14.6, 19.0, 22.2 and 24.0 % respectively in comparison with that of the virgin HDPE.

For the $CaCO_3$-filled HDPE system with 1.0 % titanate coupling agent, an increase in the $CaCO_3$ content from 10, 20, 30, 40 and 50 phr results in an increase in the corresponding modulus increase by 7.3, 13.0, 17.6, 20.7 and 22.2 % respectively in comparison with that of the virgin HDPE.

For the $CaCO_3$-filled HDPE system with 1.5 % titanate coupling agent, an increase in the $CaCO_3$ content from 10, 20, 30, 40 and 50 phr results in an increase in the corresponding modulus increase by 6.8, 12.0, 16.0, 19.1 and 20.7 % respectively in comparison with that of the virgin HDPE.

The sequence of the ability of the titanate coupling agent to decrease the modulus of elasticity is 0.5, 0.75, 1.0 and 1.5 % respectively as shown in Figure 4.40.

The effect of $CaCO_3$ content and the titanate coupling agent concentrations on the yield stress of $CaCO_3$-filled HDPE is shown in Figure 4.41.

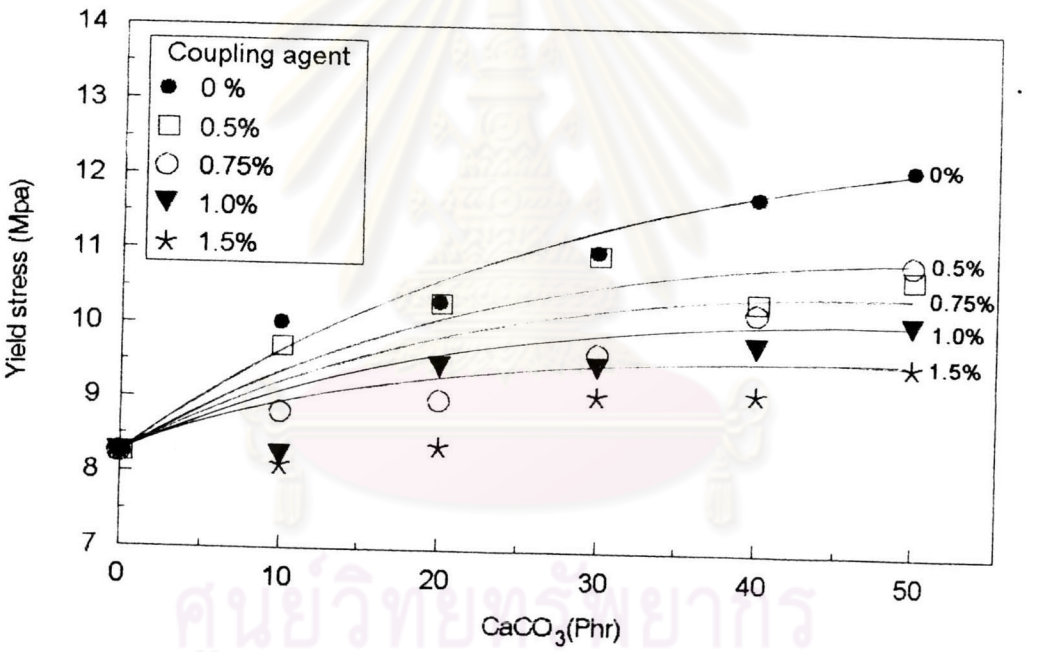

Figure 4.41: The yield stress of $CaCO_3$-filled HDPE, with and without the titanate coupling agent.

In Figure 4.41, for the $CaCO_3$-filled HDPE systems with and without the titanate coupling agent, the appearent of the yield stress increases with the adding of $CaCO_3$ content. This effect may be due to the higher modulus composite than virgin HDPE. The incorporation of

titanate coupling agent into the system decreases yield stress compare with the untreated $CaCO_3$-filled HDPE samples, which may be due to lower modulus of composites

For the untreated $CaCO_3$ system in Figure 4.41, an increase in the $CaCO_3$ content from 10, 20, 30, 40 and 50 phr results in an increase in the corresponding yield stress by 17.1, 28.9, 36.8, 42.4 and 45.4 % respectively in comparison with that of the virgin HDPE.

For the 0.5 % titanate coupling agent treated $CaCO_3$ system in Figure 4.41, an increase in the $CaCO_3$ content from 10, 20, 30, 40 and 50 phr results in an increase in the corresponding yield stress by 11.8, 22.4, 27.5, 30.7, and 32.5 % respectively in comparison with that of the virgin HDPE.

For the $CaCO_3$-filled HDPE system with 0.75 % titanate coupling agent , an increase in the $CaCO_3$ content from 10, 20, 30, 40 and 50 phr results in an increase in the corresponding yield stress by 8.4, 15.1, 19.5, 22.9 and 25.7 % respectively in comparison with that of the virgin HDPE.

For the $CaCO_3$-filled HDPE system with 1.0 % titanate coupling agent, an increase in the $CaCO_3$ content from 10, 20, 30, 40 and 50 phr results in an increase in the corresponding yield stress by 5.0, 10.3, 13.9, 17.1, and 18.9 % respectively in comparison with that of the virgin HDPE.

For the $CaCO_3$-filled HDPE system with 1.5 % titanate coupling agent, an increase in the $CaCO_3$ content from 10, 20, 30, 40 and 50 phr results in an increase in the corresponding yield stress by 3.0, 8.0, 12.4, 12.7 and 13.9 % respectively in comparison with that of the virgin HDPE.

The sequence of the ability of the titanate coupling agent to decrease the yield stress of elasticity is 0.5, 0.75, 1.0 and 1.5 % respectively as shown in Figure 4.41.

The effect of $CaCO_3$ content and the titanate coupling agent concentration on the yield strain of $CaCO_3$-filled HDPE is shown in Figure 4.42.

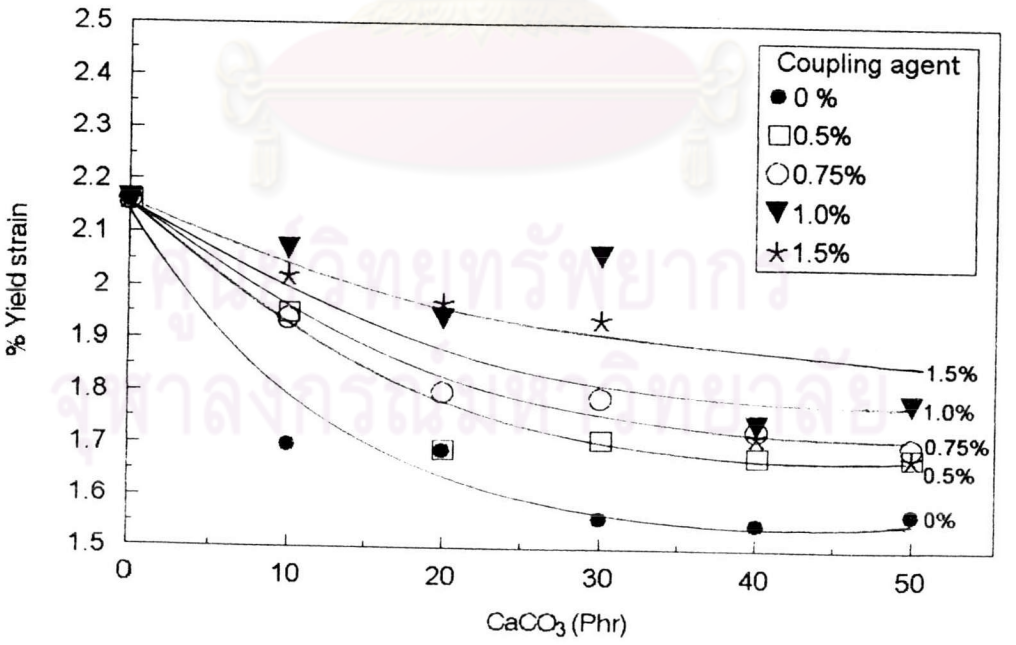

Figure 4.42: The yield strain of $CaCO_3$-filled HDPE, with and without titanate coupling agent.

In Figure 4.42, for the $CaCO_3$-filled HDPE systems with and without titanate coupling agent, the appearent of the yield strain decreases with the adding of $CaCO_3$ content. This effect may be due to the greater elasticity of the HDPE matrix than that of the $CaCO_3$, the deformation of composite Is thus lower than that of the virgin HDPE. The incorporation of the titanate coupling agent into the system increases the yield strain as compared with the untreated $CaCO_3$-filled HDPE. This may be due to may be due to the plasticizing action of titanate coupling agent and lower modulus of composites.

For the untreated $CaCO_3$ system in Figure 4.42, an increase in the $CaCO_3$ content from 10, 20, 30, 40 and 50 phr results in a decrease in the corresponding yield strain decrease by 20.2, 26.6, 28.6, 28.6 and 28.6 % respectively in comparison with that of the virgin HDPE.

For the 0.5 % titanate coupling agent treated $CaCO_3$ system in Figure 4.42, an increase in the $CaCO_3$ content from 10, 20, 30, 40 and 50 phr results in a decrease in the corresponding yield strain by 12.5, 19.5, 22.5, 22.5 and 22.5 % respectively in comparison with that of the virgin HDPE.

For the $CaCO_3$-filled HDPE system with 0.75 % titanate coupling agent , an increase in the $CaCO_3$ content from 10, 20, 30, 40 and 50 phr results in a decrease in the corresponding yield strain by 10.2, 16.4, 19.6, 19.6 and 19.6 % respectively in comparison with that of the virgin HDPE.

For the $CaCO_3$-filled HDPE system with 1.0 % titanate coupling agent, an increase in the $CaCO_3$ content from 10, 20, 30, 40 and 50 phr results in a decrease in the corresponding yield strain by 7.6, 12.6, 15.9, 17.5 and 17.5 % respectively in comparison with that of the virgin HDPE.

For the $CaCO_3$-filled HDPE system with 1.5 % titanate coupling agent, an increase in the $CaCO_3$ content from 10, 20, 30, 40 and 50 phr results in a decrease in the corresponding yield strain by 6.0, 10.2, 13.0, 14.3 and 14.3 % respectively in comparison with that of the virgin HDPE.

The sequence of the ability of the titanate coupling agent to increase the yield strain of elasticity is 0.5, 0.75, 1.0 and 1.5 % respectively as shown in Figure 4.42.

The effect of the $CaCO_3$ content and the titanate coupling agent concentration on the maximum stress of the $CaCO_3$-filled HDPE is shown in Figure 4.43.

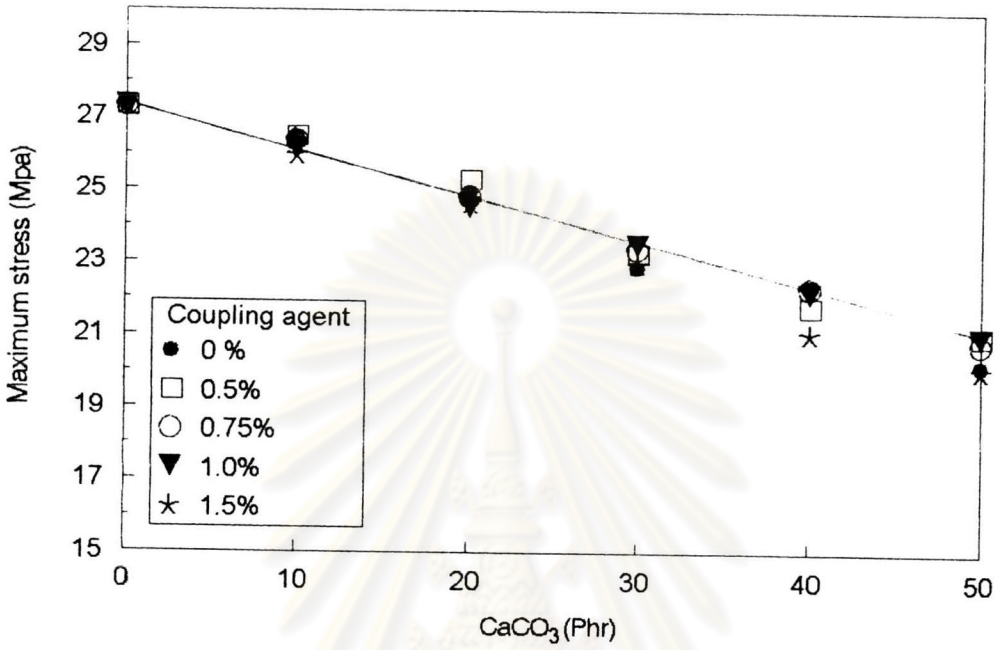

Figure 4.43: The maximum stress of $CaCO_3$-filled HDPE, with and without titanate coupling agent.

In Figure 4.43 for the $CaCO_3$-filled HDPE systems with and without the titanate coupling agent, the maximum stress apparently decreases with the $CaCO_3$ content. Before the maximum stress point is reached, the HDPE chains are uncoiled as shown in Figure 4.36. The increasing $CaCO_3$ content has a tendency to reduce the mass fraction of the HDPE, hence the number of the uncoiling chain during the deformation of the filled-HDPE is less than that of the virgin HDPE. Other possible effect may be due to the presence of the $CaCO_3$ particles which may act as a constraint or barrier to restrict the uncoiling deformability of the HDPE matrix. The maximum stress of the $CaCO_3$-filled HDPE is reduced with the $CaCO_3$ content as show in Figure 4.31 to Figure 4.35. It is obvious

from the plot in Figure 4.43 that the presence of the titanate coupling agent does not have any effect on the maximum stress of the $CaCO_3$-filled HDPE.

For the $CaCO_3$-filled HDPE systems with and without titanate coupling agent in Figure 4.43, an increase in the $CaCO_3$ content from 10, 20, 30, 40 and 50 phr, decreases the maximum stress by 3.7, 9.0, 15.0, 19.6 and 24.4 % respectively in comparison with that of the virgin HDPE.

The effect of the $CaCO_3$ content and the titanate coupling agent concentration on the fracture strain of the $CaCO_3$-filled HDPE is shown in Figure 4.44.

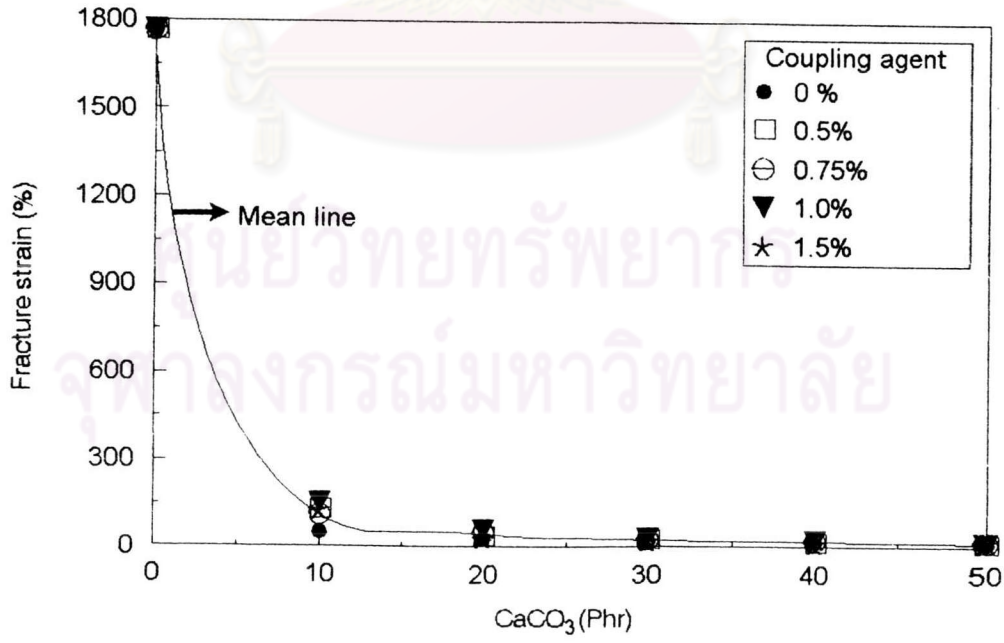

Figure 4.44: The fracture strain of $CaCO_3$-filled HDPE, with and without the titanate coupling agent.

For the $CaCO_3$-filled HDPE systems with and without titanate coupling agent in Figure 4.44, the fracture strain greatly decreases by 93.69 % when $CaCO_3$ content was added by 10 phr. Beyond 10 phr concentration, the fracture strain is approximately constant. The mechanism of the pure or unfilled HDPE is that the chains deform abundantly chain slipping and necking by before fracture takes place in a ductile manner as show in Figures 4.36. The incorporation of the $CaCO_3$ content decreases the fracture strain. This may be due the restriction on the slipping deformability of the HDPE matrix brought about by the $CaCO_3$ particles. The fracture strain of the $CaCO_3$-filled HDPE are reduced with the $CaCO_3$ content as show in the stress-strain curve of Figures 4.31 to 4.35.

Crack during necking of a ductile filled-polymer may be due to the voids developed around the fillers. To observe the voids, the drawn region of the tensile tested filled-HDPE was fractured cryogenically in the direction parallel to the draw direction as shown in Figure 4.45.

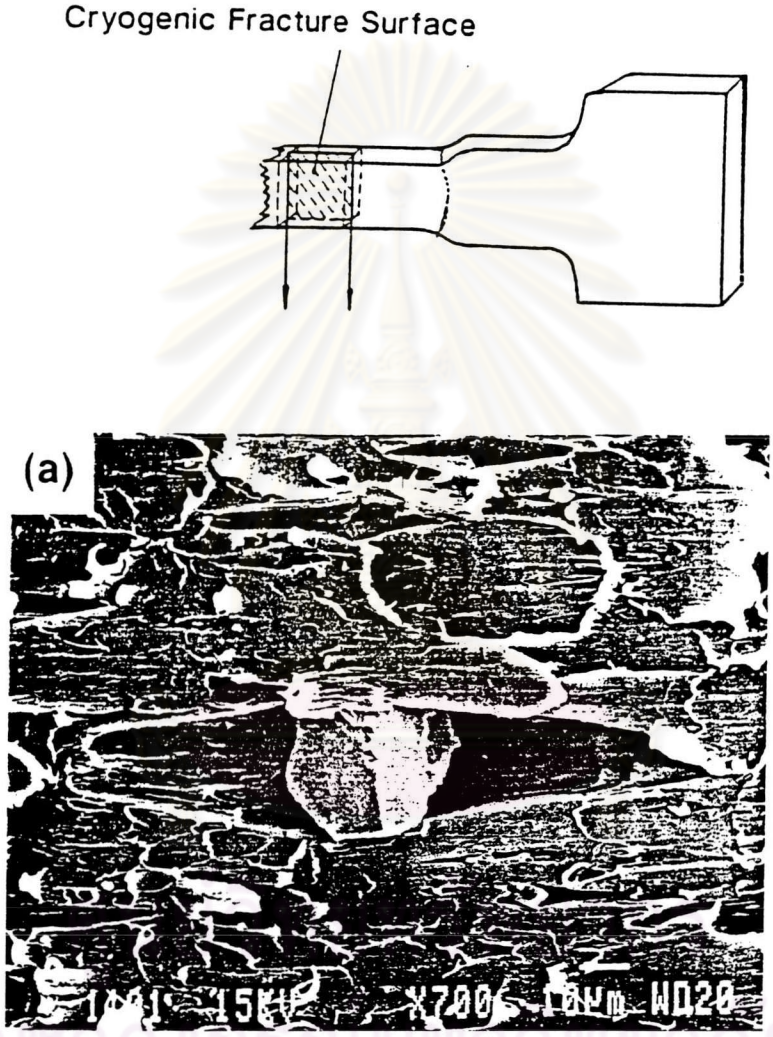

Figure 4.45: SEM micrograph of the neck region of a filled-ductile polymer.

The filler particles of Figure 4.45 are assumed to be spherical of uniform size and arrayed in a cubic lattice as shown in Figure 4.46.

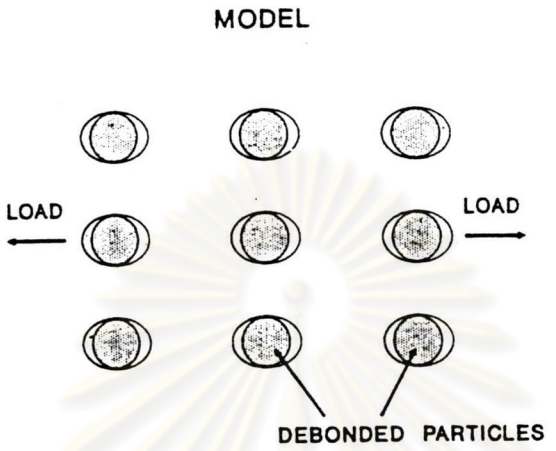

Figure 4.46: The model of voiding in necking region of filled-ductile polymer.

For filled-ductile polymer, these are 5 modes of tensile failure as shown in Figure 4.47. Each is differentiated by the corresponding fracture strain and is very much dependent on the filler content. The five modes of fracture were observed by Hiltner [35 - 37] who proposed the schematic model as shown in Figure 4.47 to the brittle manner when the filler content increases as shown in Mode E. The fracture gradually changed from the ductile manner of pure HDPE as shown in Mode A to the brittle manner when the filler content increased as shown in Mode E. The ductile behavior pure HDPE and very low filler content fractured during strain-hardening (Mode A) and during neck propagation (Mode B). As the filler content increases, quasi-brittle fracture occurred during neck formation (Mode C and D). Mode C fracture occurred through the thinned region at the site of incipient neck formation. In Mode D, the

specimens fractured shortly after the maximum stress. In Mode E, specimens fractured in a brittle manner perpendicular to the loading direction before reaching the maximum point.

In the present study, pure HDPE was found to exhibit much ductility prior to its fracture. Filled HDPE was found to undergo less tensile deformation as the filler content is increased. The greater the amount of the filler content, the closer is the filled HDPE behavior forwards the brittle fracture. However, the shift in the fracture pattern from Mode A towards Mode E as the filler becomes greater.

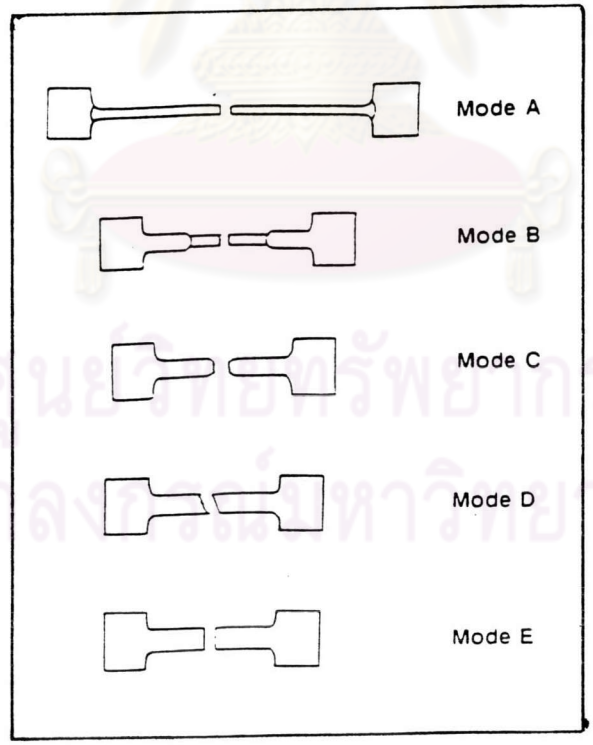

Figure 4.47: Schematic representation of the five tensile fracture modes.

Mode A fracture behavior was observed in the 10 phr $CaCO_3$-filled HDPE with prior surface treatment by titanate coupling agent on the $CaCO_3$ particles. The microscopic process detail of Mode A fracture which is observed when only a small amount of filler particles was added is schematically represented in Figure 4.48. The filler particles is debonded from the HDPE matrix during yielding. As a result, voids are formulated around the particles as the HDPE matrix is plastically deformed during neck propagation. The width of the ligaments between the particles is decreased during neck propagation while the width of the void remains constant and equals to the particle diameter. Because of the low filler content, the ligament between the voids is thick enough that they could undergo thinning during necking without fracturing. Mode A fracture surface consisted of two regions: a pullout region of the slower crack growth and a rosette region of the faster crack growth.

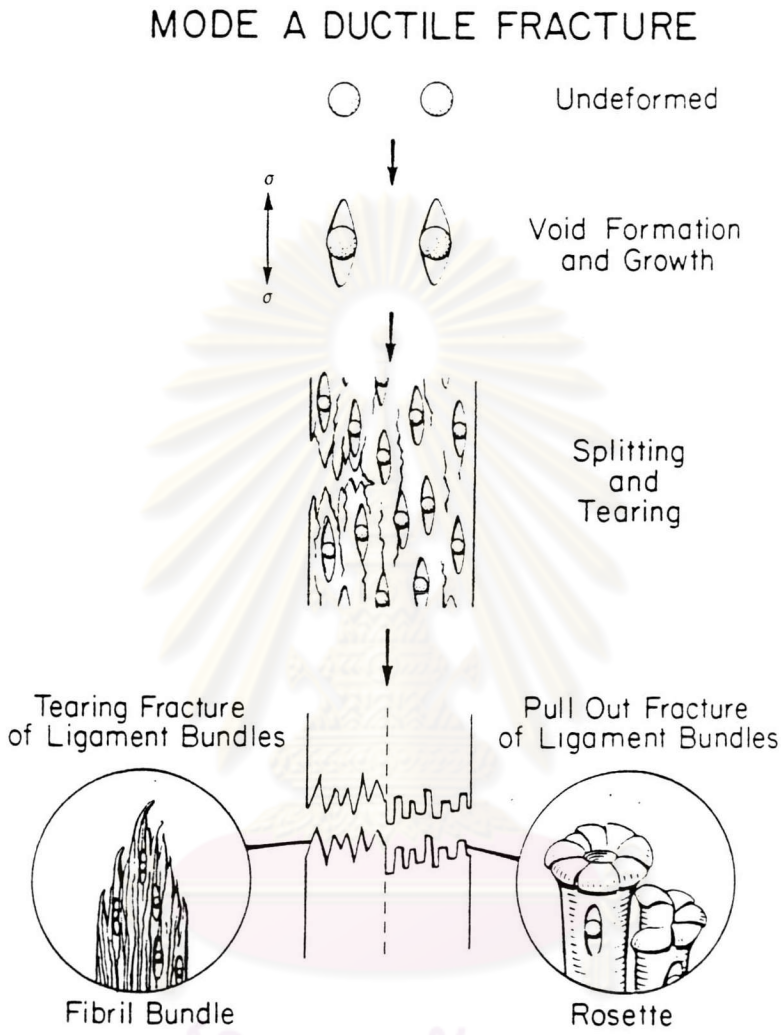

Figure 4.48: Schematic representation of Mode A fracture.

Mode B fracture behavior was observed in the 20 phr $CaCO_3$-filled HDPE with prior surface treatment by titanate coupling agent on the $CaCO_3$ particles. The microscopic process detail of Mode B fracture is shown schematically in Figure 4.49. The greater filler content means that the fillers particles are closer than those in Mode A. The ligaments between the particles are also thinner but they are still thick enough to extend during necking without fracturing. Upon stretching, the elongated

voids coalesce longitudinally. Hence, the resulting longitudinal cracks are longer and more numerous than those in Mode A. In some places, especially where the filler particles are not well dispersed, the ligaments are sometimes thin enough that necking causes these thin ligaments to fracture. Mode B fracture contains only a ductile pullout texture.

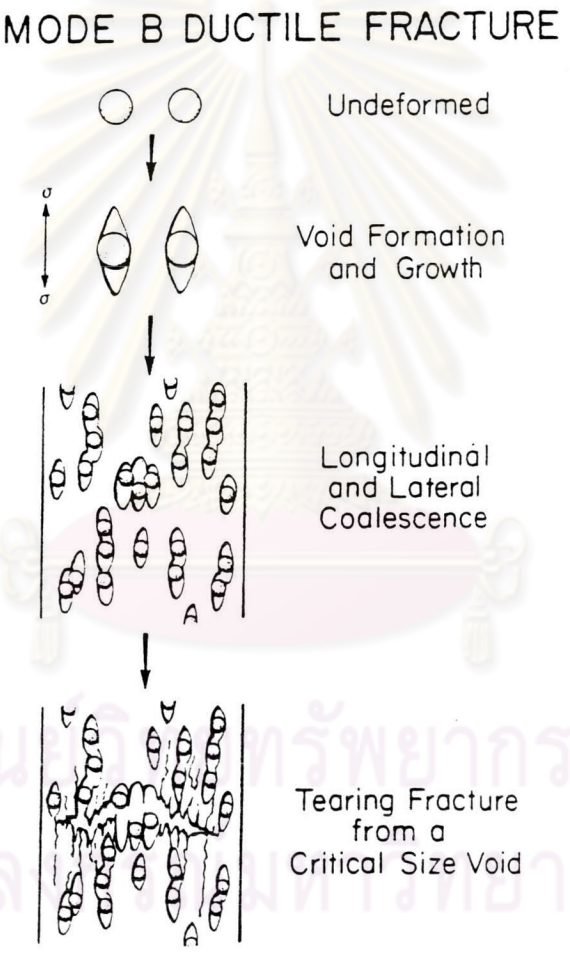

Figure 4.49: Schematic representation of Mode B fracture.

Mode C fracture behavior was observed in the 30 phr $CaCO_3$-filled HDPE with prior surface treatment by titanate coupling agent on the $CaCO_3$ particles. The microscopic Mode C fracture is presented

schematically in Figure 4.50. With even greater concentration of the filler, the fillers particles are close enough to each other that when global or macroscopic necking starts the high local stress concentration on the thin ligaments between the fillers particles can produce local necking with a large extension. When the thin ligaments are not able to support the load, they will fracture and the voids can coalesce laterally. Mode C fracture surface exhibits secondary fracture features that sometimes include the herringbone pattern.

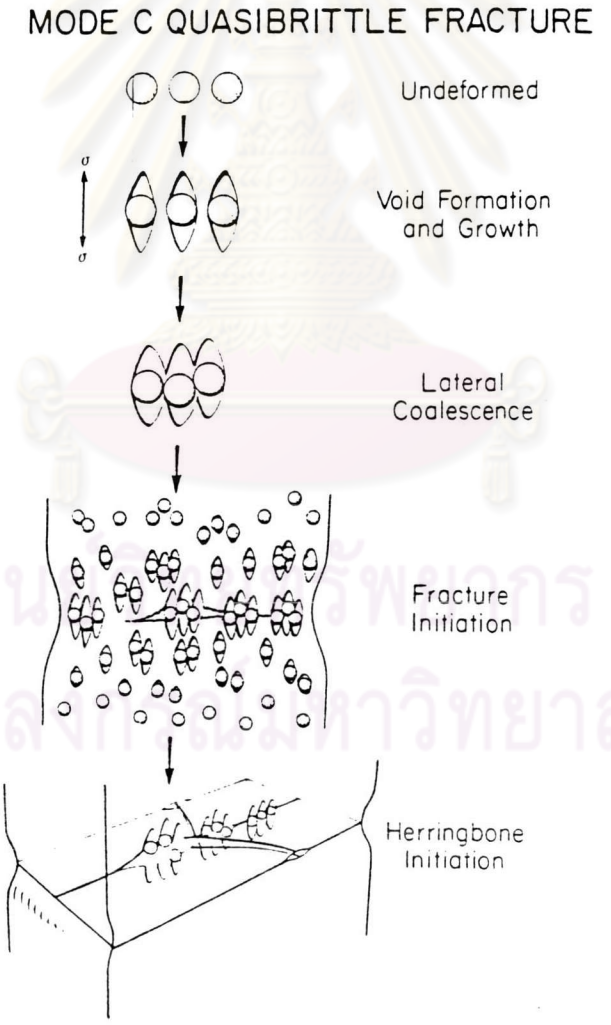

Figure 4.50: Schematic representation of Mode C fracture.

Mode D fracture behavior was observed in the 40 phr $CaCO_3$-filled HDPE with prior surface treatment by titanate coupling agent on the $CaCO_3$ particles. Mode D fracture process is schematically represented in Figure 4.51. Yielding occurs and it is observed as the formation of a macro-shearband. Within the macro-shearband, thin ligaments between the debonded filler particles are highly drawn. Tearing fracture of the ligaments occurs as the crack propagates through the macro-shearband. As a result a dimple pattern is left as a remnant on the surface. The size and the shape of the dimples are determined by the filler while the depth of dimples reflects the amount of plastic deformation in the ligaments before they fracture. The dimples becomes increasingly shallow as the crack accelerates until there is a change to brittle fracture. Mode D fracture surface consisted of a stress-whitened dimple region and a brittle fracture region.

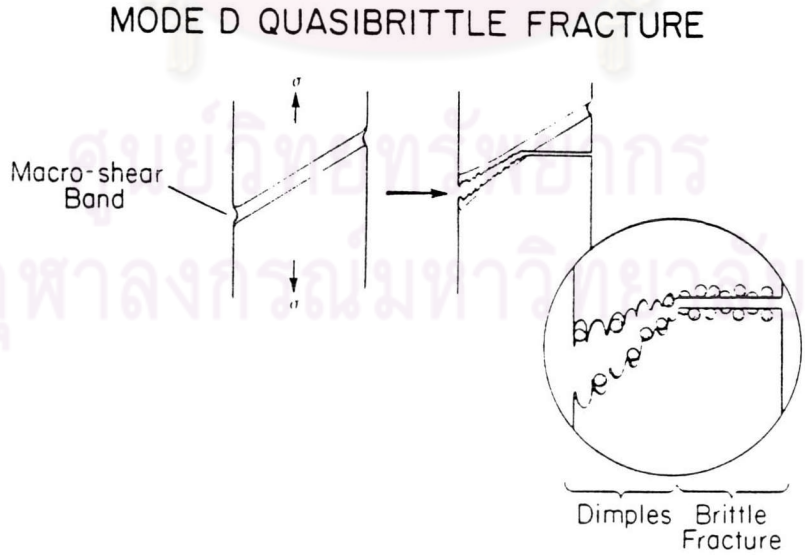

Figure 4.51: Schematic representation of Mode D fracture.

Mode E fracture behavior was observed in the 50 phr $CaCO_3$-filled HDPE with prior surface treatment by titanate coupling agent on the $CaCO_3$ particles. Mode E fracture surface exhibits primarily the rough texture characteristic of brittle fracture.

The fracture mode and the fracture strain can be summarized with an increase in the filler content as shown in Figure 4.52.

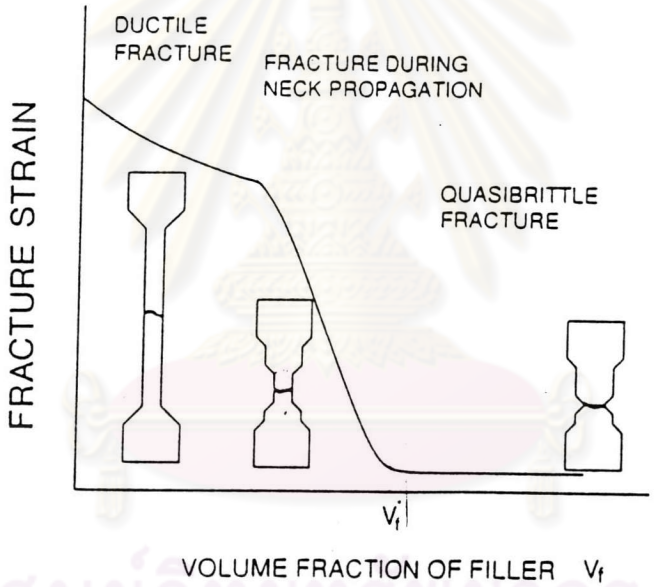

Figure 4.52: The effect of the filler content on the fracture strain of filled-HDPE.

In Figure 4.52, three fracture modes are distinguished. At low filler content, the fracture is ductile with the propagation of the neck throughout the entire gauge length of the specimen. Filler-HDPE with intermediate filler content fails during neck propagation. This fracture mode is the transition between the ductile and the Quasi-brittle fracture modes. With

the highest filler content, the fracture occurs during the formation of the neck without necking propagation.

The titanate coupling agent when applied at concentration ranges from 0.5 to 1.5 % can improve the fracture strain as shown in the plot in Figure 4.53.

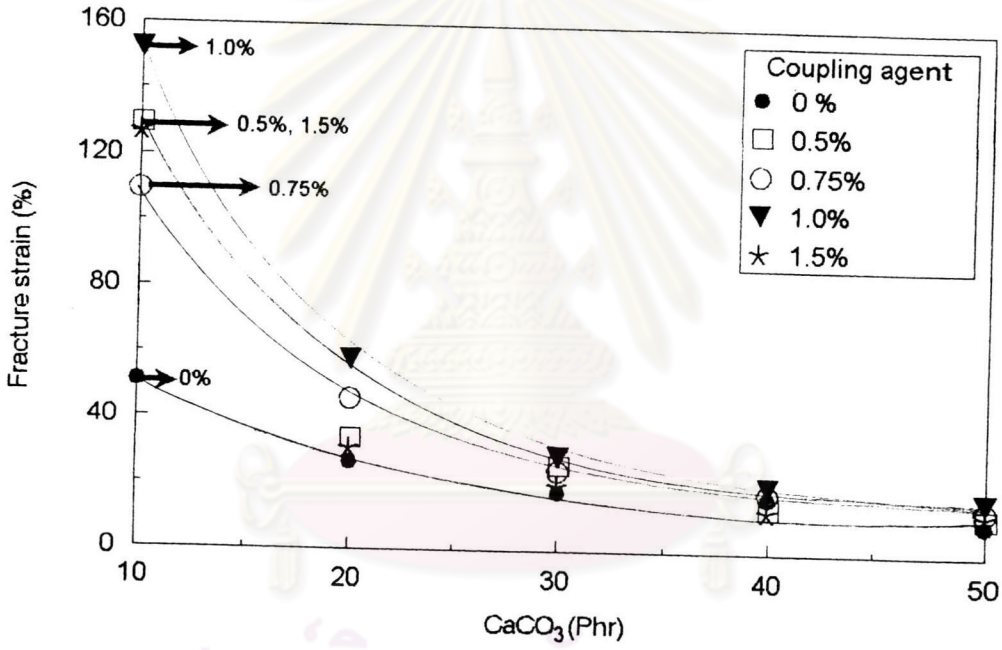

Figure 4.53: The fracture strain with and without the titanate coupling agent of $CaCO_3$-filled HDPE.

For the untreated $CaCO_3$ system in Figure 4.53, an increase in the $CaCO_3$ content from 10, 20, 30, 40 and 50 phr decrease the corresponding fracture strain by 97.0, 98.0, 99.0, 99.3 and 99.4 % respectively in comparison with that of the virgin HDPE.

The incorporation of the titanate coupling agent is believed to have improve of the bonding between the interface of the $CaCO_3$ particles and the HDPE matrix because of the increase in the fracture strain. This effect is clearly seen at the lower concentration of $CaCO_3$ content such as 10 and 20 phr in which crack occurs during necking deformation. With $CaCO_3$ concentration from 20-50 phr, the fracture takes place before necking or sometimes it happens even before yielding.

The mechanism responsible for the improved bonding between the HDPE and the $CaCO_3$-filled interface is believed to be due to the necking of the filled-HDPE at the lower $CaCO_3$ content as shown in Figure 4.45. Within the neck, the interface of the HDPE-$CaCO_3$ is separated and voids are formed as shown in Figure 4.46. The addition of the titanate coupling agent seem to be able to prevent voiding or the small cavity around filler particle. Consequently, the amount of necking deformation is enhanced.

For the 0.5 % titanate coupling agent treated $CaCO_3$ system in Figure 4.53, an increase in the $CaCO_3$ content from 10, 20, 30, 40 and 50 phr increases the corresponding fracture strain by 150, 93.8, 46.3, 45.4 and 54.2 % respectively in comparison with that of the untreated $CaCO_3$ system.

For the 0.75 % titanate coupling agent treated $CaCO_3$ system, an increase in the $CaCO_3$ content from 10, 20, 30, 40 and 50 phr increases the corresponding fracture strain by 113.0, 59.2, 40.2, 45.4 and 54.2 % respectively in comparison with that of the untreated $CaCO_3$ system.

For the 1.0 % titanate coupling agent treated $CaCO_3$ system, an increase in the $CaCO_3$ content from 10, 20, 30, 40 and 50 phr increases the corresponding fracture strain by 176.6, 104.1, 46.4, 45.4 and 54.2 % respectively in comparison with that of the untreated $CaCO_3$ system.

For the 1.5 % titanate coupling agent treated $CaCO_3$ system, an increase in the $CaCO_3$ content from 10, 20, 30, 40 and 50 phr increases the corresponding fracture strain by 150, 93.82, 46.35, 45.42 and 54.25 % respectively in comparison with that of the untreated $CaCO_3$ system.

The sequence of the ability to increase the fracture strain promoted by the use of by the titanate coupling agent is 0.75, 0.5 or 1.5 and 1.0 % respectively as shown in Figure 4.53.

The effect of the $CaCO_3$ content and the titanate coupling agent concentration on the fracture stress of $CaCO_3$-filled HDPE is shown in Figure 4.54.

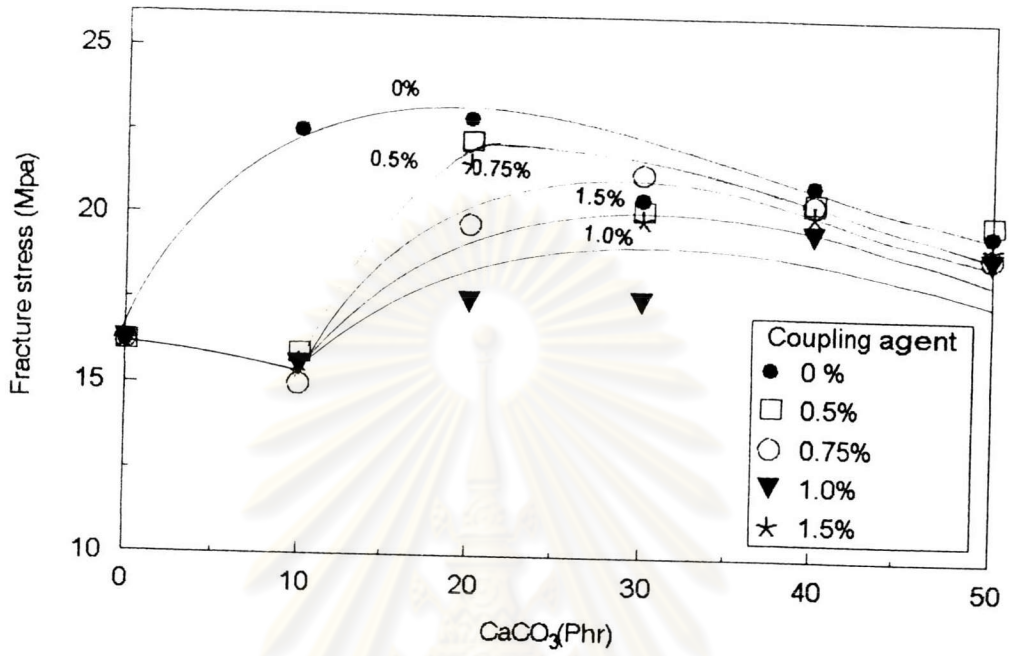

Figure 4.54: The fracture stress of the $CaCO_3$-filled HDPE with and without titanate coupling agent treated

For the untreated $CaCO_3$ system in Figure 4.54, an increase in the $CaCO_3$ content from 10, 20, 30, 40 and 50 phr increases the corresponding fracture stress by 39, 41.5, 35.4, 30.3 and 25.8 % respectively in comparison with that of the virgin HDPE. The stress-strain response shown in Figures 4.31 to 4.35. show clearly that necking did not take place when the untreated $CaCO_3$ with 10 phr was stretched. However, with the addition of the titanate coupling agent, a greater plastic deformation up to necking deformation took place in the stretched specimen. This enhancement in the fracture stress is believed to be due to the better interfacial bonding between the HDPE and the titanate coupling agent treated $CaCO_3$ and the larger voids.

For the titanate coupling agent treated $CaCO_3$ system, necking is observed only in HDPE filled with 10 phr of $CaCO_3$. The stress-strain response of the titanate treated $CaCO_3$-filled HDPE systems are shown in Figures 4.30 to 4.35. The fracture stress decreases because the reduction in the mass fraction of the HDPE-matrix can subsequently decrease the amount of necking.

For the 0.5 % titanate coupling agent treated $CaCO_3$ system in Figure 4.54, an increase in the $CaCO_3$ content from 10, 20, 30, 40 and 50 phr decreases the corresponding fracture stress by 5.92 % and increase by 35.4, 31.3, 26.5 and 22.4 % respectively in comparison with the virgin HDPE.

For the 0.75 % titanate coupling agent treated $CaCO_3$ system, an increase in the $CaCO_3$ content from 10, 20, 30, 40 and 50 phr decreases the corresponding fracture stress by 5.92 % and increase 24, 28.8, 25.4 and 20.6 % respectively in comparison with that of the virgin HDPE

For the 1.0 % titanate coupling agent treated $CaCO_3$ system, 10 phr $CaCO_3$ decrease the fracture stress by nearly 6 %. However, an increase in the $CaCO_3$ content from 20, 30, 40 and 50 phr increases the corresponding fracture strain 11.3, 16.9, 15.5 and 11.3 % respectively in comparison with that of the virgin HDPE.

For the 1.5 % titanate coupling agent treated $CaCO_3$ system, 10 phr $CaCO_3$ decrease the fracture stress by nearly 6 %. However, an increase

in the $CaCO_3$ content from 20, 30, 40 and 50 phr increase the corresponding fracture stress 18.2, 23.1, 20.6, and 16.1 % respectively in comparison with the virgin HDPE.

The fracture energy of the $CaCO_3$-filled HDPE systems with and without coupling agent is shown in Figure 4.55. Increasing the $CaCO_3$ content to 10 phr significantly decreases the average fracture energy by 97.71 % as compared with that of the virgin HDPE. Between 20 and 50 phr $CaCO_3$, the fracture energy is approximately constant. Irrespective of its concentration, the presence of the $CaCO_3$-filled particle decreases the fracture energy by 99.58 % as compared with that of the virgin HDPE.

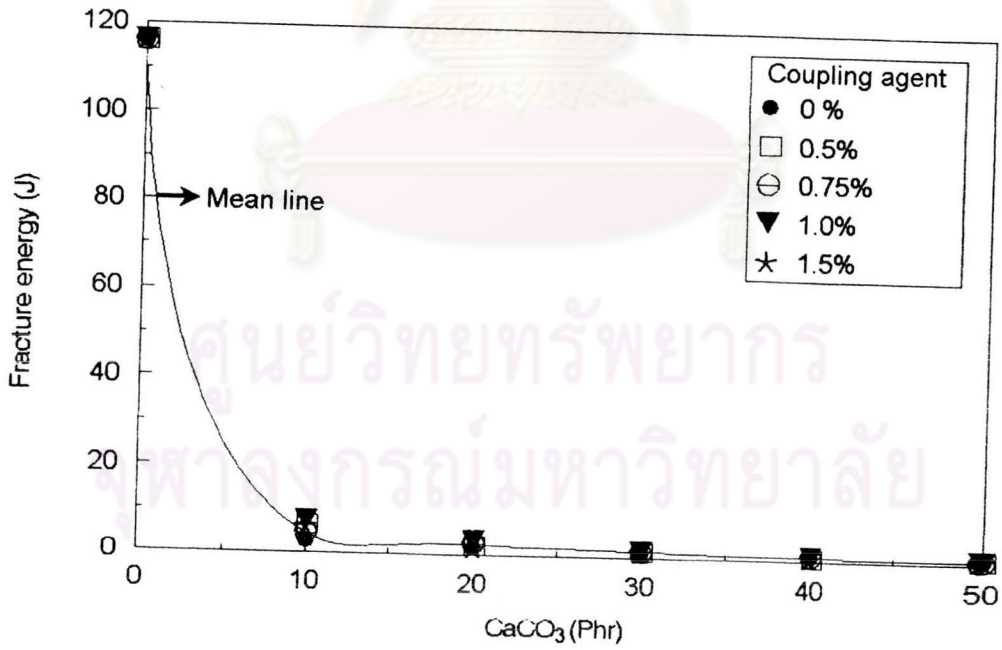

Figure 4.55: The fracture energy with and without a titanate coupling agent of $CaCO_3$-filled HDPE.

The effect of the titanate coupling agent at concentration ranges 0.5 to 1.5 % can improved fracture energy is shown in Figure 4.56.

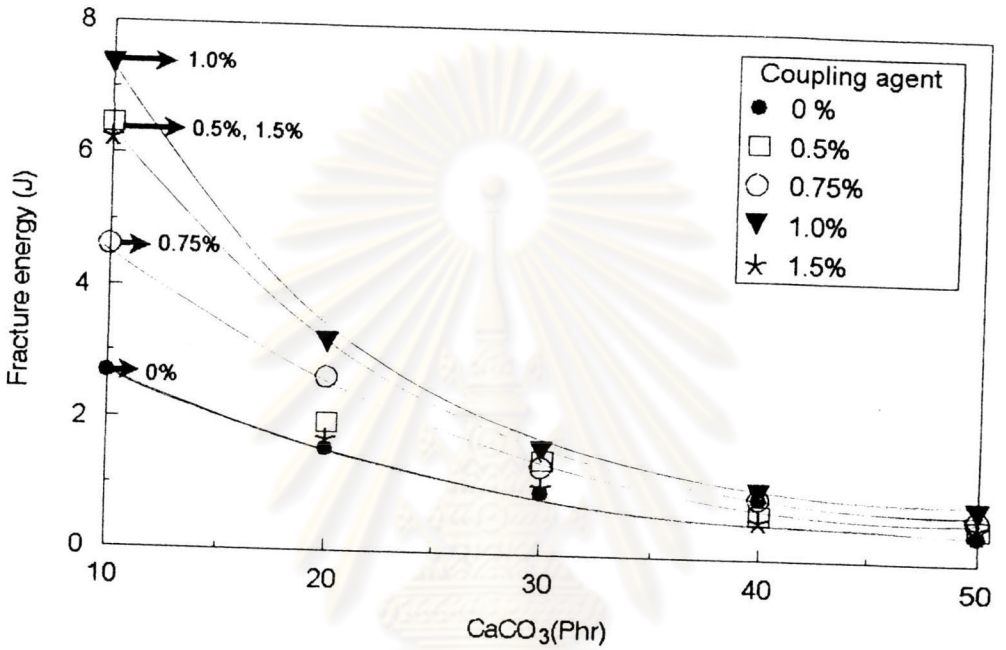

Figure 4.56: The fracture energy with and without the titanate coupling agent of $CaCO_3$-filled HDPE.

For the 0.5 % titanate coupling agent treated $CaCO_3$ system in Figure 4.56, an increase in the $CaCO_3$ content from 10, 20, 30, 40 and 50 phr increases the corresponding fracture energy by 141.4, 72, 33.7, 34.9 and 53 % respectively in comparison with that of the untreated $CaCO_3$ system.

For the 0.75 % titanate coupling agent treated $CaCO_3$ system, an increase in the $CaCO_3$ content from 10, 20, 30, 40 and 50 phr increases

the corresponding fracture energy by 73.7, 48.2, 33.7, 34.8 and 53.1 % respectively in comparison with that of the untreated $CaCO_3$ system.

For the 1.0 % titanate coupling agent treated $CaCO_3$ system, an increase in the $CaCO_3$ content from 10, 20, 30, 40 and 50 phr increases the corresponding fracture energy by 7.6, 12.6, 15.9, 17.6 and 17.6 % respectively in comparison with that of the untreated $CaCO_3$ system.

For the 1.5 % titanate coupling agent treated $CaCO_3$ system, an increase in the $CaCO_3$ content from 10, 20, 30, 40 and 50 phr increases the corresponding fracture energy by 141.4, 72, 33.7, 34.9 and 53.1 % respectively in comparison with that of the untreated $CaCO_3$ system.

The sequence of the ability to increase the fracture energy promoted by the use of by the titanate coupling agent is 0.75, 0.5 or 1.5 and 1.0 % respectively as shown in Figure 4.56.

4.3.2 Compression Properties

The compression stress-strain curve of the $CaCO_3$-filled HDPE is shown in Figure 4.57.

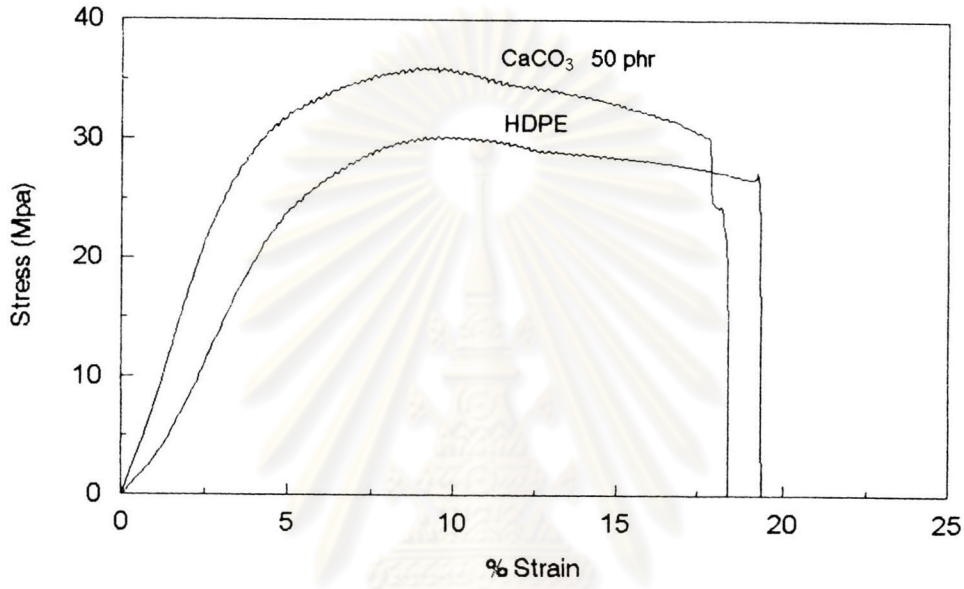

Figure 4.57: Compression stress-strain curve of $CaCO_3$-filled HDPE.

Beyond the maximum stress, the specimen tends to deform by bucking. The compression stress-strain curve was used to calculate the modulus of elasticity, the stress at yield and the stain at yield. Secant modulus was estimated as the ratio of the stress correspondent to the 2 % strain. Since the yield point is not well defined, the 0.2 % offset yield stress and yield strain will be estimated.

The effect of the $CaCO_3$ content and the titanate coupling concentration on the compressive modulus of the $CaCO_3$-filled HDPE is shown in Figure 4.58.

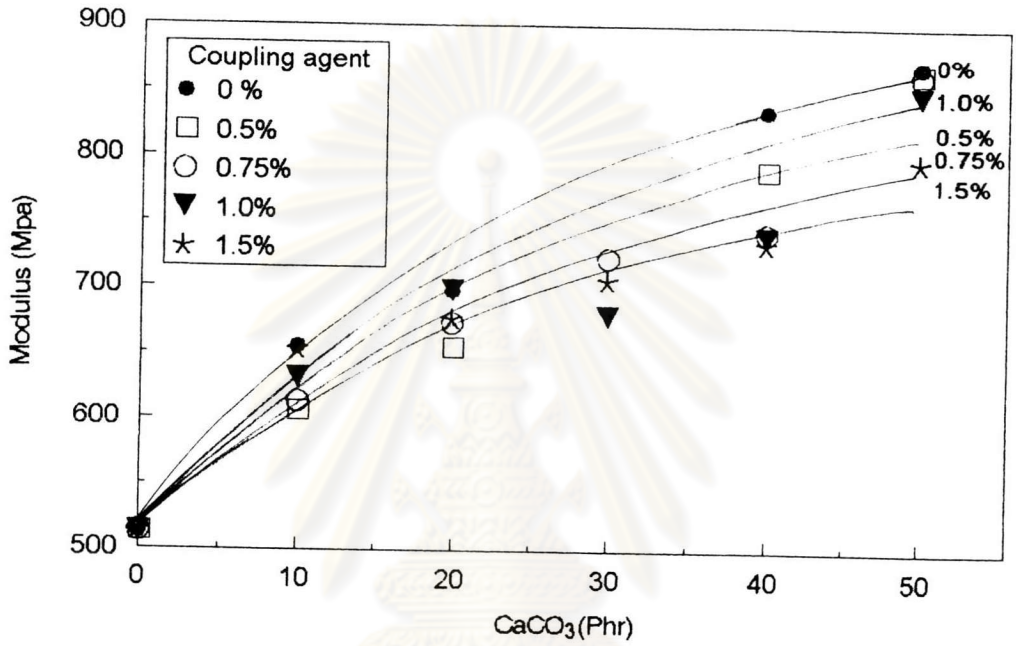

Figure 4.58: The compressive modulus of the $CaCO_3$-filled HDPE with and without titanate coupling agent.

For the $CaCO_3$-filled HDPE systems with and without titanate coupling agent shown in Figure 4.58, it is apparent that the compressive modulus increases with the $CaCO_3$ content. This may be due to the stiffness of the $CaCO_3$ which is much higher than that of the HDPE matrix. The incorporation of the titanate coupling agent in the system decreases the compressive modulus as compared with the untreated $CaCO_3$-filled HDPE system. The reduction in the compressive modulus with increasing concentration of the titanate coupling agent may be attributed to the plasticizing action of the titanate coupling agent.

For the untreated $CaCO_3$ system in Figure 4.58, an increase in the $CaCO_3$ content from 10, 20, 30, 40 and 50 phr results in an increase in the corresponding compressive modulus by 27, 41.8, 53.6, 62.2 and 69 % respectively in comparison with that of the virgin HDPE.

For the 0.5 % titanate coupling agent treated $CaCO_3$ system in Figure 4.58, an increase in the $CaCO_3$ content from 10, 20, 30, 40 and 50 phr results in an increase in the corresponding compressive modulus by 18.4, 33, 44, 53 and 60 % respectively in comparison with that of the virgin HDPE.

For the $CaCO_3$-filled HDPE system with 0.75 % titanate coupling agent, an increase in the $CaCO_3$ content from 10, 20, 30, 40 and 50 phr results in an increase in the corresponding compressive modulus by 17.1, 31.4, 43, 51 and 57 % respectively in comparison with that of the virgin HDPE.

For the $CaCO_3$-filled HDPE system with 1.0 % titanate coupling agent, an increase in the $CaCO_3$ content from 10, 20, 30, 40 and 50 phr results in an increase in the corresponding compressive modulus by 22.2, 37.3, 48.2, 58.1 and 65.3 % respectively in comparison with that of the virgin HDPE.

For the $CaCO_3$-filled HDPE system with 1.5 % titanate coupling agent, an increase in the $CaCO_3$ content from 10, 20, 30, 40 and 50 phr results in an increase in the corresponding compressive modulus by 15.6,

28.7, 38.4, 44.8 and 49.1 % respectively in comparison with that of the virgin HDPE.

The sequence of the ability of the titanate coupling agent to decrease the compressive modulus of elasticity is 1.0, 0.5, 0.75 and 1.5 % respectively as shown in Figure 4.58.

The effect of the $CaCO_3$ content and the titanate coupling concentration on the compressive yield stress of $CaCO_3$-filled HDPE is shown in Figure 4.59.

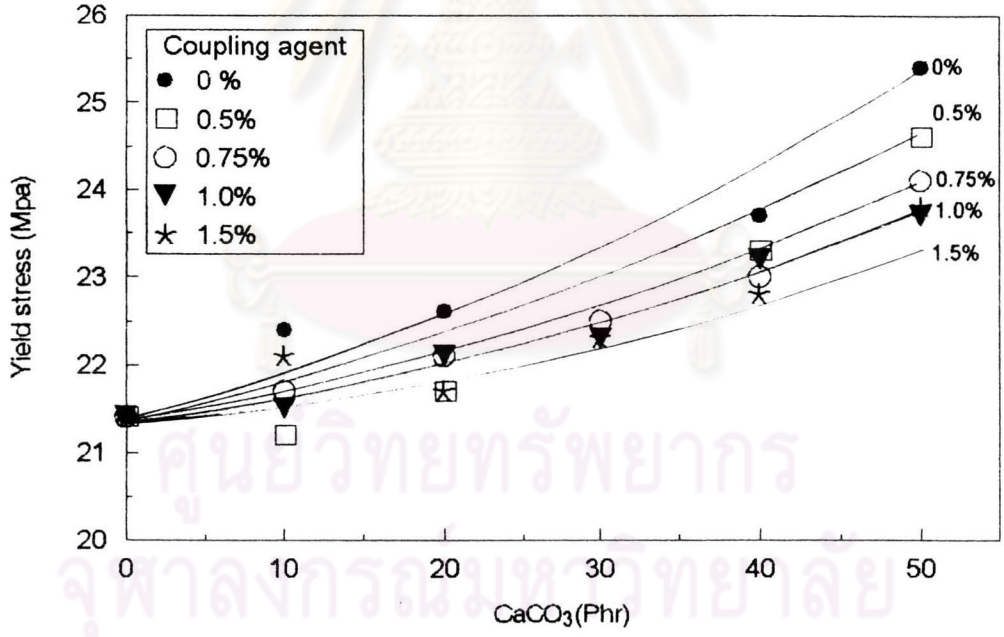

Figure 4.59: The compressive yield stress of the $CaCO_3$-filled HDPE with and without titanate coupling agent.

For the $CaCO_3$-filled HDPE systems with and without titanate coupling agent shown in Figure 4.59, it is apparent that the compressive yield stress increases with the adding of $CaCO_3$ content. This may be due to the compressive modulus of $CaCO_3$-filled HDPE higher than virgin

HDPE. The incorporation of the titanate coupling agent in the system decreases compressive yield stress as compared with the untreated $CaCO_3$-filled HDPE system, The reduction in the compressive yield stress with increasing concentration of the titanate coupling agent may be attributed to lower modulus of composites.

For the untreated $CaCO_3$ system in Figure 4.59, an increase in the $CaCO_3$ content from 10, 20, 30, 40 and 50 phr results in an increase in the corresponding compressive yield stress by 2.8, 5.4, 9.0, 13.3 and 18.5 % respectively in comparison with that of the virgin HDPE.

For the 0.5 % titanate coupling agent treated $CaCO_3$ system in Figure 4.59, an increase in the $CaCO_3$ content from 10, 20, 30, 40 and 50 phr results in an increase in the corresponding compressive yield stress by 2.2, 4.4, 7.2, 11 and 15.3 % respectively in comparison with that of the virgin HDPE.

For the $CaCO_3$-filled HDPE system with 0.75 % titanate coupling agent, an increase in the $CaCO_3$ content from 10, 20, 30, 40 and 50 phr results in an increase in the corresponding compressive yield stress by 1.3, 3.1, 5.8, 9.0 and 12.7 % respectively in comparison with that of the virgin HDPE.

For the $CaCO_3$-filled HDPE system with 1.0 % titanate coupling agent, an increase in the $CaCO_3$ content from 10, 20, 30, 40 and 50 phr results in an increase in the corresponding compressive yield stress by 0.7, 2.4, 4.8, 7.8 and 11.1 % respectively in comparison with that of the virgin HDPE.

For the $CaCO_3$-filled HDPE system with 1.5 % titanate coupling agent, an increase in the $CaCO_3$ content from 10, 20, 30, 40 and 50 phr results in an increase in the corresponding compressive yield stress by 0.2, 1.5, 3.6, 6.2 and 9.0 % respectively in comparison with that of the virgin HDPE.

The sequence of the ability of the titanate coupling agent to decrease the compressive yield stress of elasticity is 0.5, 0.75, 1.0 and 1.5 % respectively as shown in Figure 4.59.

The effect of the $CaCO_3$ content and the titanate coupling concentration on the compressive yield strain of the $CaCO_3$-filled HDPE is shown in Figure 4.60.

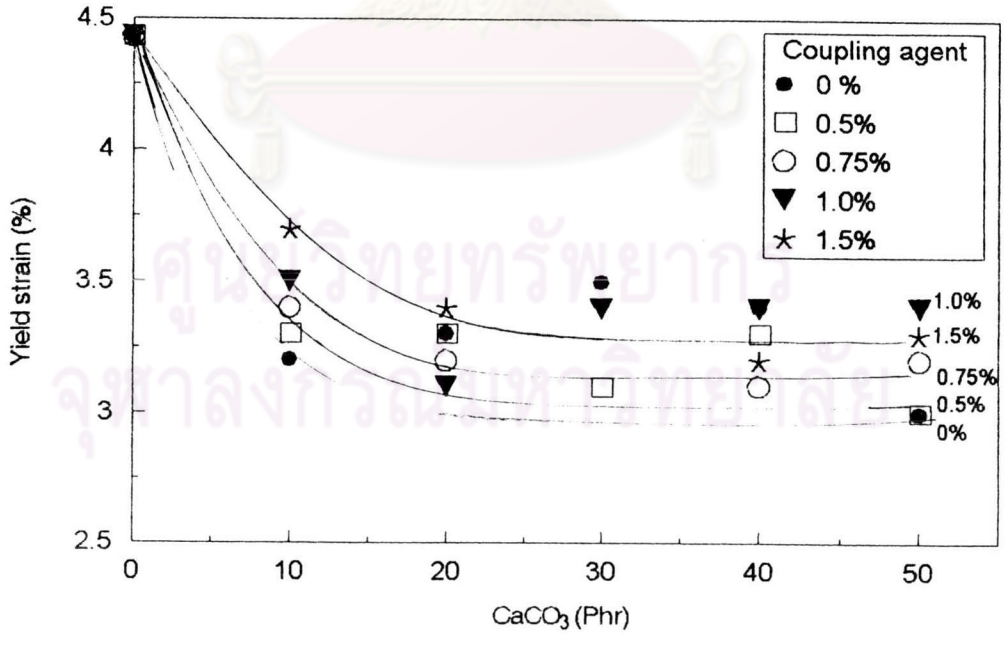

Figure 4.60: The compressive yield strain of the $CaCO_3$-filled HDPE with and without titanate coupling agent.

For the $CaCO_3$-filled HDPE systems with and without titanate coupling agent shown in Figure 4.60, it is apparent that the compressive yield strain decreases with the adding of the $CaCO_3$ content. This may be due to the elasticity of HDPE matrix higher than the $CaCO_3$ particles. The incorporation of the titanate coupling agent in the system increases compressive yield strain as compared with the untreated $CaCO_3$-filled HDPE system. The increasing in the compressive yield strain with increasing concentration of the titanate coupling agent may be attributed to lower modulus of composites.

For the untreated $CaCO_3$ system in Figure 4.60, an increase in the $CaCO_3$ content from 10, 20, 30, 40 and 50 phr results in a decrease in the corresponding compressive yield strain by 27.5, 32.3, 32.7, 32.7 and 32.7 % respectively in comparison with that of the virgin HDPE.

For the 0.5 % titanate coupling agent treated $CaCO_3$ system in Figure 4.60, an increase in the $CaCO_3$ content from 10, 20, 30, 40 and 50 phr results in a decrease in the corresponding compressive yield strain by 24.8, 30.7, 32.3, 32.3 and 32.3 % respectively in comparison with that of the virgin HDPE.

For the $CaCO_3$-filled HDPE system with 0.75 % titanate coupling agent, an increase in the $CaCO_3$ content from 10, 20, 30, 40 and 50 phr results in a decrease in the corresponding compressive yield strain by 21.7, 27.8, 29.4, 29.4 and 29.4 % respectively in comparison with that of the virgin HDPE.

For the $CaCO_3$-filled HDPE system with 1.0 % titanate coupling agent, an increase in the $CaCO_3$ content from 10, 20, 30, 40 and 50 phr results in a decrease in the corresponding compressive yield strain by 15.6, 21.7, 23.5, 23.5 and 23.5 % respectively in comparison with that of the virgin HDPE.

For the $CaCO_3$-filled HDPE system with 1.5 % titanate coupling agent, an increase in the $CaCO_3$ content from 10, 20, 30, 40 and 50 phr results in a decrease in the corresponding compressive yield strain by 17.6, 23.9, 26.2, 26.2 and 26.2 % respectively in comparison with that of the virgin HDPE.

The sequence of the ability of the titanate coupling agent to increase the compressive yield strain of elasticity is 0.5, 0.75, 1.5 and 1.0 % respectively as shown in Figure 4.60.

4.3.3 Hardness

The hardness test was conducted to determinine the indentation hardness of the unfilled and the filled HDPE systems. It is closely related to the resistance of the material to the penetration on its surface. The hardness of the unfilled and $CaCO_3$-filled HDPE is shown in Figure 4.61.

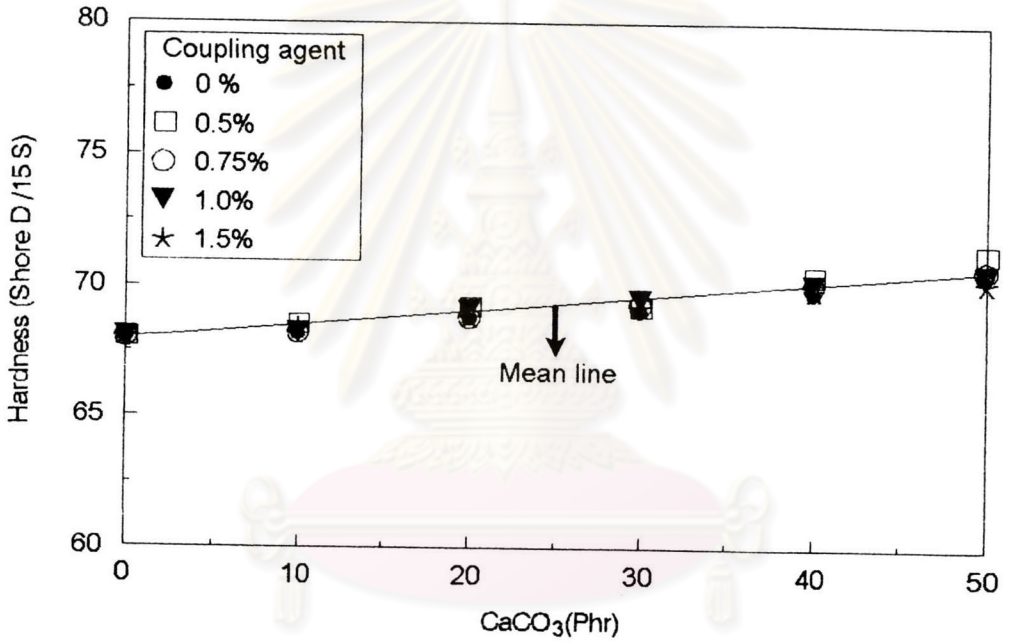

Figure 4.61: The hardness of the unfilled and the $CaCO_3$-filled HDPE.

There is an improvement in the hardness of the $CaCO_3$-filled HDPE at all concentrations. The increase is steady. With 50 phr of $CaCO_3$, the hardness is improved by 4 %. This improvement in the hardness may be attributed to the higher hardness of the $CaCO_3$ phase which has a hardness value of 3 Mohs scale. It is obvious from the plot in Figure 4.61, that the presence of a titanate coupling agent does not have any effect on the hardness of the $CaCO_3$-filled HDPE.

4.3.4 Izod Impact Strength

The Izod impact strength of the unfilled and the $CaCO_3$-filled HDPE both with and without titanate coupling agent drops dramatically by 37 % when $CaCO_3$ was added by only 10 phr. Beyond the 10 phr concentration, the impact energy is approximately constant as shown Figure 4.62. The decreasing impact strength may be attributed to the reducing deformation of HDPE matrix and thus a lower ductility is observed.

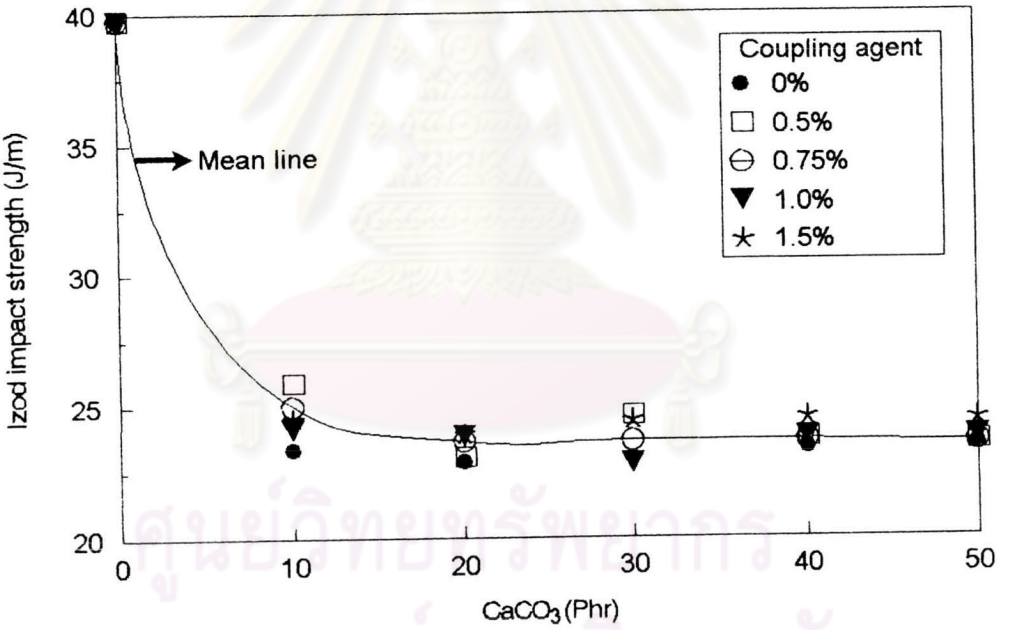

Figure 4.62: Izod impact strength of $CaCO_3$-filled HDPE.

An addition of the titanate coupling agent at the concentrations of 0.5-1.5 % can improve slightly the Izod impact strength as shown in Figure 4.63. The enhanced impact strength is due to the additional interfacial bonding at the polymer and filler interface.

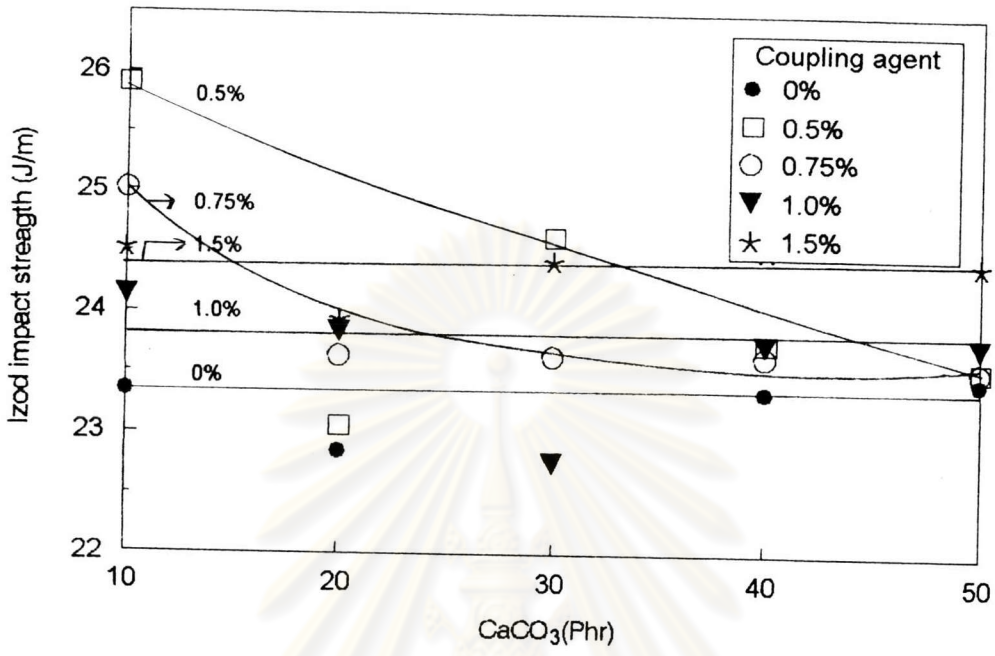

Figure 4.63: The Izod impact strength of the $CaCO_3$-filled HDPE, the plot shows $CaCO_3$ loading between 10-50 phr.

Titanate coupling contains both hydrolyzable neoalkoxy group (R′O-) and the compatibilizer group (R″-). The R′O group reacts with the available proton on the $CaCO_3$ surface giving rise to an organofunctional layer. The R″ group enhances the compatibility with HDPE chains by promoting secondary bonding of Vander Waal's type. The formulation of organofunction layer on $CaCO_3$ also leads to its deagglomeration because the reaction of the titanate coupling agent with available water of hydration and filling of air voids as shown in Figure 4.64.

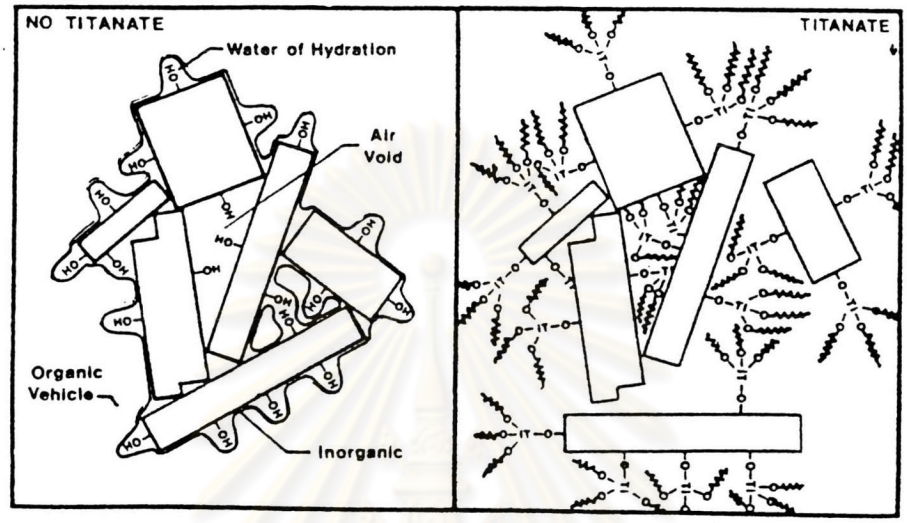

Figure 4.64: The monolayer of titanate coupling agent on $CaCO_3$ surface.

The impact strength of the $CaCO_3$-filled HDPE was measured by the Izod impact test. The Izod impact strength reflects the ability of the filled HDPE to resist an impact load before a failure will take place. Figure 4.63 shows the Izod impact strength of HDPE system filled with the $CaCO_3$ from 10 to 50 phr and various concentration of the titanate coupling agent.

For the system filled with the $CaCO_3$ but without an earlier the titanate coupling agent treatment, the impact system remains relatively unchanged from the $CaCO_3$ concentration of 10 to 50 phr. With the presence of titanate coupling agent on the $CaCO_3$ surface, the impact strength becomes greater than those without the titanate coupling agent.

At $CaCO_3$ 10 phr, a concentration of 0.5 % titanate coupling agent yields the highest elevation by 10.5 % in the impact strength.

With 0.75 % titanate coupling agent, the increase in the impact strength is about 7.1 % at $CaCO_3$ 10 phr.

With the greater concentration of titanate coupling agent i.e., at 1 % and 1.5 %, the impact strength increased only slightly. This probably due to the effect imparted by the coupling agent. Excess titanate coupling agent may have extra lubricant.

4.3.5 Falling Weight

The falling weight event is displayed as plot between the force and the displacement curve as illustrated in Figure 4.65. The area to any point under this curve is the energy required by the specimen. The energy of crack initiation and propagation can be computed on the basic of crack initial at maximum force. The force-displacement yields information on the brittle and ductile fracture of the tested samples.

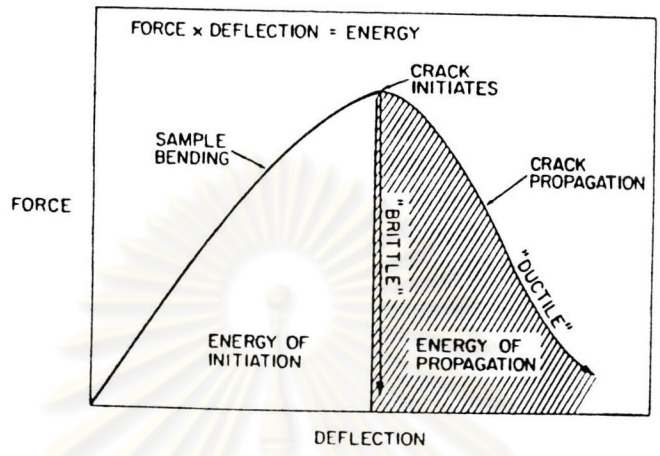

Figure 4.65: Schematic representation of the force-displacement curve for brittle and ductile fracture.

The falling weight test is carried out to predict the energy required for impact and the deformation upon fracture while the Izod impact test yields only the impact strength. The impact energy of unfilled and the filled HDPE systems is plotted against the concentrations of the $CaCO_3$ with and without prior surface treatment with the titanate coupling agent in Figure 4.66.

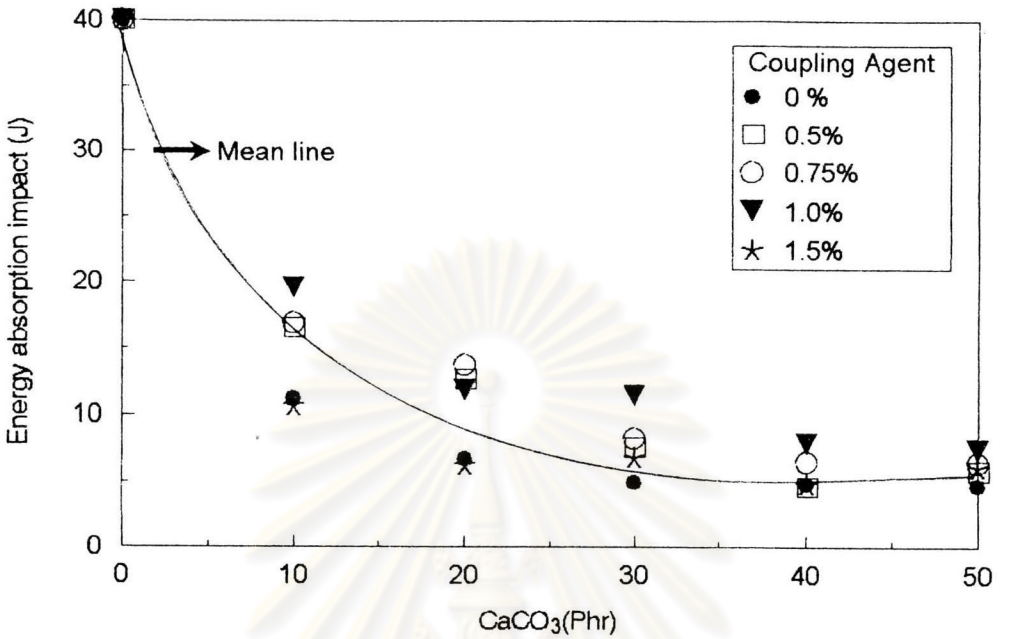

Figure 4.66: Absorption impact energy of the $CaCO_3$-filled HDPE with and without coupling agent.

For the $CaCO_3$-filled HDPE systems with and without coupling agent in Figure 4.66, increasing the $CaCO_3$ content from 10 to 20 phr significantly decreases the average impact energy by 62.6 % and 74.5 % as compared with that of the virgin HDPE. Between 20 to 50 phr of $CaCO_3$, there is a gradual depress in the impact energy by 33.3 %.

The titanate coupling agent at the concentration ranges from 0.5 to 1.5 % can improve the impact energy absorption as shown in Figure 4.67.

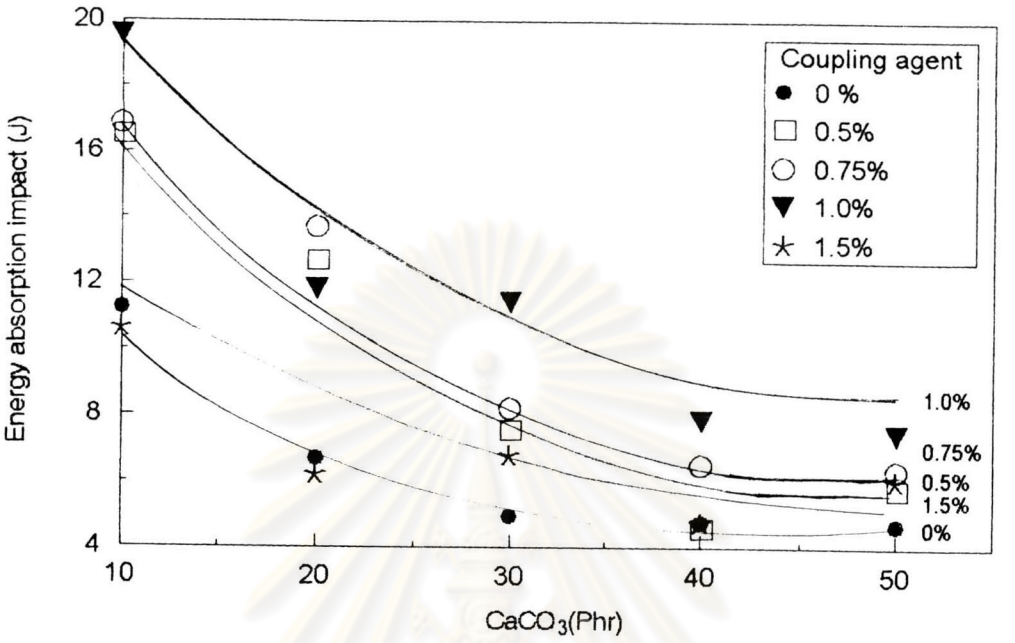

Figure 4.67: Absorption impact energy of the $CaCO_3$-filled HDPE with and without coupling agent.

For the untreated $CaCO_3$ system in Figure 4.67, an increase in the $CaCO_3$ content from 10, 20, 30, 40 and 50 phr decreases the corresponding impact energy by 72, 83.3, 87.6, 88 and 88 % respectively in comparison with that of the virgin HDPE.

For the 0.5 % titanate coupling agent treated $CaCO_3$ system in Figure 4.67, an increase in the $CaCO_3$ content from 10, 20, 30, 40 and 50 phr increases the corresponding impact energy by 43.2, 31, 40.2, 31.3, and 31.3 % respectively in comparison with that of the untreated $CaCO_3$ system.

For the 0.75 % titanate coupling agent treated $CaCO_3$ system, an increase in the $CaCO_3$ content from 10, 20, 30, 40 and 50 phr increases the corresponding impact energy by 47.7, 56.8, 45.8, 40.5 and 40.5 % respectively in comparison with that of the untreated $CaCO_3$ system.

For the 1.0 % titanate coupling agent treated $CaCO_3$ system, an increase in the $CaCO_3$ content from 10, 20, 30, 40 and 50 phr increases the corresponding impact energy by 76.1, 92.5, 100.6, 90.8 and 90.8 % respectively in comparison with that of the untreated $CaCO_3$ system.

For the 1.5 % titanate coupling agent treated $CaCO_3$ system, an increase in the $CaCO_3$ content from 10, 20, 30, 40 and 50 phr increases the corresponding impact energy by 8.3, 17.6, 24.7, 15.3 and 15.3 % respectively in comparison with that of the untreated $CaCO_3$ system.

The sequence of the ability to increase the impact energy promoted by the use of by the titanate coupling agent is 1.5, 0.5, 0.75 and 1.0 % respectively as shown in Figure 4.67.

The falling weight impact deformation of unfilled and the filled HDPE systems is plotted against the concentrations of the $CaCO_3$ with and without prior surface treatment with the titanate coupling agent in Figure 4.68.

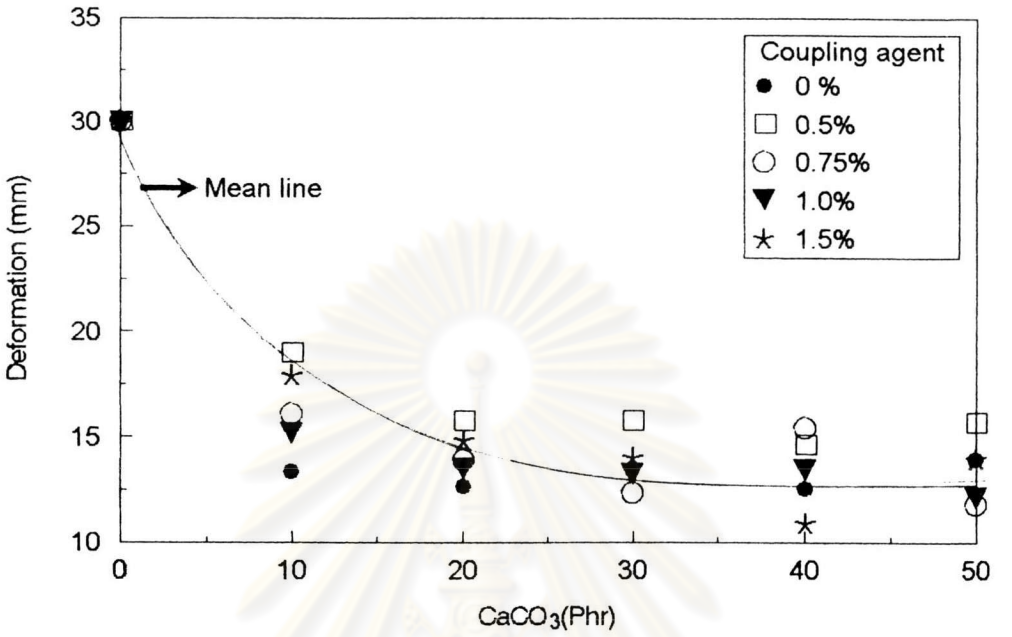

Figure 4.68: Falling weight impact deformation at fracture of the $CaCO_3$-filled HDPE.

For the $CaCO_3$-filled HDPE systems with and without coupling agent in Figure 4.68, increasing the $CaCO_3$ content from 10 to 20 phr significantly decreases the average the falling weight impact deformation by 44.24 % and 54.7 % as compared with that of the virgin HDPE. Between 20 to 50 phr of the $CaCO_3$, there is approximately constant.

The titanate coupling agent at the concentration ranges from 0.5 to 1.5 % can improve the falling weight impact deformation absorption as shown in Figure 4.69.

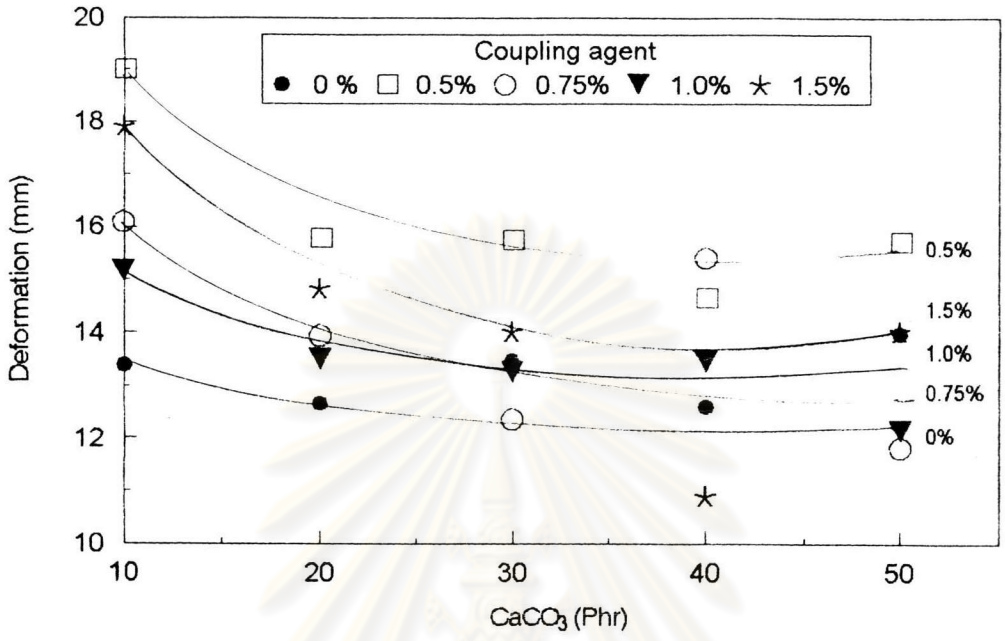

Figure 4.69: Falling weight impact deformation at fracture of the $CaCO_3$-filled HDPE.

For the untreated $CaCO_3$ system in Figure 4.69, an increase in the $CaCO_3$ content from 10, 20, 30, 40 and 50 phr decreases the corresponding falling weight impact deformation by 55.4, 57.8, 60.2, 60.2 and 60.2 % respectively in comparison with that of the virgin HDPE.

For the 0.5 % titanate coupling agent treated $CaCO_3$ system in Figure 4.69, an increase in the $CaCO_3$ content from 10, 20, 30, 40 and 50 phr increases the corresponding falling weight impact deformation by 39, 31.5, 26.5, 26.5, and 26.5 % respectively in comparison with that of the untreated $CaCO_3$ system.

For the 0.75 % titanate coupling agent treated $CaCO_3$ system, an increase in the $CaCO_3$ content from 10, 20, 30, 40 and 50 phr increases the corresponding falling weight impact deformation by 17.3, 8.5, 2.7, 2.7 and 2.7 % respectively in comparison with that of the untreated $CaCO_3$ system.

For the 1.0 % titanate coupling agent treated $CaCO_3$ system, an increase in the $CaCO_3$ content from 10, 20, 30, 40 and 50 phr increases the corresponding falling weight impact deformation by 11, 8.5, 6.6, 6.6 and 6.6 % respectively in comparison with that of the untreated $CaCO_3$ system.

For the 1.5 % titanate coupling agent treated $CaCO_3$ system, an increase in the $CaCO_3$ content from 10, 20, 30, 40 and 50 phr increases the corresponding falling weight impact deformation by 30.4, 17.6, 17.1, 17.1 and 17.1 % respectively in comparison with that of the untreated $CaCO_3$ system.

The sequence of the ability to increase the falling weight impact deformation promoted by the use of by the titanate coupling agent is 0.75, 1.0, 1.5 and 0.5 % respectively as shown in Figure 4.69.

4.4 Characterization of $CaCO_3$-Filled HDPE

4.4.1 Differential Scanning Calorimeter (DSC)

DSC thermal scans in the form of the heat flow and the temperature were obtained from the DSC test for unfilled and filled HDPE. An example of the plot is shown in Figures 4.70 to 4.75.

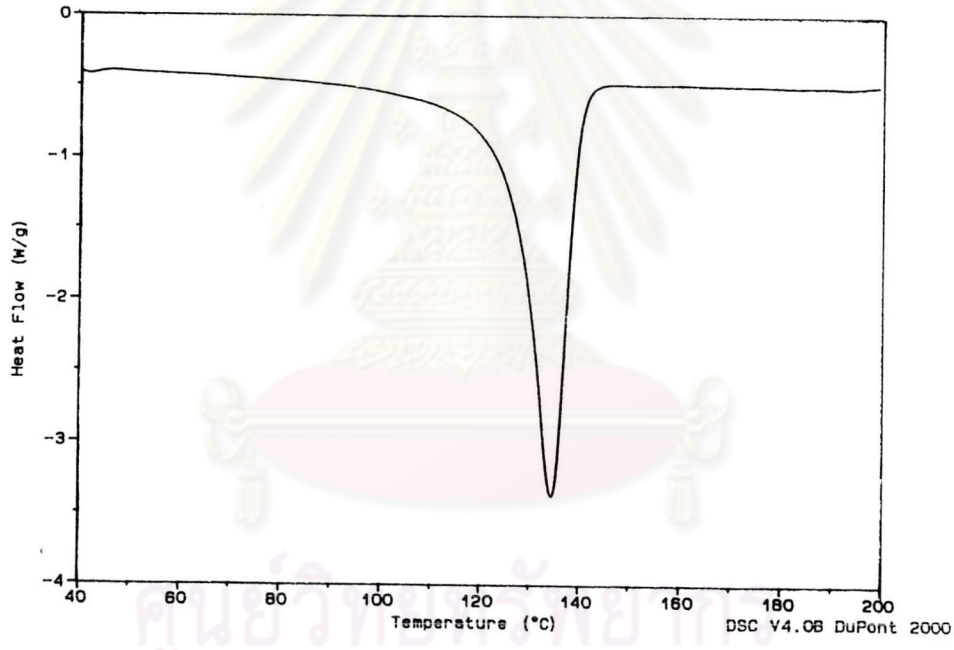

Figure 4.70: DSC thermal scan for virgin HDPE a heating rate of 10 °C/ min.

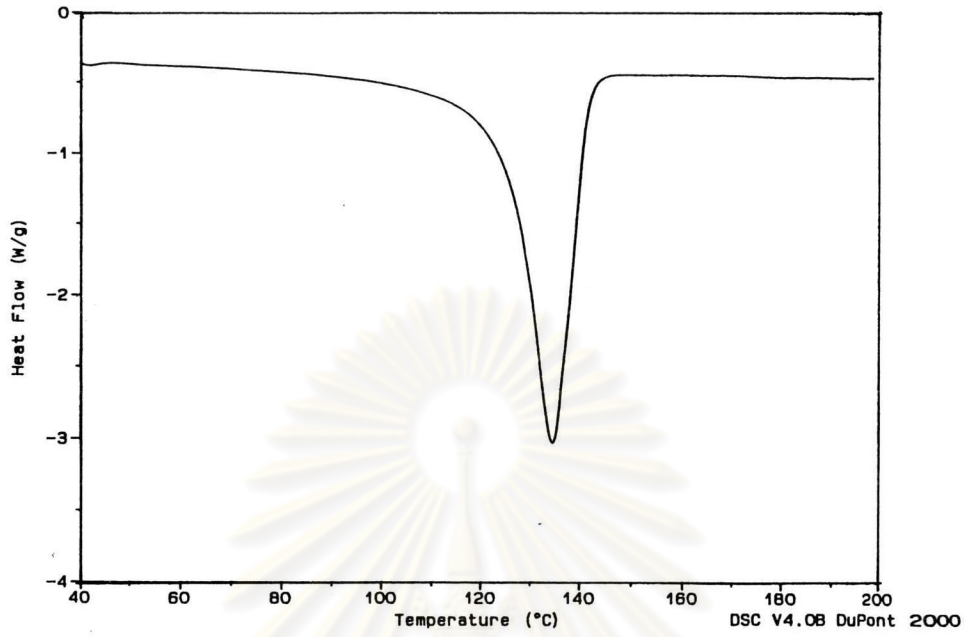

Figure 4.71: DSC thermal scan for $CaCO_3$-filled HDPE with $CaCO_3$ 10 phr at a heating rate of 10 °C/min.

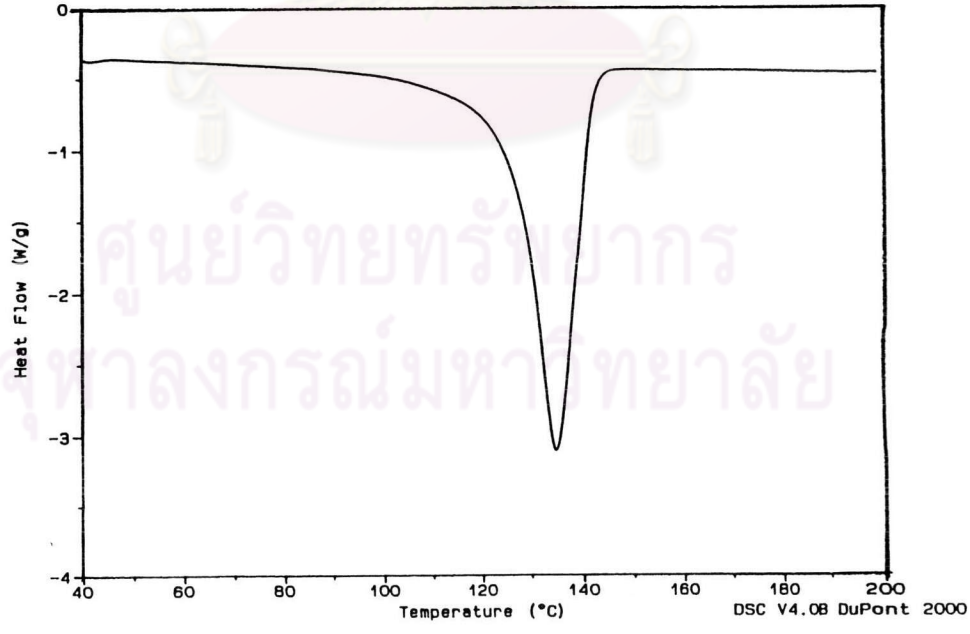

Figure 4.72: DSC thermal scan for $CaCO_3$-filled HDPE with $CaCO_3$ 20 phr at a heating rate of 10 °C/min.

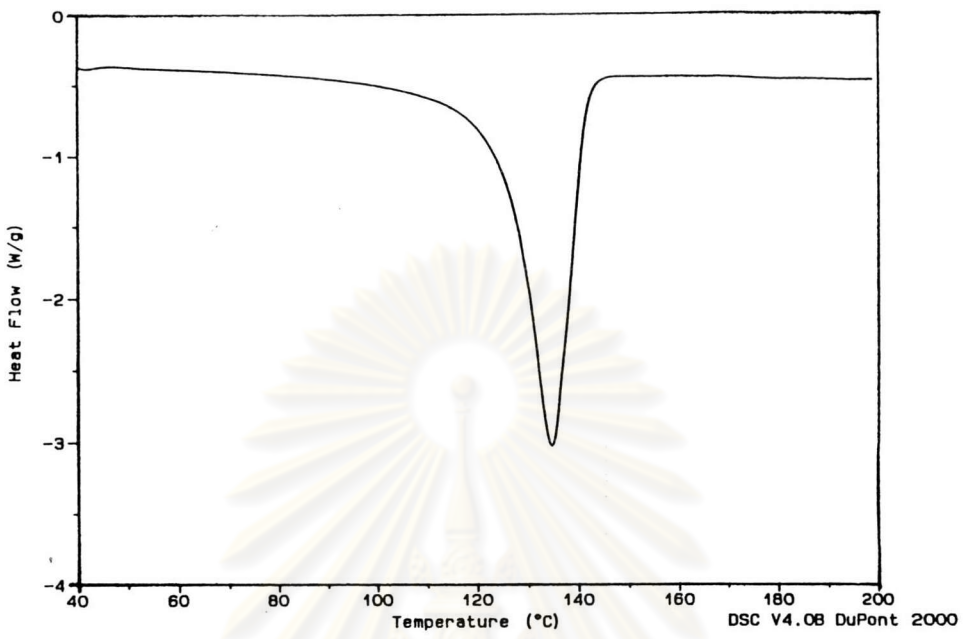

Figure 4.73: DSC thermal scan for $CaCO_3$-filled HDPE with $CaCO_3$ 30 phr at a heating rate of 10 °C/min.

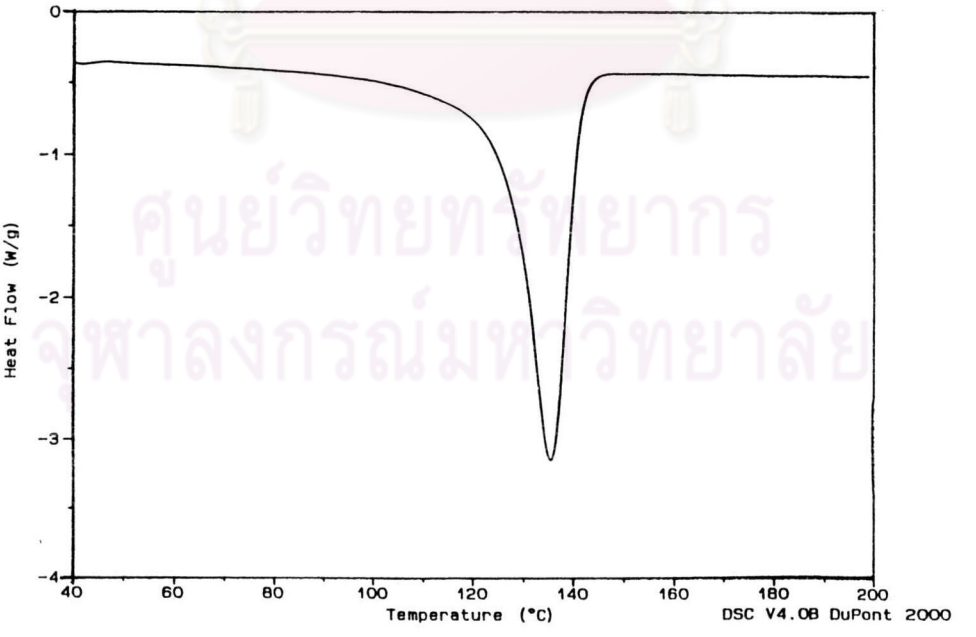

Figure 4.74: DSC thermal scan for $CaCO_3$-filled HDPE with $CaCO_3$ 40 phr at a heating rate of 10 °C/min.

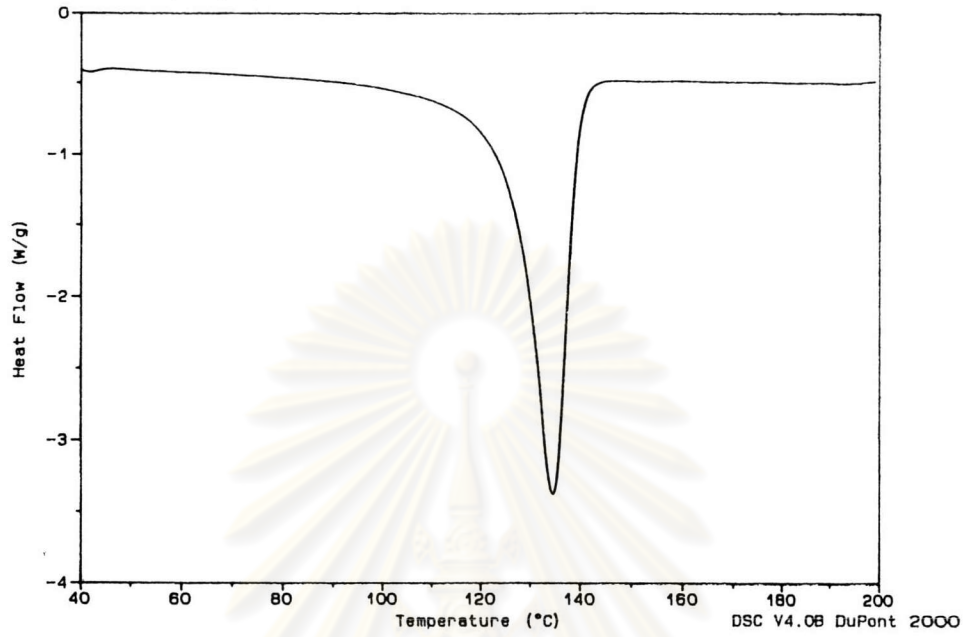

Figure 4.75: DSC thermal scan for $CaCO_3$-filled HDPE with $CaCO_3$ 50 phr at a heating rate of 10 °C/min.

An addition of the $CaCO_3$ content and the titanate coupling agent concentration does not significantly effect the melting temperature and the percent crystallinity of the HDPE.

The melting temperature and the percent crystallinity of all the unfilled and the filled HDPE systems is about 126 °C and 59 % respectively as shown in Figures 4.76 and 4.77 respectively. The constant melting temperature of the system implies that the filler particles and the HDPE are totally immisible. This is also verified by the existence of the two phases in the microscopic study by SEM as shown in Figure 4.78.

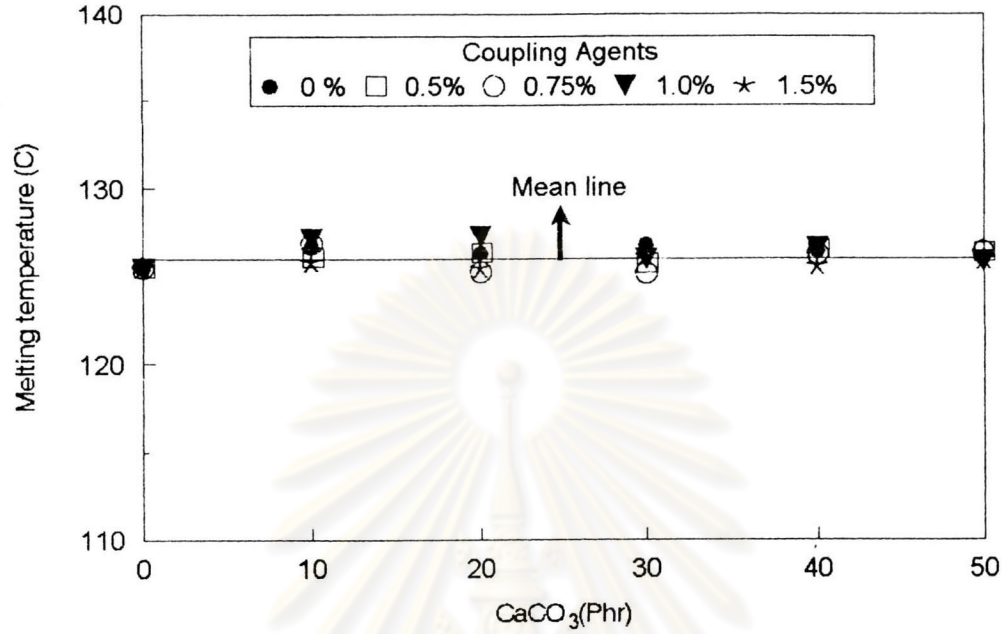

Figure 4.76: The melting temperature of the unfilled and $CaCO_3$-filled HDPE with and without titanate coupling agent.

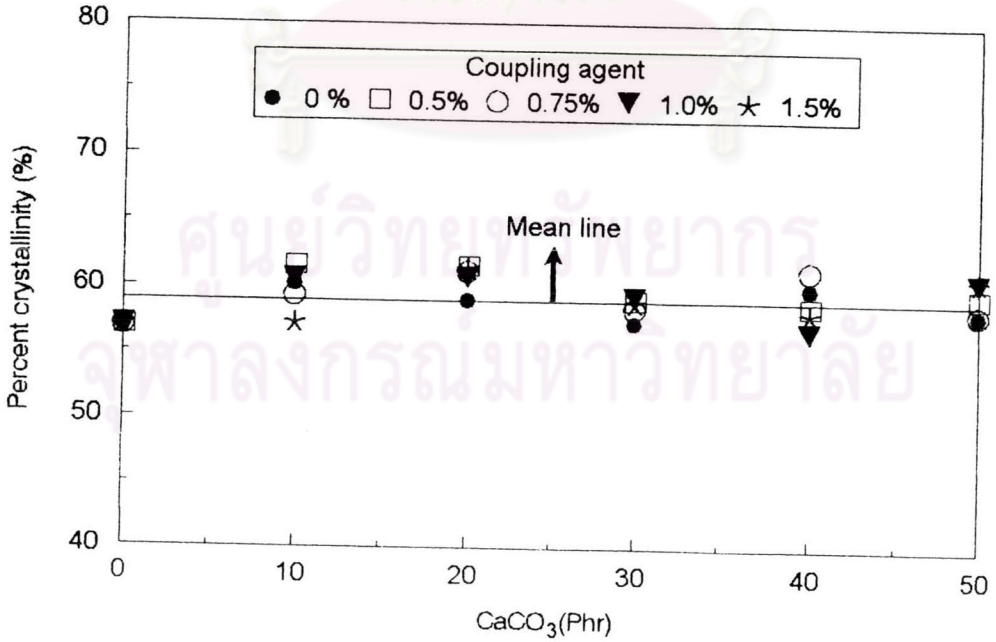

Figure 4.77: The degree of crystalinity of the unfilled and $CaCO_3$-filled HDPE with and without titanate coupling agent.

Figure 4.78: SEM micrograph of HDPE/50 phr $CaCO_3$.

4.4.2 Dynamic Mechanical Thermal Analysis (DMTA)

The storage (elastic) modulus (E′) and the loss tangent (tan δ) are obtained from the DMTA test and plotted against the temperature as shown in Figure 4.79. The test was conducted under a bending mode. The glass transition temperature of the HDPE is defined at loss tangent peak.

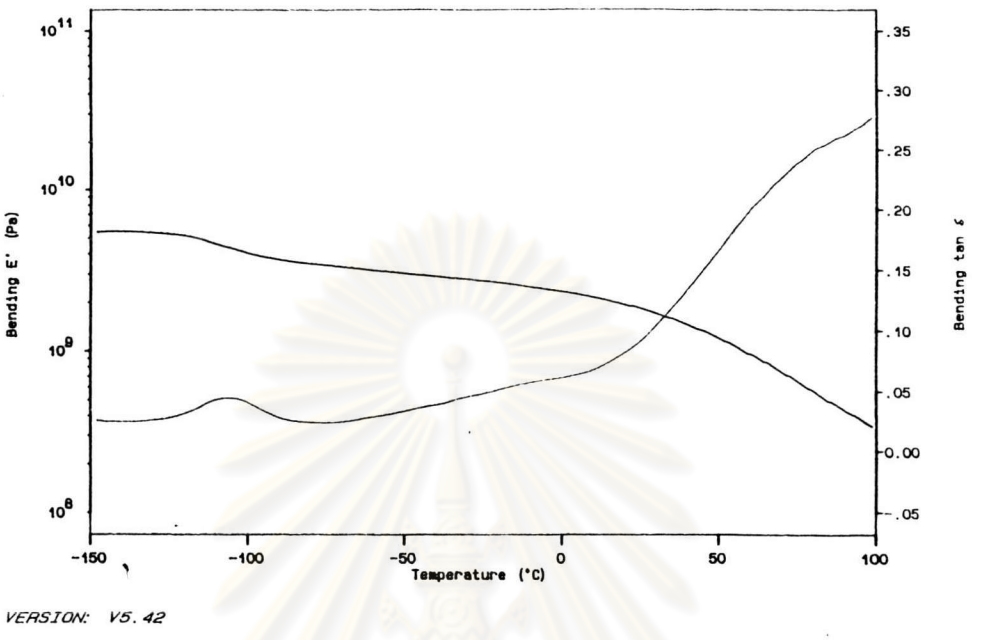

Figure 4.79: Temperature dependence of the bending modulus and loss the tangent of filled HDPE at 1 Hz.

The glass transition temperature of the HDPE composites system is about -105.5 °C as shown in Figure 4.80.

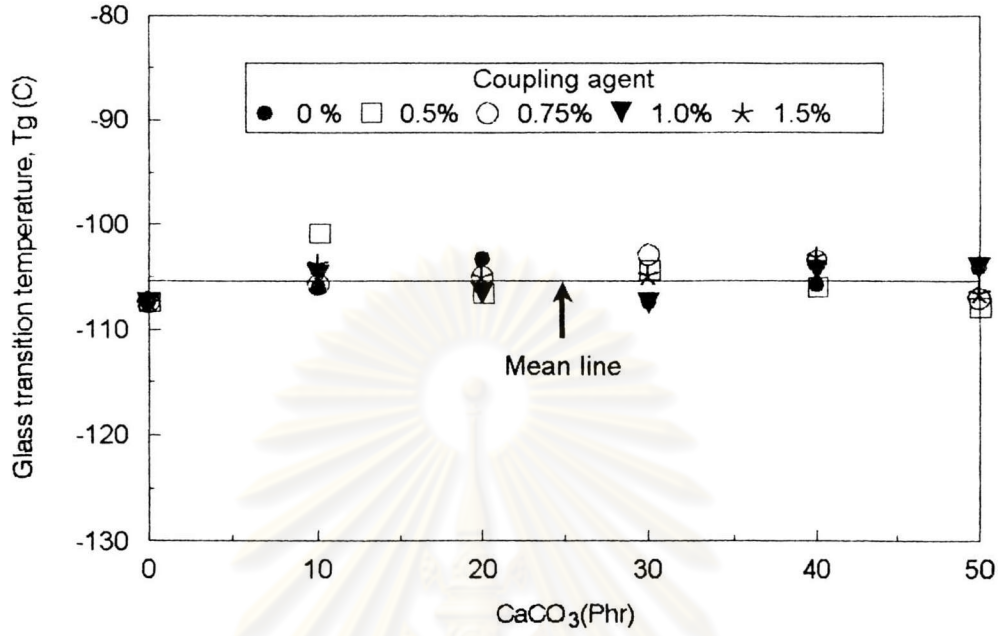

Figure 4.80: The glass transition temperature of the unfilled and $CaCO_3$-filled HDPE.

Though both the $CaCO_3$ content and the concentration of the titanate coupling agent have increased, the glass transition temperature does not change. The glass transition temperature is the property of the amorphous part of the HDPE system. The greater the degree of crystallinity in the system, the lower is the amount of the amorphous part. According to the differential scanning calorimeter test, the degree of crystallinity of the filled HDPE composite systems, however, does not change.

Other study by Flocke [48] observed the glass transition on both the low density (branches) and high density (linear) polyethylene as shown in Figure 4.81.

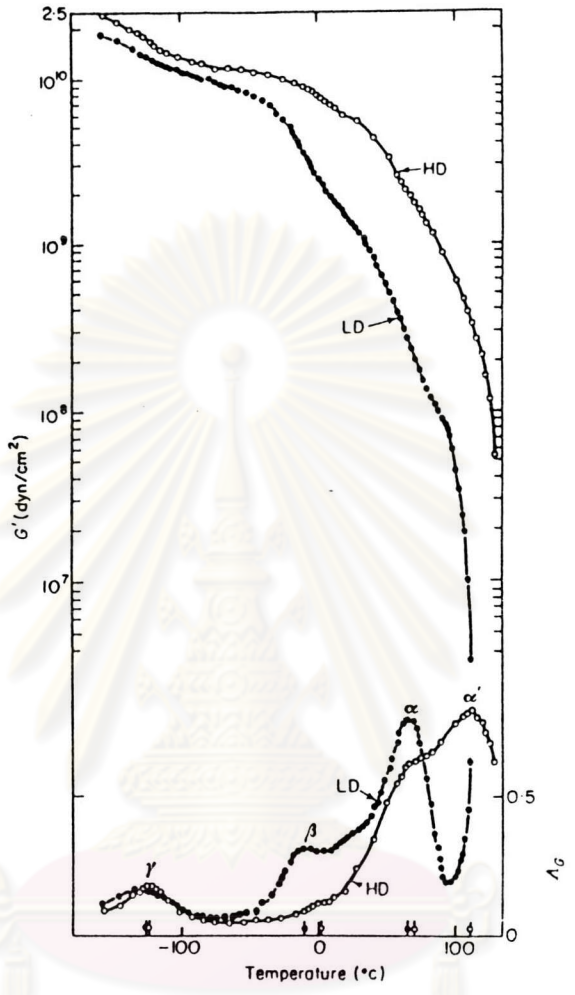

Figure 4.81: Temperature dependence of the shear modulus and the loss tangent of the high density (HD) and the low density (LD) polyethylene at 1 Hz.

The parameters of loss tangent peaks are labeled as α, β and γ for the highest peak, the middle peak and the lowest peak respectively as shown in Figure 4.81.

The α peak is due to the vibrational or reorientational motion of the PE chains within the crystal line region. In LDPE, the narrowing of α

peak appears at room temperature and it occurs at a higher temperature in HDPE, as shown in Figure 4.81. The temperature of the α peak depends on both the side-branch content and the method of crystallization which tends to lower the melting point and affects the lower α temperature peak. Quenching appears to lower α temperature peak.

In the present study, the tan δ at temperature above 100°C can not be measured. At such temperature, one is within the softening temperature range and is approaching the melting temperature of HDPE.

The β peak is attributed to the rotation of the side-branching group. The β peak of HDPE does not appear in the present study as HDPE has very few branching. On the contary, the β peak can be observed in LDPE which has many long side branches. The observation of the β peak in LDPE by Flocke is shown in Figure 4.82. The increase of side-branch group content greatly increases the magnification of the β peak but it does not change the corresponding peak temperature as shown in Figure 4.82.

The γ peak is most significant for the glass transition temperature of polyethylene. This is because the γ peak is associated with the rotation of the main chain C-C bond in the amorphous part. The magnitude of the γ peak is a function of the volume fraction of the amorphous region.

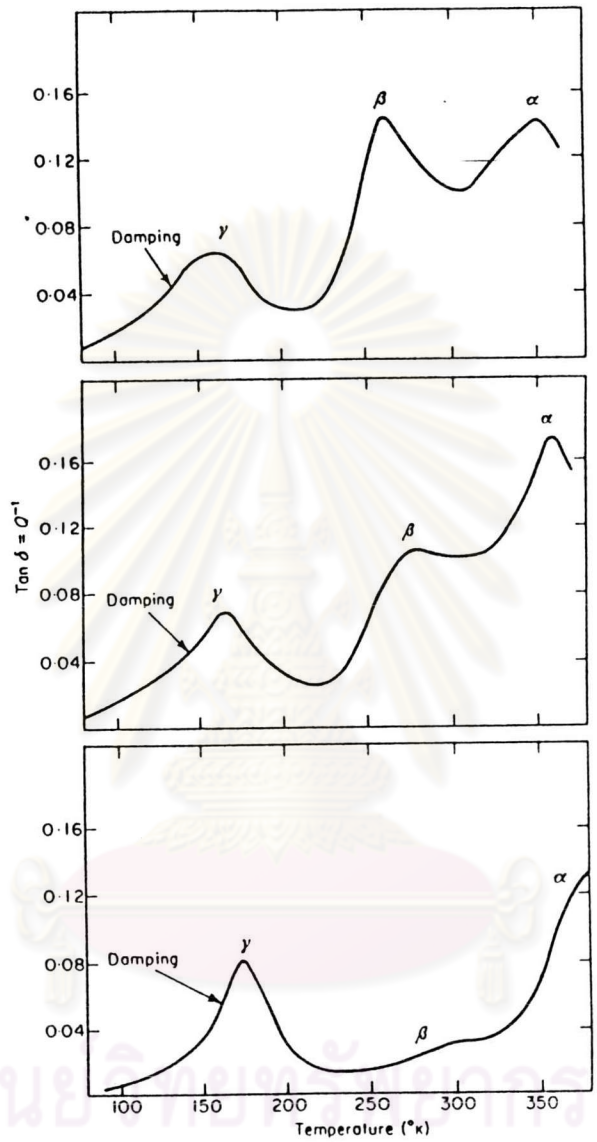

Figure 4.82: The effect of the side-branch content on the β peak magnitude in polyethylene. The upper, the middle and the lower curves are for specimens containing 32, 16 and 1 methyl group per 1000 carbon atoms.

4.4.3 Heat Deflection Temperature (HDT)

The heat deflection temperature of the $CaCO_3$-filled HDPE system is shown in Figure 4.83.

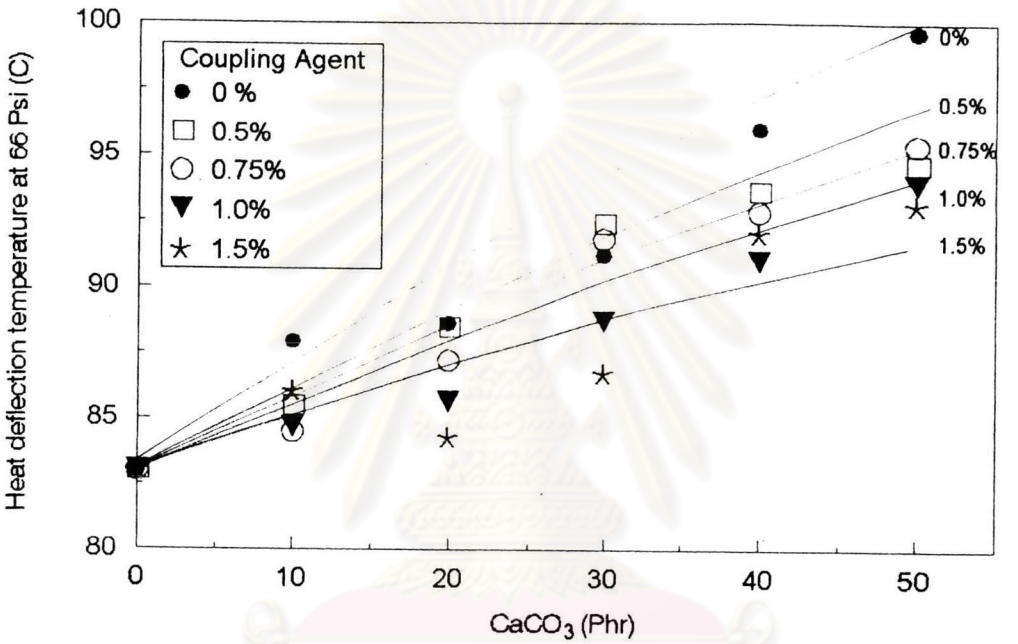

Figure 4.83: Shown the heat deflection temperature of $CaCO_3$-filled HDPE.

The heat deflection temperature increases with increasing $CaCO_3$ content. This is because the $CaCO_3$ content which has a tendency to increase the modulus, as is evident in the study in Section 4.3.1, has made the filled HDPE a thermally stable material. The decomposition temperature of $CaCO_3$ is 800-900°C. The HDPE matrix is stiffened by the $CaCO_3$ particle. At $CaCO_3$ content ranges from 0 to 50 phr, the heat deflection temperature of untreated-$CaCO_3$ filled HDPE increases by 20.48%. The increase in heat deflection temperature may be due to the

restriction to mobility and deformability of HDPE chains. When the titanate coupling agent is incorporated into the system by 0.5 %, 0.75 %, 1.0% and 1.5%, the heat deflection temperature of the $CaCO_3$-filled HDPE increases by 15.7, 13.2, 11.4 and 9.5 % respectively. The effect of the titanate coupling agent on heat deflection temperature was attributed to reduction of high temperature creep. Incorporation of titanate coupling agent was also found in plasticizing action as indicated by the yield strain and modulus as evident in the section 4.3.1.

4.4.4 Density

The density of the $CaCO_3$-filled HDPE increases with the increase in the $CaCO_3$ content as shown in Figure 4.84.

The density of $CaCO_3$-filled HDPE gradually increases by 10.6 %, 16.8 %, 22.2 %, 27.7 % and 32.6 % when the $CaCO_3$ content is raised by 10, 20, 30, 40 and 50 phr. The density of both the $CaCO_3$ and the HDPE are 2.7 and 0.9471 g/cm^3 respectively. Hence, the density of the composite systems is naturally higher than that of the virgin HDPE. When titanate coupling agent is used, the density of the composite is not significantly affected. By application of the rule of mixture, the calculated density from the mass fraction of the composite are slightly less than those measured by the density gradient method by about 12.3 %.

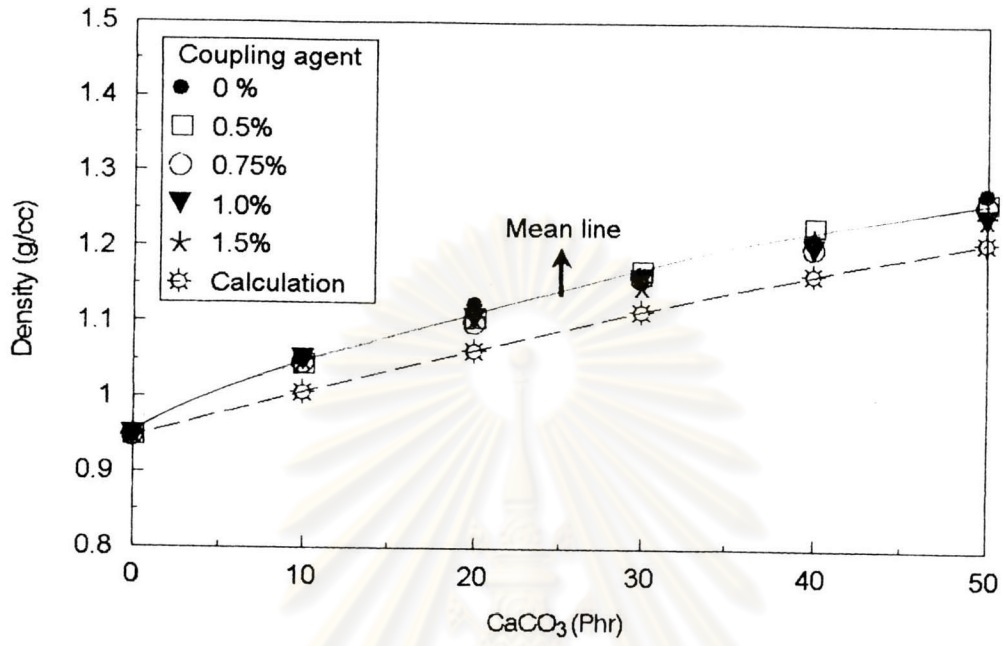

Figure 4.84: The density of the unfilled and $CaCO_3$-filled HDPE composite.

4.4.5 Crystallization and Spherulites in HDPE

In the present study, crystallization and spherulites can not be observed due to the lack of a polarizes in the microscope. Despite the lack of appropriate equipments, on attempt was still made by crystallizing the unfilled and filled HDPE at 120 °C for 10 hrs. A micrograph of pure HDPE crystallites and spherulites are shown in Figure 4.85.

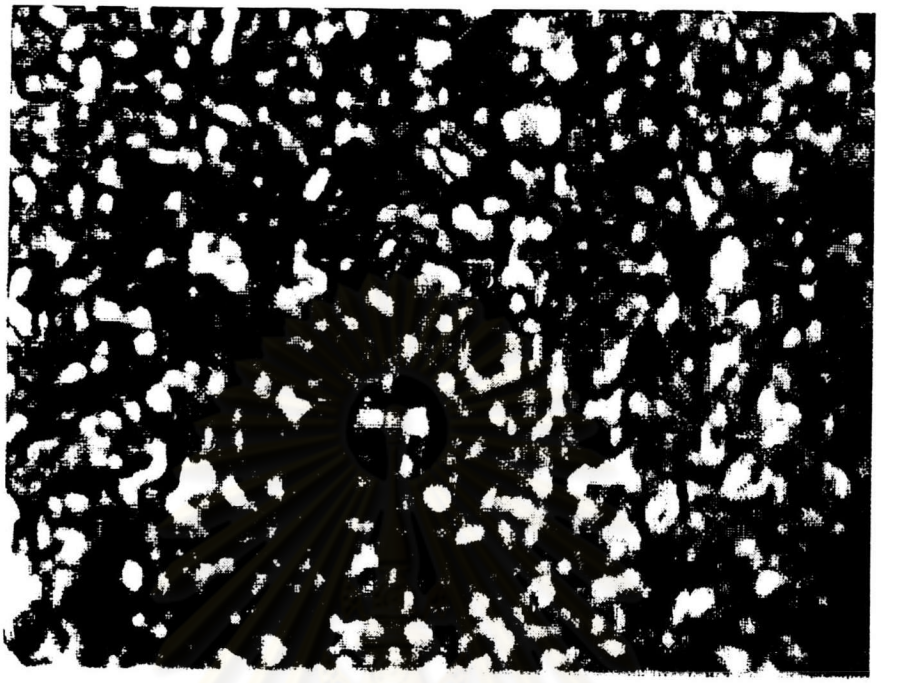

Figure 4.85: The light microscope shows spherulite of pure HDPE.

Crystallization kinetics of HDPE was explained by Chew [21] to be related to the spherulite radius, the number of nuclei and the crystallization temperature (T_e).

The number of nuclei was plotted against the time of crystallization of HDPE as shown in Figure 4.86.

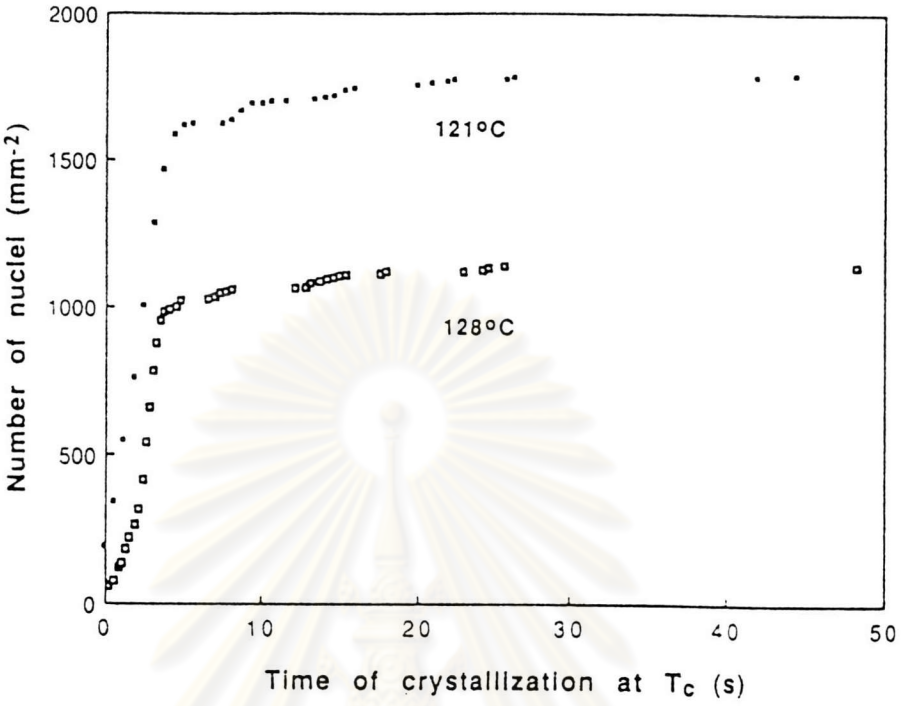

Figure 4.86: The number of spherulite plotted against the time of crystallization at the crystallization temperature of 121°C and 128°C.

From Figure 4.86, the number of nucleation rate is very high at the first five second, beyond that period the number of nucleation rate is constant. At low crystallization temperature of 121°C, the nucleation rate is higher than that at crystallization temperature of 128°C.

The growth of spherulite radius is plotted against the time of crystallization of HDPE as shown in Figure 4.87.

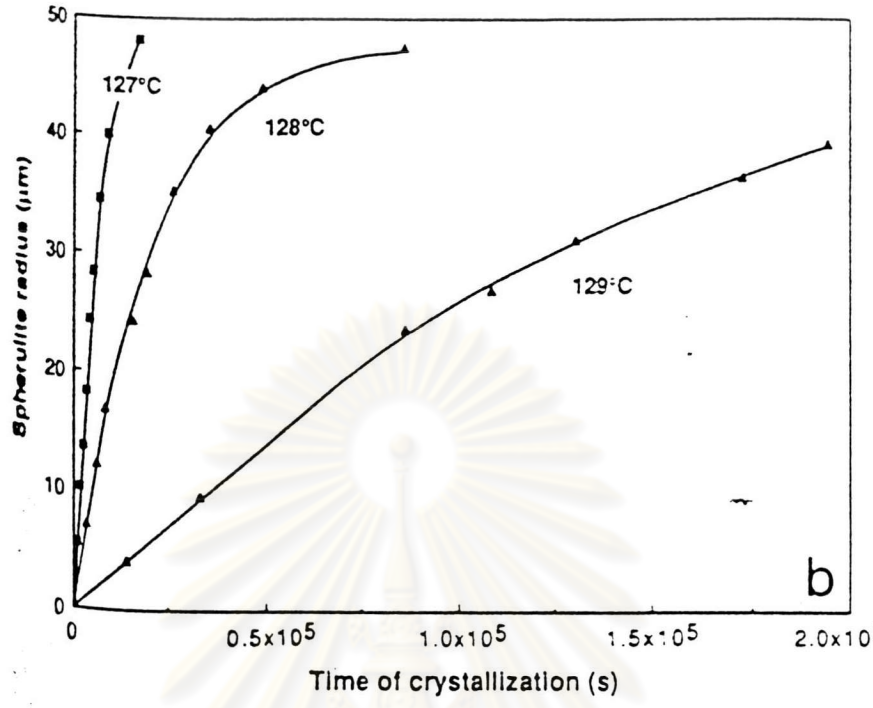

Figure 4.87: Spherulite size is plotted against the time of crystallization of HDPE at various T_c

From Figure 4.87, the growth rates of spherulite size greatly increases with the decrease in the T_c even if the crystalline temperature is changed by only 1 °C.

The spherulite morphology depends strongly on the temperature of crystallization as shown in Figure 4.88. Three distinct morphologies had been observed within the range of temperature from 120 to 127 °C, namely (a) round, ringed spherulites at the crystalline temperature of 121 °C. Then was a gradual transformation to (b) which were coarse, non-ringed spherulites at the crystalline temperature of 126 °C. Eventually, to (c) at the crystalline temperature top of 127 °C, axialite growth takes place [21].

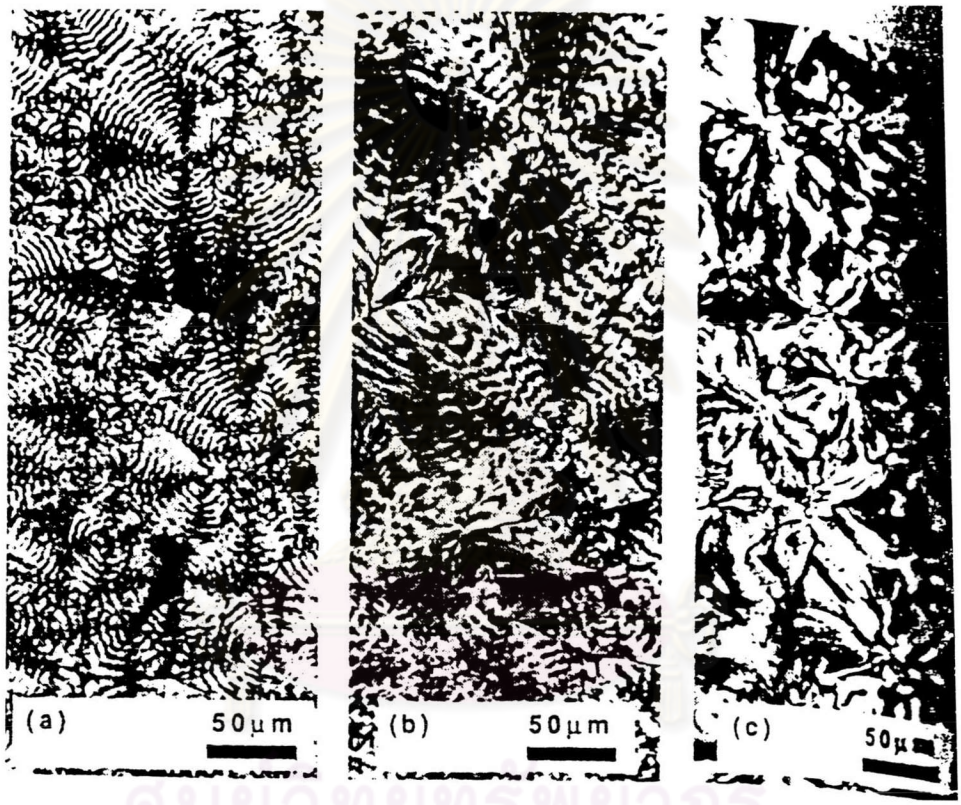

Figure 4.88: Three morphologies of spherulite observed in HDPE; (a) ringed shperulites crystallized at 120 °C; (b) coarse grained spherulites crystallized at 126 °C; (c) axialites growth at 127 °C.

4.5 Fracture Behavior of $CaCO_3$-Filled HDPE

The study of the fracture surface of 50 phr $CaCO_3$-filled HDPE with and without the titanate coupling agent are shown in Figure 4.89 to 4.94.

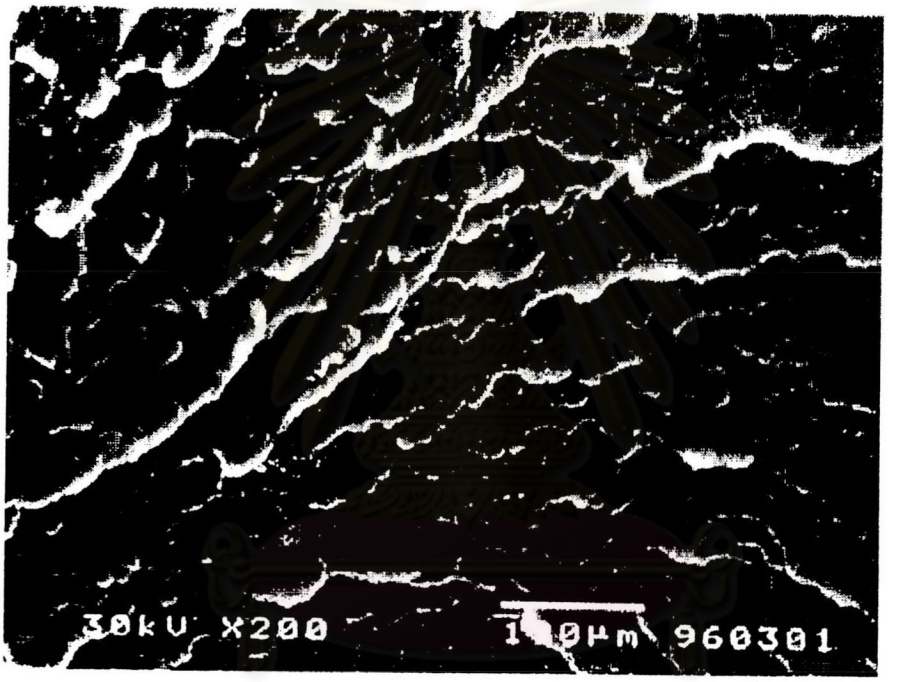

Figure 4.89: SEM photomicrograph of virgin HDPE.

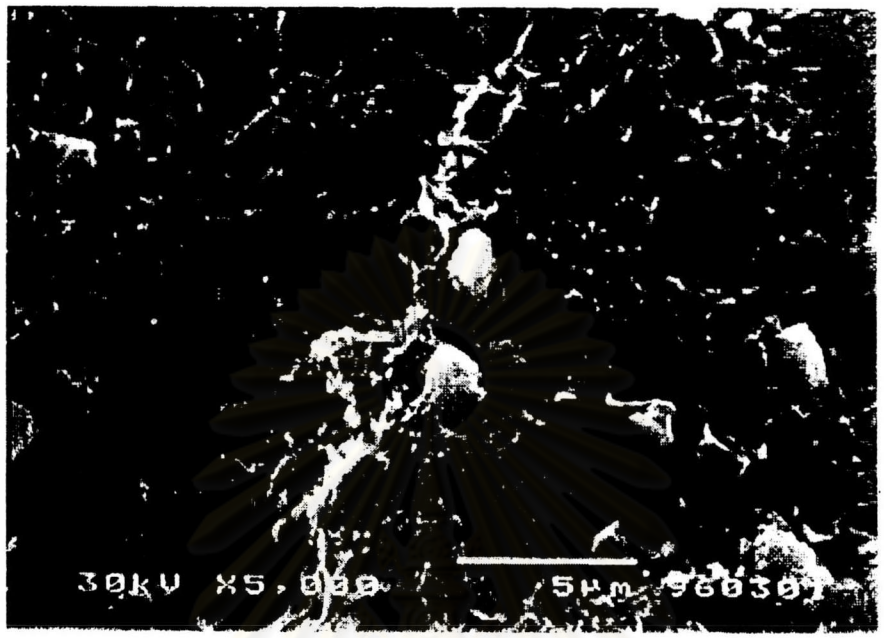

Figure 4.90: SEM photomicrograph of 50 phr $CaCO_3$-filled HDPE.

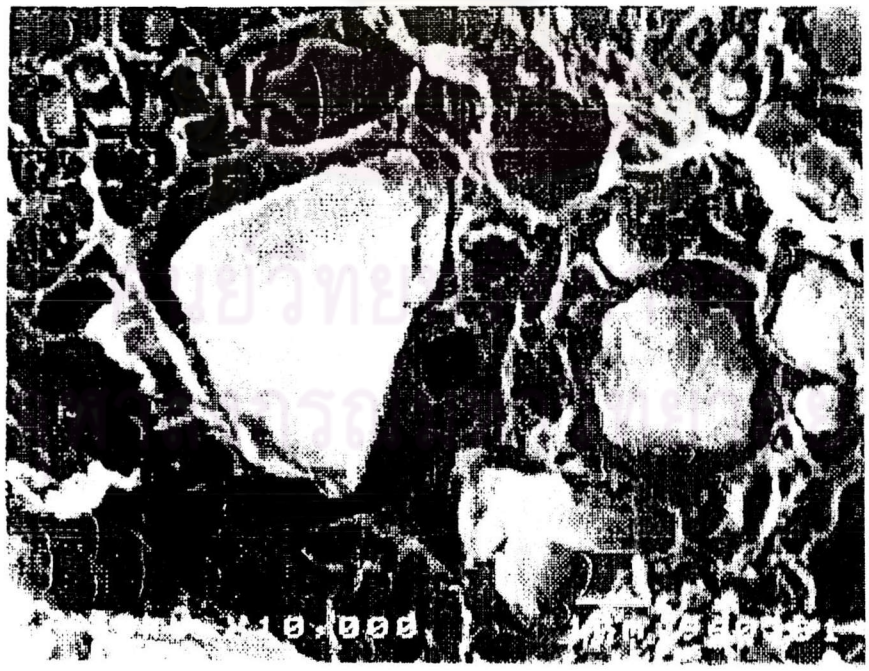

Figure 4.91: SEM photomicrograph of 50 phr $CaCO_3$-filled HDPE with 0.5 % titanate coupling agent.

Figure 4.92: SEM photomicrograph of 50 phr $CaCO_3$-filled HDPE with 0.75 % titanate coupling agent.

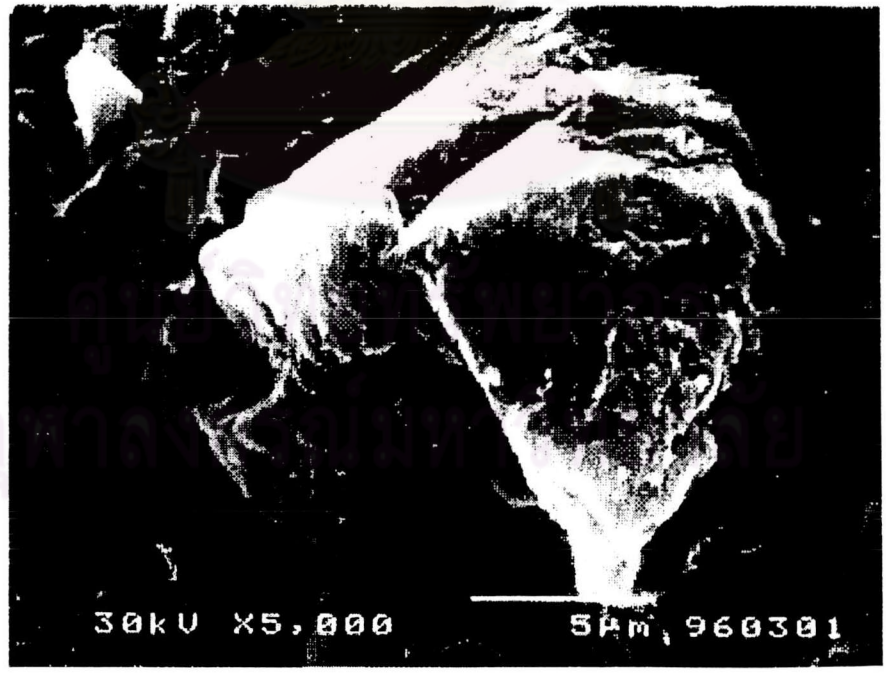

Figure 4.93: SEM photomicrograph of 50 phr $CaCO_3$-filled HDPE with 1.0 % titanate coupling agent.

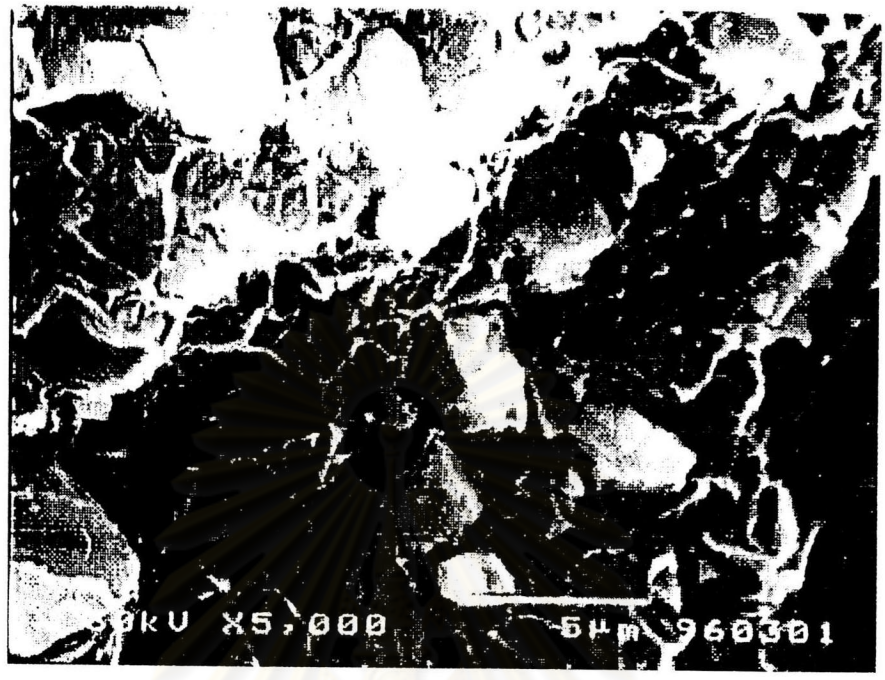

Figure 4.94: SEM photomicrograph of 50 phr $CaCO_3$-filled HDPE with 1.5 % titanate coupling agent.

For the untreated $CaCO_3$ system in Figure 4.90, it seems that the $CaCO_3$ particles is pulled out from the HDPE matrix. This effect attributable to poor bonding between $CaCO_3$ and HDPE.

The effect of titanate coupling agent on the fracture behavior of $CaCO_3$-filled HDPE are shown in Figure 4.91 to 4.94. It is found that the better adhesion between $CaCO_3$ particles and HDPE matrix as compared to the untreated system.